# Ground Motion and Site Effect Evaluation in Cretan Stations for the 2021 Arkalochori Earthquake Sequence

National Technical University of Athens

Department of Structural Engineering

Mevlut Ziya Cekinmez

October 2022

# Dedication

To my family, especially my nephews Eray and Ege...

# Acknowledgement

I would like to thank everyone who was with me from the start of my Master's degree journey till the end.

First and special thanks to Dr. Olga-Joan Ktenidou. She never stopped being so kind, patient and helpful from the first day till the last one. I have learned a lot from her not only on Engineering Seismology but also every aspect of life. Much thanks to her for being one of her kind. It was an honor to be her student.

I would also like to thank Assoc. Prof. Dimitrios Vamvatsikos. I was lucky have started my Engineering Seismology journey by taking the course from him. His unique way of explaining complicated science with interesting ways took and hold my attention on the subject.

Secondly, I would like to thank all my professors on National Technical University of Athens. It was once in a lifetime opportunity to take classes from all the professors which are one of the bests in their subjects.

Special thanks to Dr. Faidra Gikka of National Observatory of Athens. She helped and taught me a lot during my learning days in the observatory. Also she has done a lot on the signal processing of the massive amount of data. Signal processing of almost 10000 time histories one by one...She has taught me how and also patiently done in her free time with or without me. I could never finish without her.

Another special thanks to Dr. Chris Van Houtte for showing me how to use Openquake tools, Jupyter Notebooks and sharing his materials. He has spent some of his Sunday early mornings in New Zealand for this and it is precious. I have learnt a lot from him.

I would also like to thank my family as they were always supportive and with me even from another country. Last thanks to my dear friend Emilyo Celik, during these two years he was my family!

# Contents


**1 INTRODUCTION** **10**

**2 STATE-OF-THE-ART** **13**

2.1 Strong Ground Motion . . . . . . . . . . . . . . . . . . . . . . . . . . 14
2.2 Source, Path and Site Effects . . . . . . . . . . . . . . . . . . . . . . 19
2.3 Wave Theory . . . . . . . . . . . . . . . . . . . . . . . . . . . . . . 21
2.4 Local Site Effects . . . . . . . . . . . . . . . . . . . . . . . . . . . . 23
2.5 Soil Non-linearity . . . . . . . . . . . . . . . . . . . . . . . . . . . . 26
2.6 Estimation of Ground Motion Parameters-Attenuation Relationships 27
2.7 Design Codes . . . . . . . . . . . . . . . . . . . . . . . . . . . . . . 30

**3 AREA AND THE DATA SET, STATIONS AND TECHNIQUES USED FOR THE STUDY** **34**

3.1 General Information about Crete and Arkalochori . . . . . . . . . . . 35
3.2 Seismicity in Crete . . . . . . . . . . . . . . . . . . . . . . . . . . . 38
3.3 Arkalochori Earthquake Sequence in 2021 and the Damage Caused by it 41
3.4 Data Set Used and the Recording Stations in Crete . . . . . . . . . . 44
3.5 Effect of Earthquake Sequence on the Gravestones in Cretan Cemeteries 47

**4 DATA ANALYSIS** **50**

4.1 Signal Processing . . . . . . . . . . . . . . . . . . . . . . . . . . . . 51
4.2 Acceleration Response Spectra . . . . . . . . . . . . . . . . . . . . . 54
4.3 H/V Spectral Ratio (HVSR) . . . . . . . . . . . . . . . . . . . . . . 55
4.4 Distance Scaling and Residual Analysis and the GMPEs Used for both 58

**5 ANALYSIS OF THE RESULTS** **63**

5.1 H/V Fourier Analysis Combined with GMPE Residuals for Stations with Arkalochori Sequence Data . . . . . . . . . . . . . . . . . . . . 64
5.1.1 Stations with Strong Amplification . . . . . . . . . . . . . . . . 64
5.1.2 Reference Stations . . . . . . . . . . . . . . . . . . . . . . . . . 74
5.1.3 Stations with Flat H/V Ratio which Decreases with Higher Frequencies . . . . . . . . . . . . . . . . . . . . . . . . . . . . . . 78
5.1.4 Stations with Small Broadband Amplification . . . . . . . . . . 83
5.1.5 Station with a Likely Error in Sensor or Metadata . . . . . . . 86

5.2 H/V Fourier Analysis Results for Stations with no Arkalochori Sequence Data . . . . . . . . . . 88
5.3 Distance Scaling . . . . . . . . . . 94
5.3.1 Mw=5.9 . . . . . . . . . . 94
5.3.2 Mw=5.1 . . . . . . . . . . 97
5.3.3 Mw=4.5 bin . . . . . . . . . . 100

**6 CONCLUSIONS 103**

**A Parameters of the 6 Events of Sequence for the Residual Analysis 107**

# List of Figures


1.1 Seismic Map of Greece, by Technical Chamber of Greece . . . . . . . 11
1.2 Seismic Hazard Map of the region including Greece from ESHM 2020 project with 10 % probability in exceedance in 50 Years by Danciu et al. 2020 . . . . . . . . . . . . . . . . . . . . . . . . . . . . . . . 12

2.1 Seismic Wave Radiation . . . . . . . . . . . . . . . . . . . . . . . . . 14
2.2 Acceleration time history and Fourier Spectrum . . . . . . . . . . . . 16
2.3 Response spectrum example . . . . . . . . . . . . . . . . . . . . . . . 17
2.4 Response design spectrum example . . . . . . . . . . . . . . . . . . . 18
2.5 Factors affecting the ground motion . . . . . . . . . . . . . . . . . . . 19
2.6 Forward and backward directivity effect . . . . . . . . . . . . . . . . . 19
2.7 Deformation produced by body and surface waves . . . . . . . . . . . 22
2.8 Acceleration time history of SCT and UNAM stations in 1985 Mexico Earthquake . . . . . . . . . . . . . . . . . . . . . . . . . . . . . . . 23
2.9 Acceleration time history of Yerba and Treasure Island Stations in 1985 Mexico Earthquake . . . . . . . . . . . . . . . . . . . . . . . . . . . 24
2.10 Propagation of seismic wave on one layer soil and basin case (Vittoz et al. 2001) . . . . . . . . . . . . . . . . . . . . . . . . . . . . . . . 25
2.11 Stress-strain relationship of soil in cyclic shear deformation . . . . . 26
2.12 SA(1.0 sec) results in g per different Mw values with rupture distance 100 km from GMPE Abrahamson et al 2014, created by Openquake software . . . . . . . . . . . . . . . . . . . . . . . . . . . . . . . . . 27
2.13 PGA results in per different rjb values with Mw=6.3 km from GMPE n Kotha et al 2020, by Openquake software . . . . . . . . . . . . . . . 28
2.14 Empirical Attenuation relationship function . . . . . . . . . . . . . . 29
2.15 Design spectra . . . . . . . . . . . . . . . . . . . . . . . . . . . . . . 30
2.16 Response Spectra . . . . . . . . . . . . . . . . . . . . . . . . . . . . . 30
2.17 Eurocode 8-Site Clasification . . . . . . . . . . . . . . . . . . . . . . 32
2.18 Normalized elastic design spectra for Type 1 (a) and Type 2 (b) seismicity and for different ground types, according to EC8-1 . . . . . . . 33

3.1 Agios Nikolaos, Crete . . . . . . . . . . . . . . . . . . . . . . . . . . 35
3.2 Famous Minoan Palace in Knossos, Crete . . . . . . . . . . . . . . . . 36
3.3 Arkalochori view from South Wikipedia . . . . . . . . . . . . . . . . . 36
3.4 Seismotectonic map of Crete by Caputo et Al. . . . . . . . . . . . . . 38

3.5 Seismic Map of Greece, by Technical Chamber of Greece . . . . . . . 39
3.6 Distribution of aftershock epicenters for magnitudes above l2.0, according to the GI/EAA list. Earthquakes from June 2021 to the ML5.8 mainshock are shown in red. The seismic sequence from 9/27/2021 to May 2022 is shown in blue. Seismicity around Arkalochori from the 1960s to June 2021 is shown in grey. Figure is from ETAM report on Arkalochori sequence . . . . . . . . . . . . . . . . . . . . . . . . . . 40
3.7 Moment tensors of the main shock and the largest aftershock, from ETAM report on the sequence . . . . . . . . . . . . . . . . . . . . . 41
3.8 Damage photos from the Arkalochori earthquake site trip . . . . . . . 42
3.9 Damage photos from the Arkalochori earthquake site trip . . . . . . . 43
3.10 Map of Crete created with the Stations of Study created on Qgis . . 45
3.11 Photos of rotated gravestones after Arkalochori earthquake sequence . 47
3.12 Photos of rotated headstone and smaller objects . . . . . . . . . . . 47
3.13 Drawings with measurements made for the three gravestones on Figure 3.10 . . . . . . . . . . . . . . . . . . . . . . . . . . . . . . . . 48
3.14 Map of the rotated and measured graves . . . . . . . . . . . . . . . 49

4.1 Matlab program to find lowest and highest usable frequency, wave picking part . . . . . . . . . . . . . . . . . . . . . . . . . . . . . . . . 51
4.2 Matlab program to find lowest and highest usable frequency, Fourier analysis part . . . . . . . . . . . . . . . . . . . . . . . . . . . . . 52
4.3 Matlab program to find lowest and highest usable frequency, Fourier analysis part . . . . . . . . . . . . . . . . . . . . . . . . . . . . . 52
4.4 A response spectrum of a time history from IMOD..HH station, created by Matlab code . . . . . . . . . . . . . . . . . . . . . . . . . . . . 54
4.5 H/V Fourier Profile for GVD.00.HN . . . . . . . . . . . . . . . . . . 55
4.6 H/V PSA Profile for GVD.00.HN . . . . . . . . . . . . . . . . . . . 56
4.7 Single degree of freedom oscillator transfer function at different oscillator frequencies by Bora et al 2016 . . . . . . . . . . . . . . . . . . 57
4.8 GMPE distance parameters by Kaklamanos et al, 2021 . . . . . . . . 58
4.9 Example of a distance scaling graph for several GMPEs and different IMTs . . . . . . . . . . . . . . . . . . . . . . . . . . . . . . . . . . 59
4.10 Example of GMPE residuals with several parameters . . . . . . . . . 60
4.11 Example of distance scaling graph with real events created on Openquake 61
4.12 Example of residuals for station SIVA . . . . . . . . . . . . . . . . . 62

5.1 ARK1..HN H/V and Residuals with Vs30=800 m/s . . . . . . . . . . 64
5.2 H/V - Frequency graph created by ITSAK for the Arkalochori sequence report 2021 . . . . . . . . . . . . . . . . . . . . . . . . . . . . . . 65
5.3 ARK1..HN H/V and Residuals with Vs30=400 m/s . . . . . . . . . . 66
5.4 IACM..HN H/V and Residuals with Vs30=800 m/s . . . . . . . . . . 67
5.5 IACM..HN H/V and Residuals with Vs30=400 m/s . . . . . . . . . . 68
5.6 H/V Fourier Amplification Graph for IACM..HH . . . . . . . . . . . 69

5.7 SIT2..HN H/V and Residuals with Vs30=400 m/s . . . . . . . . . . . 70
5.8 SIVA.00.HN H/V and Residuals with Vs30=400 m/s . . . . . . . . . . 71
5.9 SIVA.00.HN H/V and Residuals with Vs30=800 m/s . . . . . . . . . . 72
5.10 H/V Fourier Amplification Graph for SIVA..HH . . . . . . . . . . . . 72
5.11 H/V and Residuals for IDI..HH . . . . . . . . . . . . . . . . . . . . . 74
5.12 H/V and Residuals for NPS..HH . . . . . . . . . . . . . . . . . . . . . 75
5.13 H/V and Residuals for VAM..HH . . . . . . . . . . . . . . . . . . . . . 76
5.14 H/V and Residuals for VAM..HH . . . . . . . . . . . . . . . . . . . . . 77
5.15 H/V and Residuals for CHAN..HH . . . . . . . . . . . . . . . . . . . . 78
5.16 H/V Fourier and Residual Results for KNDR..HH . . . . . . . . . . . . 79
5.17 H/V Fourier and Residual Results for IMMV..HN . . . . . . . . . . . . 80
5.18 H/V Fourier Amplification Graph for IMMV..HH . . . . . . . . . . . . 81
5.19 H/V Fourier Amplification Graph for IMMV..HH . . . . . . . . . . . . 81
5.20 H/V and Residuals for GVDS..HH . . . . . . . . . . . . . . . . . . . . 83
5.21 H/V and Residuals for CHAN..HH . . . . . . . . . . . . . . . . . . . . 84
5.22 H/V and Residuals for PFKS..HH . . . . . . . . . . . . . . . . . . . . 85
5.23 H/V and Residuals for ZKR..HH . . . . . . . . . . . . . . . . . . . . . 86
5.24 H/V and Residuals for ZKR.00.HN . . . . . . . . . . . . . . . . . . . . 87
5.25 H/V amplification graph for CRE1..HH . . . . . . . . . . . . . . . . . 88
5.26 H/V amplification graph for CRE3..HH . . . . . . . . . . . . . . . . . 89
5.27 H/V Profile for GVD..HH . . . . . . . . . . . . . . . . . . . . . . . . 89
5.28 H/V amplification graph for GVD.00.HN . . . . . . . . . . . . . . . . 90
5.29 H/V and Residuals for IMOD..HH . . . . . . . . . . . . . . . . . . . . 91
5.30 H/V and Residuals for IPPL..HH . . . . . . . . . . . . . . . . . . . . . 91
5.31 H/V and Residuals for KNSS..HH . . . . . . . . . . . . . . . . . . . . 92
5.32 H/V and Residuals for KSTE..HH . . . . . . . . . . . . . . . . . . . . 93
5.33 H/V and Residuals for KSTE..HN . . . . . . . . . . . . . . . . . . . . 93
5.34 Distance Scaling Graphs for for GMPEs using rrup with Mw=5.9 and Vs30=800 m/s and 400 m/s . . . . . . . . . . . . . . . . . . . . . . . . 95
5.35 Distance Scaling Graphs for for GMPEs using rjb with Mw=5.9 and Vs30=800 m/s and 400 m/s . . . . . . . . . . . . . . . . . . . . . . . . 96
5.36 Distance Scaling Graphs for for GMPEs using rrup with Mw=5.1 and Vs30=800 m/s and 400 m/s . . . . . . . . . . . . . . . . . . . . . . . . 98
5.37 Distance Scaling Graphs for for GMPEs using rjb with Mw=5.1 and Vs30=800 m/s and 400 m/s . . . . . . . . . . . . . . . . . . . . . . . . 99
5.38 Distance Scaling Graphs for for GMPEs using rrup with Mw=4.5 and Vs30=800 m/s and 400 m/s . . . . . . . . . . . . . . . . . . . . . . . . 101
5.39 Distance Scaling Graphs for for GMPEs using rjb with Mw=4.5 and Vs30=800 m/s and 400 m/s . . . . . . . . . . . . . . . . . . . . . . . . 102

6.1 PGA Residuals for All Stations . . . . . . . . . . . . . . . . . . . . . 104
6.2 SA (1.0 sec) Residuals for All Stations . . . . . . . . . . . . . . . . . 105
6.3 Map of Crete with Analyzed Stations including Amplification Classification . . . . . . . . . . . . . . . . . . . . . . . . . . . . . . . . . 106

# List of Tables


3.1 Events used from the Arkalochori earthquake sequence for the detailed analysis of stations . . . . . . . . . . . . . . . . . . . . . . . . . . . . . 44
3.2 Total amount of data used and the date range of events per station (Total number of events = 2770) . . . . . . . . . . . . . . . . . . . . . 46

4.1 Lowest and highest usable frequency values calculated for each station 53
4.2 GMPEs used in Distance Scaling and Residual Analyses . . . . . . . . 60

# Abstract

Seismic design codes account for soil conditions and near-surface geology in a very approximate way, namely through the classification of sites into generic classes (based on NSPT or Vs30). However, ground response is more complex. Different soil profiles belonging to the same class may yield different amplification effects (different amplitudes at different frequencies). In addition to that, this effect may not even be the same in all horizontal directions, as is implicitly assumed in typical analyses.

Aim of this thesis to evaluate the ground motion and site effects for the Cretan seismic stations. To do that, empirical methods (e.g. empirical spectral ratios using Fourier and elastic response spectra) will be applied to estimate the near-surface geological effect on seismic ground motion in the frequency domain. Also variety of ground motion prediction equations made for active shallow crustal tectonic regions will be used to do residual analysis and find the difference between the observations and predictions with related site parameters to get a deeper idea on the station by station evaluation on ground motion and site effects. Selected locations of the National Observatory's seismographic/accelerometric network will be used. Overall station performance will be evaluated by using real data from 2021 Arkalochori earthquake sequence from all possible sites.

Results will be the estimation of the variability in response for different soil profiles within the same generic class as per the design code. Also information about the sites will be compared to the results of the analyses and possible discrepancies will be discussed.

# Chapter 1

# INTRODUCTION

It is a well known fact that Greece is one of the most seismically active regions in the world. It has the highest seismic activity in Europe with about 2 % of the whole world's seismic energy release. This is accomplished within an area amounting to only 0.09 % of the total area of the world.

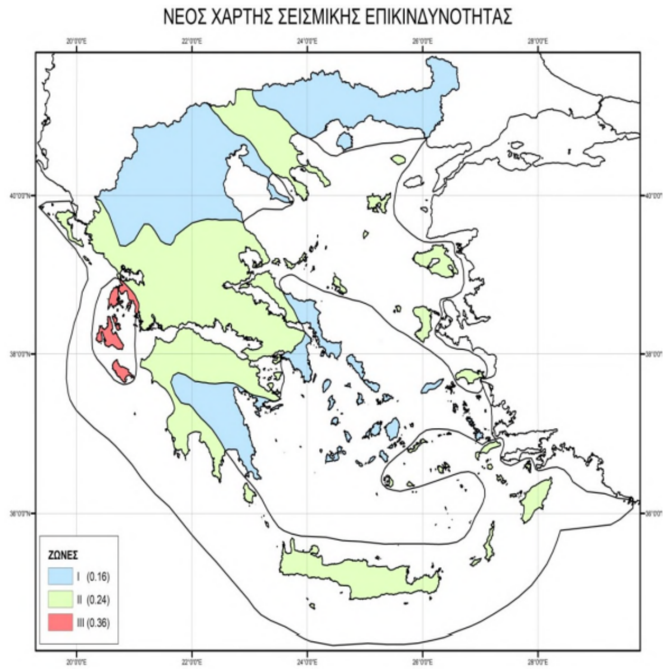


Figure 1.1: Seismic Map of Greece, by Technical Chamber of Greece

Figure 1.1 above and 1.2 below, show the seismic maps of Greece. First map was created by the Technical Chamber of Greece and also used actively in the Greek seismic codes. According to this map, Greece is divided into three seismic hazard:
Zone I(a=0,16 g), II (a=0,24 g), III (a=0,36 g).
These values of peak ground accelerations were found using 10 % probability of exceedance in 50 years.
Second map was created by Danciu et al. (2020) and it is the seismic hazard map of Greece for PGA with 10 % POE in 50 years again. This is the most updated seismic hazard map created for European Seismic Hazard Model 2020. Both maps clearly show us Greece is a seismically very active zone and always have potential for damage causing big earthquakes.

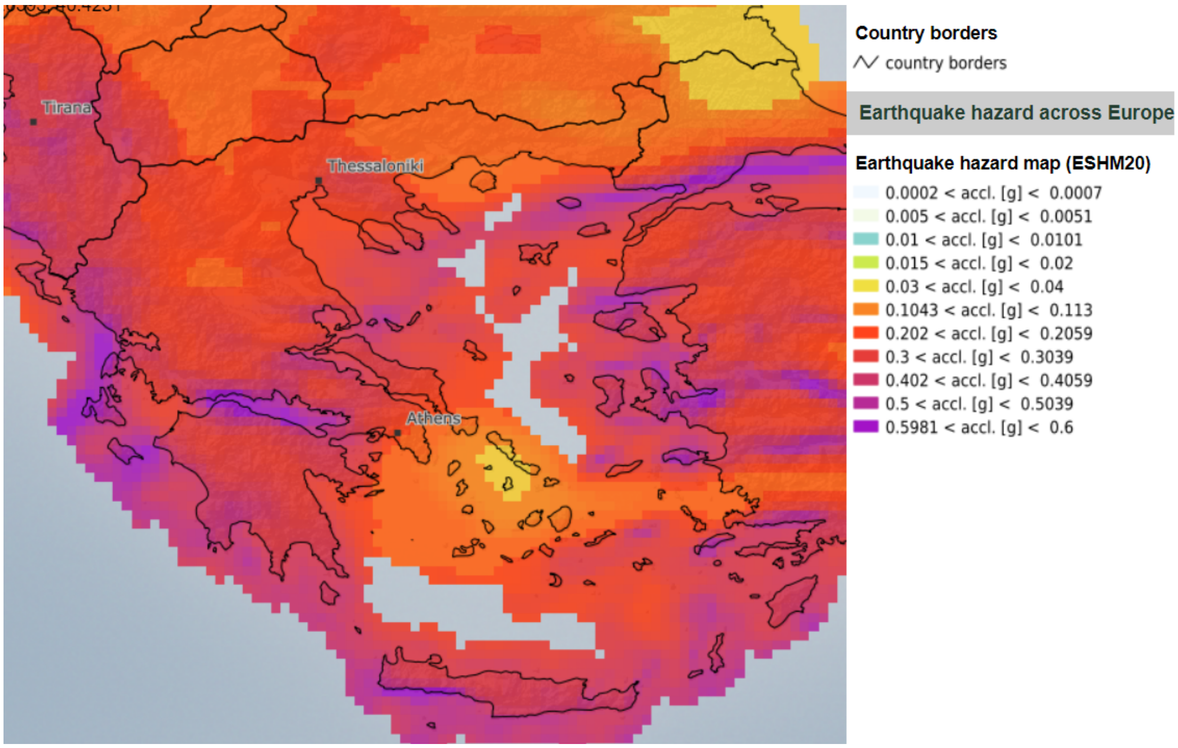


Figure 1.2: Seismic Hazard Map of the region including Greece from ESHM 2020 project with 10 % probability in exceedance in 50 Years by Danciu et al. 2020

As it can also be seen from the above seismic maps, Crete, this dissertation's interest of study, is also an active seismic zone and it was hit by an earthquake sequence recently in September 2021, including a large earthquake of Mw = 5.9 which caused causalties, injuries and severe damage especially at the Arkalochori village at central Crete.
Various seismic hazard analyses (as on the figures) made on the island used for design purposes with estimation of intensity measure types (like PGA, SA(1.0 sec)) by using ground motion prediction equations but most of these GMPEs do not take the site effects into account deeply enough so this causes underestimation of earthquake parameters. Irregular geological structures are known to affect seismic ground response in complex ways and these effects are usually named 'site effects'. Local geology can modify the amplitude,frequency content and duration of seismic motion as it travels from bedrock to the ground surface.

This thesis is to find out the site effects on Crete. A large data set of almost 10000 time histories from 21 stations were used to calculate the amplification in various sites of the island, also the fundamental frequency by using the H/V method. Moreover, by using the 6 sequence earthquakes in 2021, 3 European and 3 American GMPEs on active shallow crustal regions were analysed by using distance scaling graph and residuals and their comparison with the real data was made.

# Chapter 2

# STATE-OF-THE-ART

## 2.1 Strong Ground Motion

There are always vibrations on earth in very small to very big amplitudes and periods. Number of these small vibrations are much higher than the big ones but since the big ones, called strong ground motions, are much more dangerous and have sufficient amplitude and duration to affect the environment and the people, also potentially damage the structures, they get more interest from the engineers. For many years, even though the technology has developed a lot, new and better construction techniques, materials etc. were found there always have been strong ground motions to cause devastation so it is vital to describe strong ground motions in an objective and quantitative way to evaluate effects of earthquakes at a particular site.

Ground motions are the results of the ground shaking caused by the seismic waves starting to transmit from an epicenter through the ground. In general, the release of the accumulated elastic strain energy by the sudden rupture of the fault is the cause of the earthquake shaking. It is composed of 6 components which are 3 translations

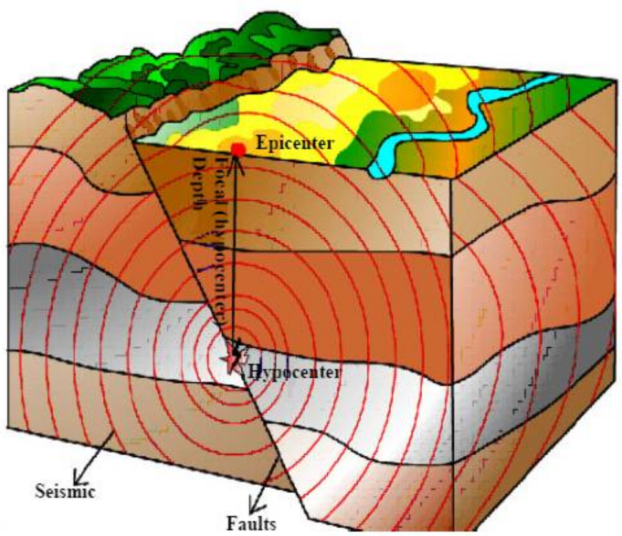


Figure 2.1: Seismic Wave Radiation

and 3 rotations. Rotational components are one torsional component, as it is rotation around the vertical axis, and 2 rocking components, which are rotations around horizontal axes. In general, these rotational components are ignored. So the time histories of ground motions, which are composed or derived of 2 horizontal and one vertical translational components are used in research to characterize the ground motion with characteristics like amplitude, frequency content, duration. From these characteristics, a lot of ground motion parameters like peak ground acceleration, Fourier spectra, predominant period, bracketed duration etc. are derived so that we can characterize the particular ground motions in a deeper manner.

To find out the ground motion parameters, ground motions should be measured accurately in a quantitative way. This is the very start point of hazard assessment and seismic design of structures. The most common used instruments used to measure the ground motions are seismographs and accelerographs. Seismometer, which is a sensor that detects the velocity of the ground, detects and measures earthquakes by translating the seismic waves into electric signals. Those electric signals are displayed as time histories mentioned above. Seismometers are very sensitive devices. The other common instrument, accelerometer, which measures the acceleration of the ground, are way less sensitive than the seismometers but can measure very high ranges of accelerations, like almost $\pm 2$g. In other words, seismometers are to measure small ground motions or distant events but accelerometers measure strong ground motions which have potential to damage on the measured location.

Data received from the seismometers and accelerometers are raw data and might include errors. Most common cause of the errors is the background noise that might be detected by seismometers. To eliminate this possible error, time histories must be processed and this background noise should be eliminated. In this thesis, more than 8000 time histories measured by 20 seismometers and 7 accelerometers in Crete were analyzed. These time histories were processed against the background noise to find the lowest and highest usable frequencies of each recording. These stations, used instruments and technique used to process the data will be mentioned in another chapter.

As mentioned earlier, using the processed data from seismometers and accelerometers; some parameters are found out and strong ground motions are characterized in many ways like in amplitude, frequency content and duration. In a general way, amplitude is defined in dictionaries as the maximum or peak value of a quantity or wave that varies in an oscillatory manner. If we specify it to an earthquake dictionary, it is the size of the wiggles on an earthquake recording, which might be high, medium or low. Considering that what we get from the time histories are time vs. acceleration-velocity or displacement, amplitude parameters are related to those. In the engineering practice, most common used amplitude parameters are peak ground acceleration, peak ground velocity and peak ground displacement. These parameters are equal to the maximum ground acceleration, velocity and displacement at a location during a ground shaking. Since the structures are done with enough resistance to dynamic forces coming from the vertical component of the earthquakes, these parameters are also called as peak horizontal acceleration, velocity or displacement as well. Peak ground acceleration can easily be related to the inertial force on a very short building and it is easy to measure because the response of most instruments is proportional to ground acceleration. Usually, ground motions with higher PGAs are more destructive than the ones with smaller values but since the frequency content and duration also matter, we can not make a certain comment on this. Another useful amplitude parameter is peak ground velocity. Considering that the velocity is less sensitive to high frequencies, it characterizes the intermediate frequency better like bridges or intermediate height buildings. For the lower frequencies-higher periods, peak displacement parameter is used. as due to signal processing errors, it is hard to measure them, it is used less than the other two amplitude parameters of earthquakes.

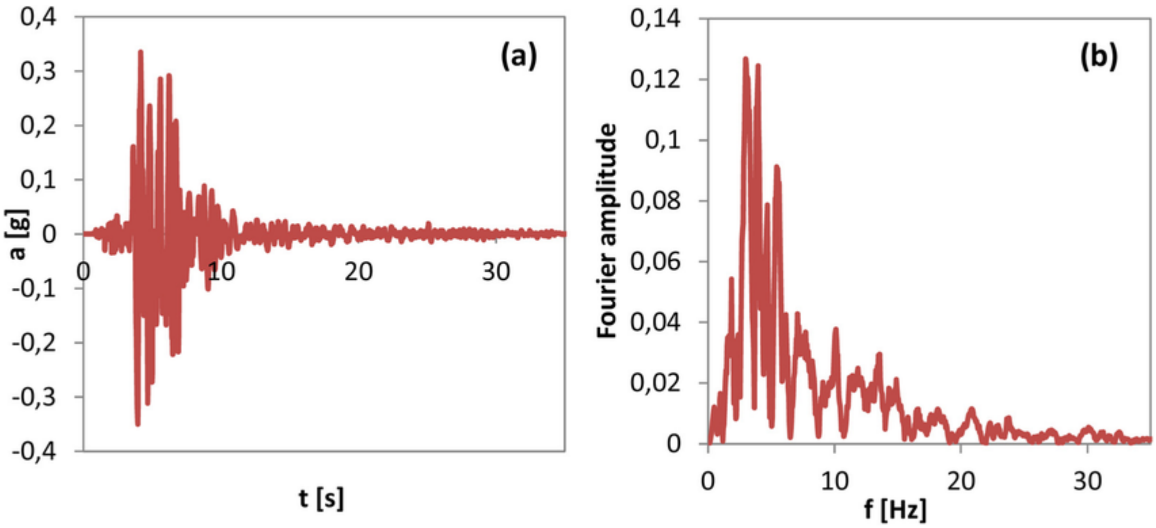


Figure 2.2: Acceleration time history and Fourier Spectrum

Second main type of earthquake parameters are derived from the frequency content of the time histories.These parameters are the most important ones to explain the structural damage caused by earthquakes. In general, frequency describes the number of waves that pass a fixed place in a given amount of time, for earthquakes these waves are seismic waves. To describe frequency content of ground motion, we can say that it shows us how the amplitudes are distributed among different frequencies. Most important ground motion spectra derived from the frequency content are, Fourier, power and response spectra. The Fourier spectrum consists of series of harmonic terms with different amplitude, frequency and phase. It decomposes a signal into its constituent frequency components. It shows how the amplitude of the motion was distributed to frequencies very clearly, however, we can not identify their temporal localization.

If Fourier spectrum is narrow, we can say that the motion has a dominant frequency and a smooth, almost sinusoidal time history. A broad one tells us that the amplitude of the motion is distributed to many frequencies and gives us no clue on dominant frequency. To make the characteristic shape easier to see, Fourier spectra are plotted on logarithmic scales. Another spectra related to frequency content is power spectra. Total intensity of a ground motion in the time domain is described by the area under the time history squared acceleration. After expressing total intensity in the frequency domain, power spectral density is calculated. Power spectrum has a close relationship with Fourier spectrum. Like in Fourier spectrum, we can understand in which frequencies the variations are strong and week.Third and the most widely used frequency content ground motion spectra is the response spectra. Response spectra are functions frequencies or periods showing the peak response of a simple harmonic oscillator that is subjected to a transient event. It is not a direct representation of the frequency content of the motion but it shows the response of the structure to the various frequencies. Or we can also define it as the responses of various structures

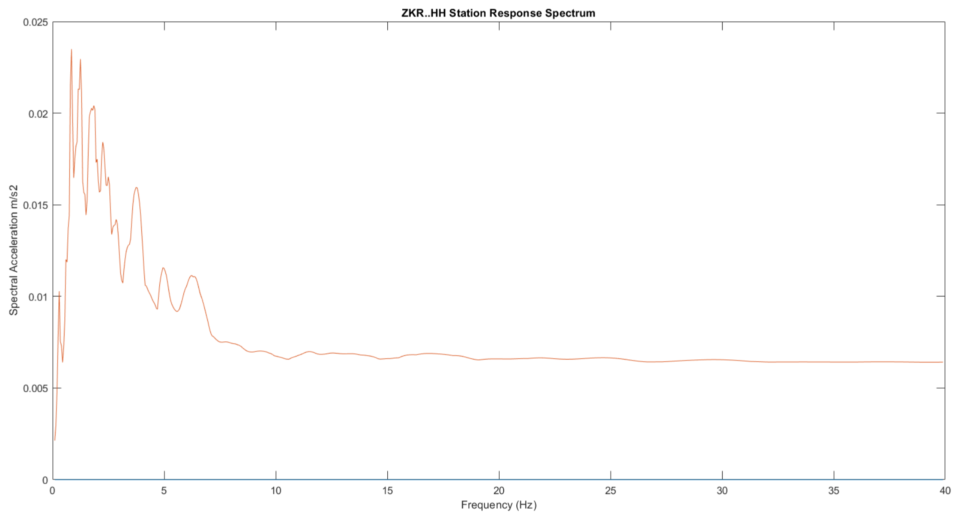


Figure 2.3: Response spectrum example

with different natural frequencies to a given earthquake.

Response spectra reflect the characteristics of the ground motion indirectly since it is only for the single degree of freedom structures.Most widely used one is acceleration to period but velocity-period or displacement-period response spectra are also used.

As the main spectra of the ground motions are described, next is to explain the main parameters found out using these spectra. There are various parameters extracted from these spectra like predominant period, bandwidth, shape factor and Kanai-Tajimi parameters. Predominant period of the earthquake is the period of vibration corresponding to the maximum value of Fourier amplitude. This parameter does not give info about the dispersion of the spectral amplitudes about the predominant period. Bandwidth, another parameter coming from Fourier, is the range of frequency over which some level of Fourier amplitude is exceeded. Central frequency is a measure of the frequency and shows us where the power spectral density is concentrated. Shape factor parameter is found from the power spectra and indicates the dispersion of the power spectral density function about the central frequency.

Third main type of earthquake parameters is the duration. Earthquake duration is the total time of ground shaking from the arrival of seismic waves until the return to ambient conditions. Duration of strong ground motion might effect the amount of damage on structures caused by the earthquakes since i.e. stiffness, strength degradation of the structures are sensitive to loading cycles. When there is low duration, even if the earthquake amplitude is high, there might not be any damage but in high duration earthquakes, as mentioned above, structures can be damaged easily by moderate amplitude earthquakes due to the number of loading cycles. Duration of the earthquakes depend on the way of the seismic waves from the rupture through the ground. If there are a lot of reflections and resonance like in a sedimentary valley, duration will be higher.Also as area and length of the fault rupture increases, duration increases. Bracketed duration and cumulative e energy duration are important parameters characterising earthquakes based on their durations. Bracketed duration is the time between the first and the last exceedance of a threshold acceleration. This threshold value is 0.05g in general. The cumulative energy duration is defined as the time interval between the points at which 5% and 95 % of the total intensity was recorded.

There are also some other important strong ground motion parameters like total intensity, average intensity, Arias intensity.

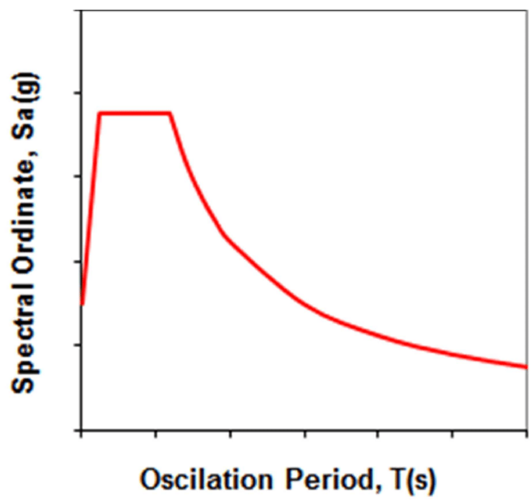


Figure 2.4: Response design spectrum example

As the strong ground motion parameters are the main characteristics and level of shaking is describing by using these parameters, good estimation of them are vital to design earthquake-resistant structures. Predictive equations to express ground motion parameters as a function of distance, magnitude and some other variables are called attenuation relationships or prediction equations. It will be the next topic of this thesis.

## 2.2 Source, Path and Site Effects

Seismic waves can be characterized by its source, path it follows and the local site conditions on where it reaches on the civil engineering structures. All these three are needed to be taken into account for the estimation of ground motion parameters discussed.

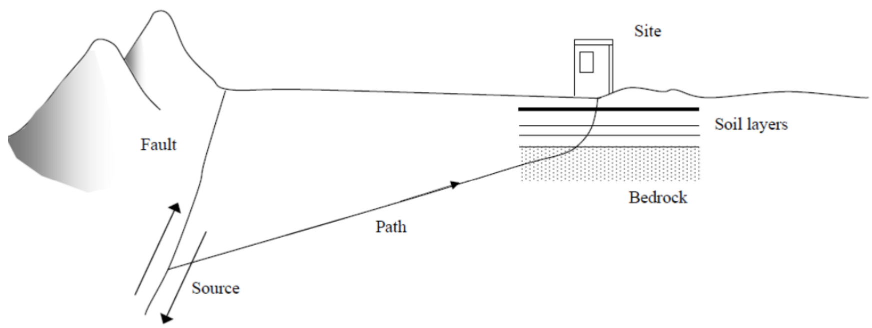


Figure 2.5: Factors affecting the ground motion

The first one these three, is the rupture of the fault and release of the energy from the source mechanism and it is related to the rupture mechanism, rupture size and radiation pattern. It affects the magnitude of the earthquake and also directivity. Earthquake stress waves propagation is more intense and stronger in the direction of the fault than the other directions. Distribution of ground motion parameters and shaking intensity is directly affected by this phenomenon. Waves propagate away from the rupture with different intensity along different directions and this is called directivity. It occurs since fault ruptures are moving sources of waves. In the direction of rupture propagation, larger amplification in shorter duration is observed, on the contrary, longer total duration and smaller ground motion amplification is observed in the opposite direction.

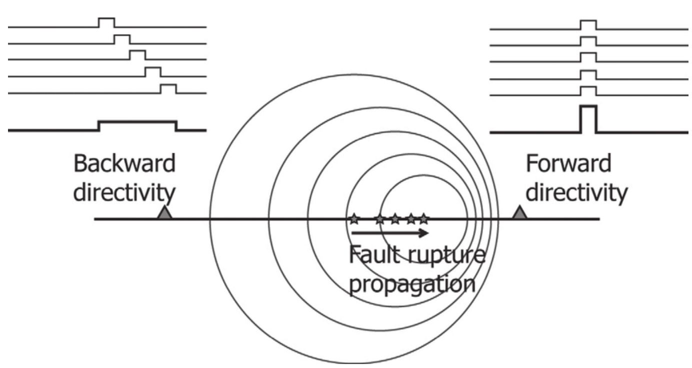


Figure 2.6: Forward and backward directivity effect

Second one, path is the path followed by the seismic waves from the source through the site. When the waves get distant from the source, there is attenuation of energy due to geometric spreading and absorption. This is also related to the focal depth and the physical composition of the path by the ground motion prediction equations.

The third one, site effects are in general referred to the amplification of the seismic waves due to some geological conditions, surface and subsurface topography, discontinuities, heterogeneity. This is a major factor influencing the extent of damage on structures and should be considered seriously before any kind of structural design. Since the one of the aims of this paper is to measure the site effects in Crete, this subject will be explained in detailed over the next subsection.

## 2.3 Wave Theory

In general, waves are representations for propagation of the energy. For the seismic waves, energy propagates through displacements away from the seismic source with a pattern. On a seismogram, the wiggles tell us that the ground is vibrated by the seismic waves. These seismic waves are propagating vibrations and they carry energy from the shaking source through all directions. This concept is similar to the spreading circular waves created at a pond after we throw a stone on it, but of course seismic waves are way more complicated than this process.

There are many kinds of seismic waves but the two main types are the body waves and the surface waves. Among these, body waves can travel through the interior layers of the Earth and surface waves can only travel through the Earth's surface. Body waves have higher frequency than the surface waves.

First type of body waves are called P-waves. These waves are also known as primary waves and pressure (compressional) or longitudinal waves and they are the fastest to travel through the Earth, at speeds between 4-8 km/sec in the Earth's crust. Speed that the body waves travel changes due to the stiffness of the material they travel through and since geologic materials are stiffer in compression than shear, P-waves are faster than shearing S-waves. Since P-waves are the fastest ones, seismograms record the P-waves first during an earthquake. The P wave can travel through solids, gases and fluids, like water or the the inner core of the the earth. It moves as the sound waves pushing and pulling the air, by pushing and pulling the rock so they are also known as compressional waves. When the particles are subjected to P-waves, they travel in the same direction and it is also the direction that the energy is traveling so called wave propagation direction. Second type of body waves are called as S-waves. They are also known as secondary, shear or transverse waves. The reason they are called as secondary waves is that they are the second waves to arrive after the P-waves at an earthquake as they travel slower than the P-waves (2.5-4 km/sec).And since they can travel in 'transverse' direction, through a material and cause 'shear' deformations, they are called with these names as well. Unlike the P-waves, S-waves can not travel through fluids since they have no shearing stiffness (and also gases) and this was one of the reasons seismologists concluded that the outer core of the earth is liquid. As shown in the figure, S-waves move the solid particles up ad down or side to side and always travel perpendicular to the wave propagation direction.

Second type of seismic waves are the surface waves. The reason they are called as 'surface' waves is that they are trapped to the Earth's surface and they cannot travel through Earth's body. They are generated stronger when the source of the earthquake is closer to the Earth's surface so shallow earthquakes creates stronger surface waves than the deeper ones and if the earthquake is very deep, it generally does not create any surface wave. Surface waves travel slower than the body waves but since they might have much larger amplitudes, they might cause more destruction than the body waves. Two kinds of surface waves are Love waves and Rayleigh waves. Love waves produce entirely horizontal motion and causes horizontal shearing on the ground. Rayleigh waves create a rolling, up and down, forward and backward ground motion and most of the shaking felt on an earthquake are caused by Rayleigh waves, since they can be larger than the any other. Love waves usually travel slightly faster than the Rayleigh waves. Both of these surface waves are dispersive and they travel in different speed with a different frequency component. So these waves change shape as they travel.

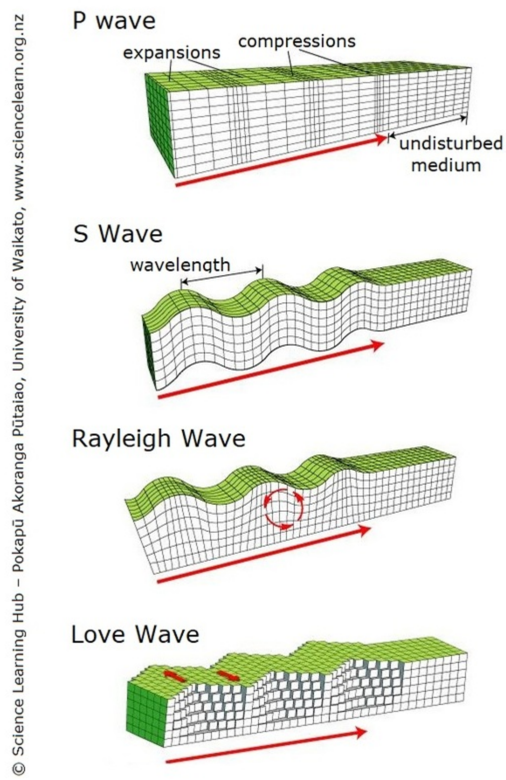


Figure 2.7: Deformation produced by body and surface waves

Amplitude of seismic waves get smaller as the distance from the source increases. This has two main reasons. First one is geometric spreading. As the area that the wave energy covers becomes larger and wave intensity decreases. As the energy drops with x-2, amplitude drops with x-1. Second one is caused by the absorption of wave energy as wave keeps traveling, caused by the frictional heating occurred since the earth materials since the earth materials are not perfectly elastic.

Another important point in wave propagation is the reflection and refraction of seismic waves as they travel through the Earth with the change of bulk modulus, rigidity modulus and density.When a wave hits an interface between two materials with differing physical properties, some of the wave energy will be reflected and the rest will be transmitted through or along the interface. Well known Snells's Law describes the relationship between the angle of incidence of a seismic wave passing through a boundary between two different (slow and faster) media.

## 2.4 Local Site Effects

With a simple definition,local site effects can be defined as the influence of local geologic and soil conditions on the intensity of ground shaking and earthquake damage. In other words, it is the amplification of seismic waves due to some geological conditions. Those effects play a vital role to characterize the ground motions since since they amplify or deamplify the seismic waves just before reaching the structures. These amplification effects all the important characteristics of ground motions like frequency content, amplitude and duration. Local site effects are a combination of ground response, basin effects and topographic effects, so it can be grouped into 3 that way as well.

Effects on the local ground response can be grouped into two as direct sediment effects soil non-linearity effects. Soil non-linearity will be discussed separately in the next subsection. Direct effects happen due to impedance between stiff soil and the soft soil and cause ground motion amplification. These effects were started to be studied more comprehensively after the 1985 Mexico City earthquake (8.0 Mw). In this earthquake areas close to the epicenter got only moderate damage but 350 km away from the epicenter, there was extensive damage.

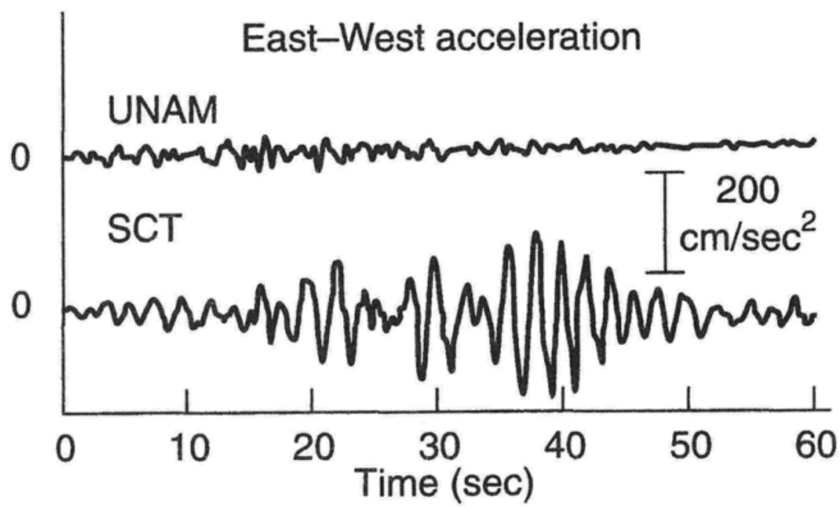


Figure 2.8: Acceleration time history of SCT and UNAM stations in 1985 Mexico Earthquake

There were several stations to record the earthquake. One of those stations, UNAM, was located in zone which was mostly rock and the other one SCT was located around a lake zone, which was composed of soft soils. Peak ground acceleration around SCT station, where the extensive damage occured, peak ground acceleration was around 0.15-0.20 g, but around UNAM station, it was only around 0.003-0.04g. In the foothill zone, where the SCT station is located, there was no to negligible damage but in the lake zone, where the UNAM station was located, most of the 5 to 20 storey buildings unfortunately collapsed. At the lake zone, there was only slight damage to the 1-5 storey buildings and this difference was caused by the 2 second predominant period.Since higher buildings' have higher fundamental frequency (storey/10 from the basic thumb rule might give an idea), they got higher earthquake response in the lake zone. Another recent example of this, is the 1989 Loma Prieta Earthquake in San Francisco. This earthquake also caused extensive damage in certain and relatively little damage in others due to local site conditions. Two recordings from two different stations with the same distance to the source in this earthquake were also giving a lot of clues of local site effects. Recording from Yerba Bueno island with a rock profile had 0.06 g peak ground acceleration and this value was 0.16 g for the recording from Treasure Island which had man-made fill underlain by San Francisco Bay mud.

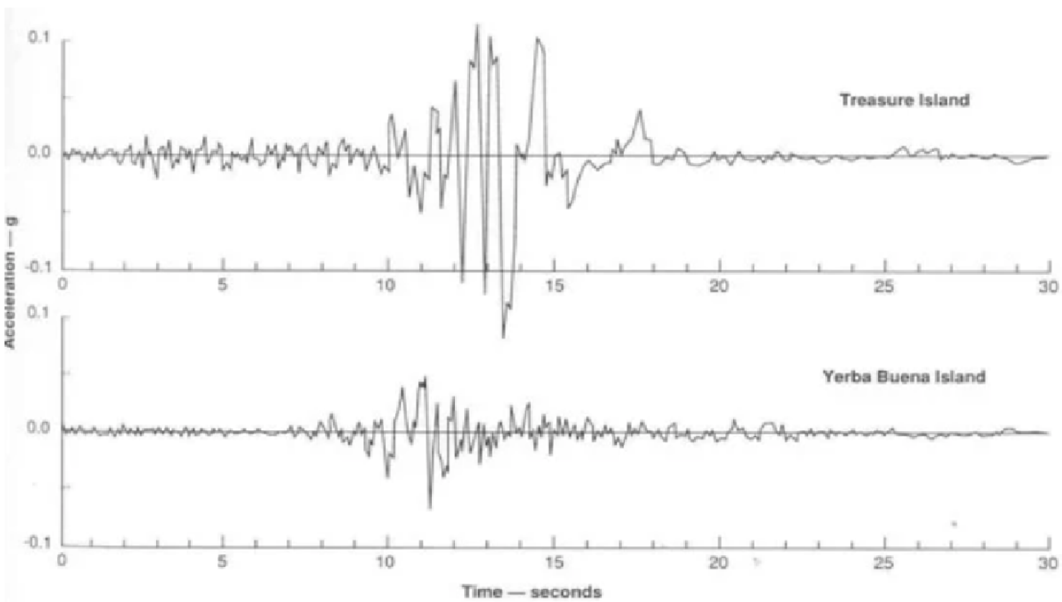


Figure 2.9: Acceleration time history of Yerba and Treasure Island Stations in 1985 Mexico Earthquake

Although the predominant period of both stations were around 0.6 sec, peak spectral acceleration at this period was around 0.7-0.75g for Surface Island and 0.20-0.22 g for Yerba Bueno Island and this was clearly showing how site effects can change it!

Basin (geometry) effects are the trapped earthquake waves in soft sedimentary deposits underlain by basement rock. This effect significantly changes the duration, amplitude and frequency content of the wave. Since a lot of large cities are around alluvial valleys, basin effects have become important in design.

As shown in Figure 2.10, when the soil layer is flat, seismic waves may resonate but can not be trapped inside the layer but in the basin case, they are trapped inside the basin if the incidence angle is larger than the critical one and this may produce stronger shaking and longer duration.

Another local site effect that creates amplification on the ground motion is topog-

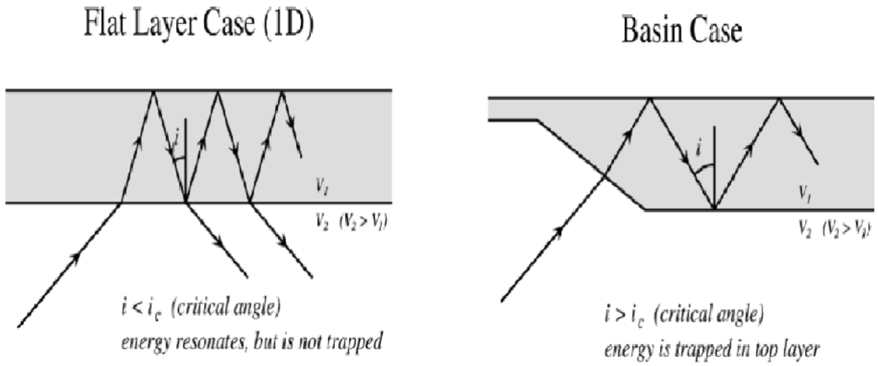


Figure 2.10: Propagation of seismic wave on one layer soil and basin case (Vittoz et al. 2001)

raphy. Observations on destructive earthquakes show that damage intensity is higher on tops of hills, ridges and canyons than the lower places or flat areas.

Methods to physically model the site effects in 1D is the main interest of this thesis and methodology will be explained in the next chapter. In this section, adding to 1D effects, 2D and 3D effects, non-linearity effects and topography effects were also explained. One should consider all of them together for earthquake design of structures. To sum up, there are various types of local site effects and each one of them is vital and underpredicting any of them might cause fatal errors in design.

## 2.5 Soil Non-linearity

Stress strain behavior of soil is highly non-linear and this has a great importance in selecting the design parameters. As mentioned in the wave propagation part, amplification of the seismic waves comes from the strong contrast between the difference in physical properties of the rock and sediment layers. Evaluation of this amplification is done by assuming the seismic response of soil as linear under low strains. But when the stress-strain levels get larger, results of many laboratory tests show that soil has a highly nonlinear character and can not be represented with linear relations.

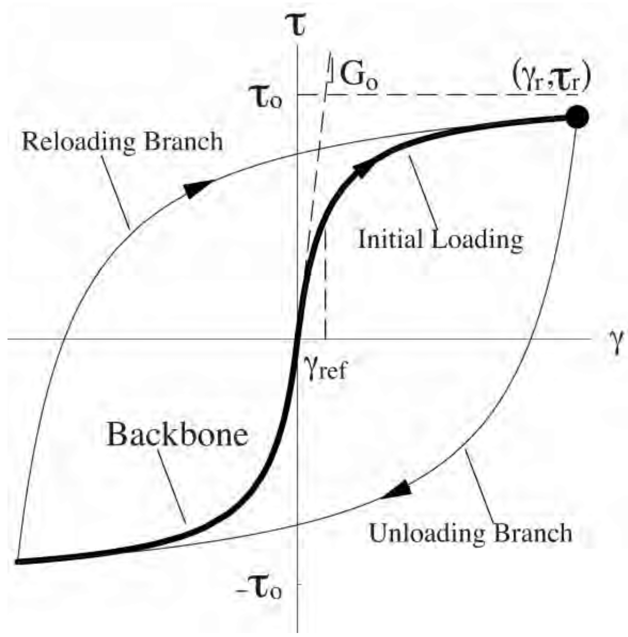


Figure 2.11: Stress-strain relationship of soil in cyclic shear deformation

Non-linearity of soil is more effective in site response for strong ground motions than the site response in weak ground motions, which is combined by site configuration and various incident wave field. Especially for a sedimentary site, if we want to predict the strong motions accurately, non-linear soil behaviour need to be taken into account carefully. As mentioned earlier, non-linear soil response is described by the stress-strain curves. By non-linearity, stiffness degrades and energy dissipation increases. So the stress-strain curves are approximate with the shear modulus decrease (G/Gmax) and increase of damping curves with shear strain.

To sum up, oil non-linearity is characterized by reduction of shear rigidity and, as a result, by the reduction of shear wave velocity, and increase of damping factor. Translating this in to the site effects, non-linearity causes extension on predominant period and decrease in amplification factors. Taking all of the these into account we can conclude that it is vital to measure it especially to predict the strong ground motions with the local site effects.

## 2.6 Estimation of Ground Motion Parameters-Attenuation Relationships

The attenuation of earthquake is known as the gradual loss of strength of shaking as the distance from the earthquake source increases. This can also be expressed as the energy loss of seismic waves during their travel through a path. For assessment and design of structures, it is crucial to estimate this, and this estimation is done by attenuation relationships (also called as ground motion prediction equations), which are describing the motion with magnitude, source distance and site condition and even style of faulting. In different parts of the world, different magnitude measures are used but the most universal one is the moment magnitude as it is used almost everywhere. An example of results from GMPE Abrahamson et al 2014 showing the results for SA(1.0 sec) in g per different moment magnitudes with rupture distance 100 km is in figure 2.12. This is also called magnitude scaling.

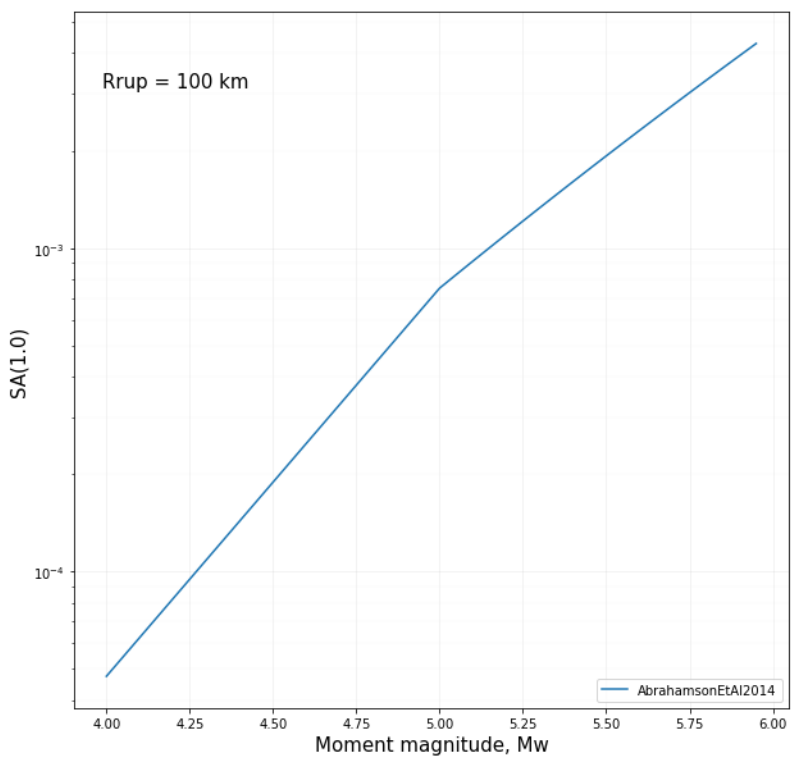


Figure 2.12: SA(1.0 sec) results in g per different Mw values with rupture distance 100 km from GMPE Abrahamson et al 2014, created by Openquake software

As the ruptures may extend for even hundreds of kilometers, distance between the source and the site is measured in many different ways. Epicentral distance was the most used one, but nowadays, Joyner-Boore distance, rupture distance and hypocentral distance are also used a lot. Shortest distance from the source to the site is defined as Joyner-Boore distance and it is compatible with almost all of the GMPEs. Figure 2.13 shows PGA results in per different Joyner-Boore distances for Mw=6.3 by GMPE Kotha et al, 2020. This is also called distance scaling.

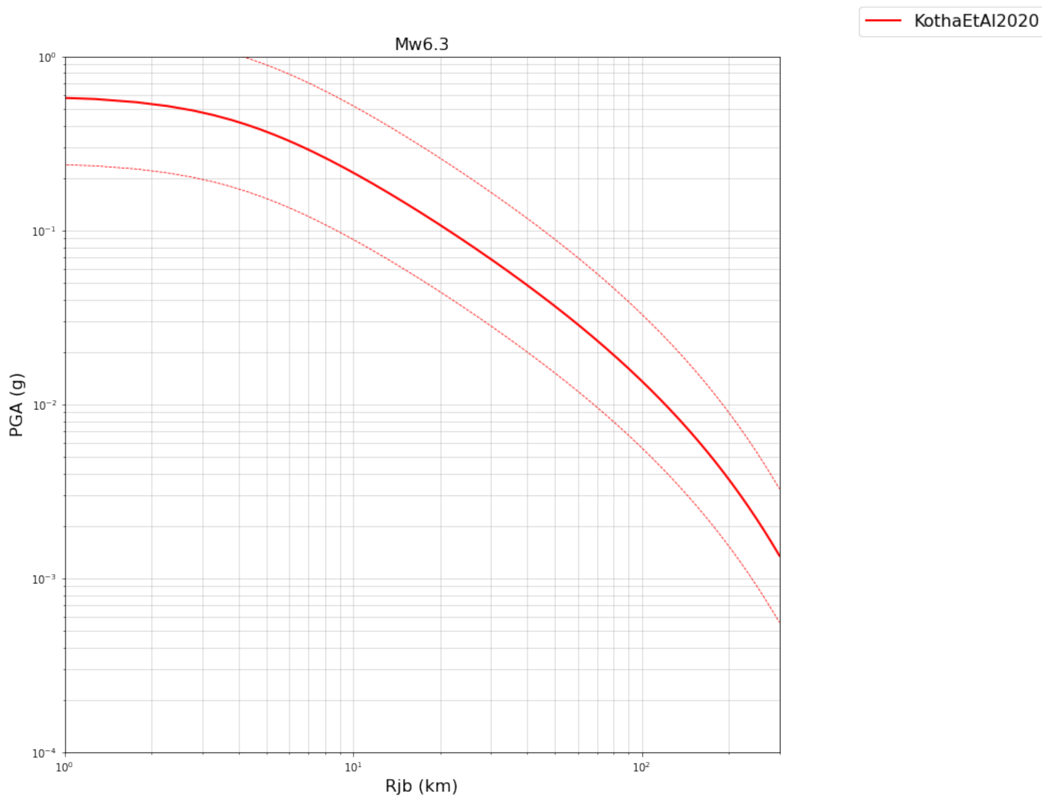


Figure 2.13: PGA results in per different rjb values with Mw=6.3 km from GMPE n Kotha et al 2020, by Openquake software

Parameters of ground motion might be affected by source characteristics. Fault types which might be strike-slip, normal or reverse faulting etc. are also taken into account in most of the attenuation relationships. Site characteristics are also considered on GMPEs, mostly with average shear wave velocity in 30 meters depth but this might not be sufficient to estimate site effects in most of them.

These relations calculate seismic ground motion intensity by statistical regression analysis of many strong motion records. There are relationships estimating every ground motion parameters but the relations based on the peak ground acceleration, velocity, displacement and spectral acceleration are the ones which are generally used in structural engineering.

With the development of technology, recording the strong ground motions became easier and database has became larger. This database all over the world are used by engineers and scientists to create regional ground motion prediction equations. Another type of data used to generate attenuation relationships is synthetic ground motions that account for source, path and site effects. These two methods may overlap.

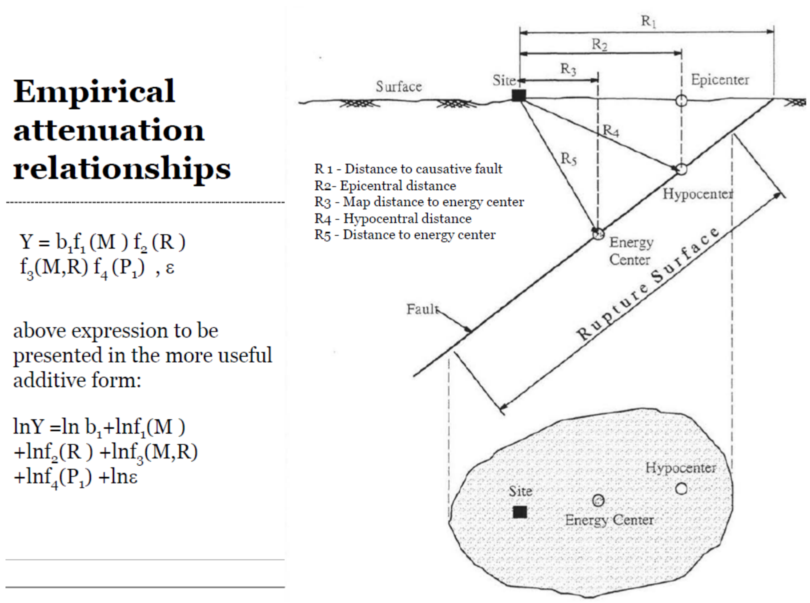


Figure 2.14: Empirical Attenuation relationship function

Choosing the correct GMPE to use among all these GMPEs, we can check different options like the tectonic regime it was done for, parameter we are interested in and the region we want to use the GMPE. Usually the ground motion source, wave propagation and site effects (which are not sufficient in general) are modelled in the attenuation relationships and Figure 2.5 shows an example for the general functional form of it.

As mentioned earlier, right now, there are hundreds of ground motion prediction equations available for all over the world. An example of this is the PEER initiation Next Generation Attenuation. NGA has developed ground motion models for shallow crustal earthquakes that cover the sources in California for the average horizontal motion. Well known attenuation relationships of Abrahamson and Silva, Boore and Atkinson, Chiou and Youngs, Campbell and Bozorgnia, and Idriss were generated as a part of this project and used all over the world in the same tectonic type regions. In this thesis 3 GMPEs from this project (Abrahamson et. Al 2014, Chiou and Youngs 2014, Campbell and Bozorgnia 2014) were used to generate distance scaling graphs of known events in Crete. Also from the European based institutions, Bindi et Al 2014, Akkar et Al 2014 and Kotha et Al 2014 were used. These ground motion prediction equations, scaling graphs and their features will be explained later in another chapter.

## 2.7 Design Codes

To be able to design the structures resistant to various earthquakes, or estimating the safety of of the existing structures against earthquakes, their response to the ground motions should be analyzed. To achieve a satisfactory performance, we need to know the possible level of shaking, which is design level of shaking described by design ground motion. Design ground motions are mostly specific with the parameters of ground motion like peak ground acceleration, peak ground velocity, response spectrum ordinates, duration and predominant period.

In the history, many terms have been used to describe level of severity of design earthquakes but the most common used term was MCE (maximum credible earthquake). It is the largest earthquake than can reasonably expected. Some other terms used in the history to describe the worst case level design earthquakes are Safe Shutdown Earthquake (for designing nuclear plants), Maximum Design Earthquake, Contingency Level Earthquake, Safety Level Earthquake, Credible Design Earthquake and Contingency Design Earthquake. These were all to design the structures to the most catastrophic scenario. Design earthquakes are specified without taking the probability of occurence into account so after the probabilistic seismic hazard analysis techniques were developed, its use has decreased.

Another term that was used in the design of earthquake resistant structures was the design spectra. Design ground motions were represented by the design spectra and this was not the same with the real response spectra of a related structure. Response spectras are found out by using the earthquakes, highly irregular in shape to reflect the specific frequency contents and phasing. But the design spectras are determined by smoothing averaging or enveloping of response spectras of a lot of earthquakes. By using the smoothing of response spectra as design spectra, uncertainty in the soil and structure properties are taken care of.

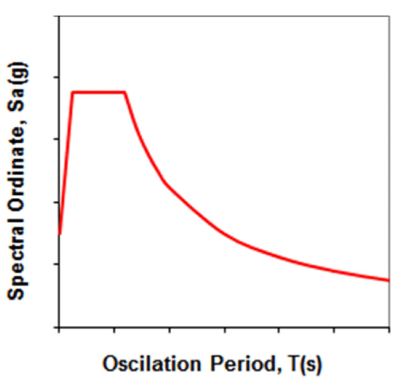


Figure 2.15: Design spectra

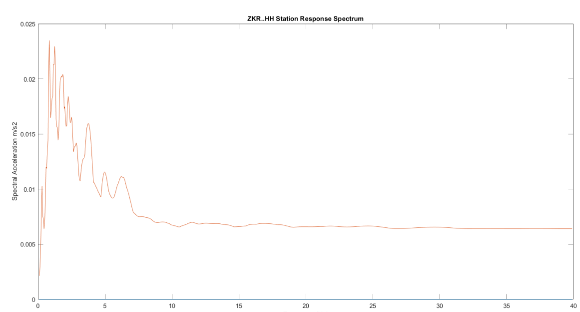


Figure 2.16: Response Spectra

Design ground motion characteristics depend on the location of the site relative to the seismic source, seismicity levels of around sources, nature of the rupture at the sources, path and local site effects and also the importance of the facility that it will be used. In general, there are two ways to design these ground motions, first one to do site-specific development and the second one is code based development.

Site-specific design tries to reflect the detailed effect of the site into the designed ground motion. For a succesful site-specific design, both of seismic hazard analysis and ground response analysis are required. Seismic hazard analysis can be done in both deterministic and probabilistic ways. Most common used method for seismic hazard analysis is probabilistic seismic hazard analysis, also known as PSHA. PSHA makes a quantitative estimation of probability of exceeding of various ground motion levels at a particular site or a map of sites, considering all reasonable earthquake scenarios. Using a risk or return factor is required in PSHA. For instance, in general, 10 % probability of exceedance in 50 years is used for design in most of the world. This method involves 3 steps. First one is to specify seismic hazard source models, second one is to specify the ground motion prediction equations to use for the region and the third one is the probabilistic calculation.

As a second alternative, design ground motions can be developed by using the code based provisions. In most of the countries, it is mandatory to consider earthquakes in the design of structure so country, region even continent based provisions were developed. In Europe, for this purpose, Eurocode 8 : Design of structures for earthquake resistance was developed and it applies to all civil engineering structures in the seismic zones. Aim of Eurocode was mentioned as protecting the human lives, limiting the damage and keeping the structures important for civil protection operational. In Eurocode, design seismic action is defined as the one for which the no collapse requirement is verified. Return periods for seismic actions are nationally determined parameters but recommended to be used as 475 years( 10 % in 50 years). Reference seismic actions are described with national zonation maps in terms of the reference peak ground acceleration on rock and by multiplying this value to an importance factor design ground acceleration on rock is calculated. Also the reference seismic action is defined with the elastic response spectrum for 5 % damping. This is the very starting point of designing the structures resistant to earthquakes by Eurocode but also one of the most vital parts.

Unfortunately, Eurocode has only one parameter to affect the site classify the site amplification, which is Vs30, the time-averaged shear-wave velocity to a depth of 30 meters.

| Subsoil class | Description of stratigraphic profile | Parameters | | |
|---|---|---|---|---|
| | | $V_{s,30}$ (m/s) | $N_{SPT}$ (bl/30 cm) | $c_u$ (kPa) |
| A | Rock or other rock-like geological formation, including at most 5 m of weaker material at the surface | >800 | – | – |
| B | Deposits of very dense sand, gravel, or very stiff clay, at least several tens of m in thickness, characterised by a gradual increase of mechanical properties with depth | 360–800 | >50 | >250 |
| C | Deep deposits of dense or medium-dense sand, gravel or stiff clay with thickness from several tens to many hundreds of m | 180–360 | 15–15 | 70–250 |
| D | Deposits of loose-to-medium cohesionless soil (with or without some soft cohesive layers), or of predominantly soft-to-firm cohesive soil | <180 | <15 | <70 |
| E | A soil profile consisting of a surface alluvium layer with $V_{s,30}$ values of class C or D and thickness varying between about 5 and 20 m, underlain by stiffer material with $V_{s,30}$ > 800m/s | | | |
| $S_1$ | Deposits consisting—or containing a layer at least 10 m thick of soft clays/silts with high plasticity index (PI > 40) and high water content | <100 (indicative) | – | 10–20 |
| $S_2$ | Deposits of liquefiable soils, of sensitive clays, or any other soil profile not included in classes A–E or $S_1$ | | | |

Figure 2.17: Eurocode 8-Site Clasification

As on the figure above, sites are categorized according to just a few parameters (most common used vs30). After categorizing the site, according to that, an S factor due to the earthquake magnitude is found out and that factor is used in the elastic design spectra calculations.

Representing the direct site effects on the site just with this factor is mostly not found sufficient so a better representation is expected for the next version of the Eurocode.

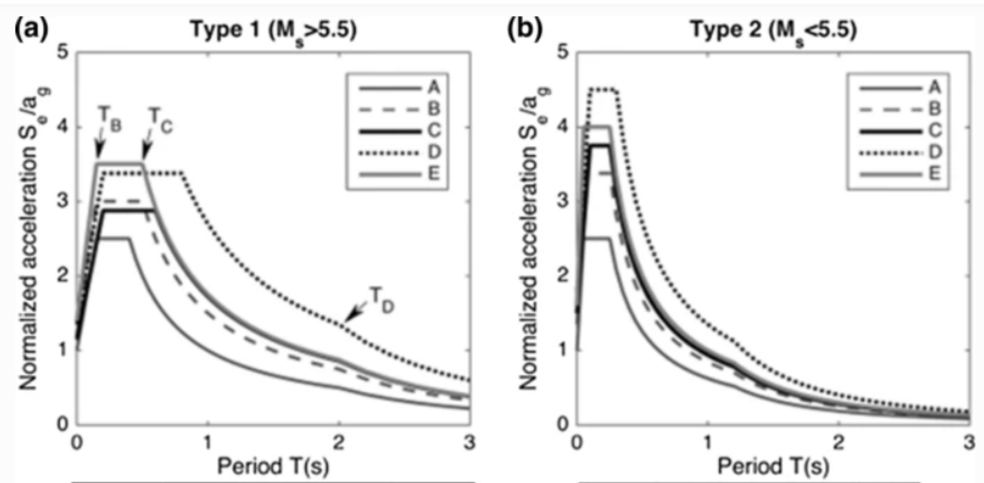


| Ground type | $S$ | $T_B$ (s) | $T_C$ (s) | $T_D$ (s) |
|---|---|---|---|---|
| A | 1.0 | 0.15 | 0.4 | 2.0 |
| B | 1.2 | 0.15 | 0.5 | 2.0 |
| C | 1.15 | 0.20 | 0.6 | 2.0 |
| D | 1.35 | 0.20 | 0.8 | 2.0 |
| E | 1.4 | 0.15 | 0.5 | 2.0 |

| Ground type | $S$ | $T_B$ (s) | $T_C$ (s) | $T_D$ (s) |
|---|---|---|---|---|
| A | 1.0 | 0.05 | 0.25 | 1.2 |
| B | 1.35 | 0.05 | 0.25 | 1.2 |
| C | 1.5 | 0.10 | 0.25 | 1.2 |
| D | 1.8 | 0.10 | 0.30 | 1.2 |
| E | 1.6 | 0.05 | 0.25 | 1.2 |

Figure 2.18: Normalized elastic design spectra for Type 1 (a) and Type 2 (b) seismicity and for different ground types, according to EC8-1

# Chapter 3

# AREA AND THE DATA SET, STATIONS AND TECHNIQUES USED FOR THE STUDY

## 3.1 General Information about Crete and Arkalochori

Crete is the largest island of Greece (among 227 inhabited) and the fifth largest island in all Mediterranian. It is around 260 km in the east-west axis and between 12 to 60 km in width. Administrative centre of Crete is Irákleio and it is on the north coast. Crete has 8336 square km area and approximately 650000 population.

Figure 3.1: Agios Nikolaos, Crete

The island was inhabited by the humans almost 130000 years ago during the Paleolithic age and it is known to host Europe's first advanced civilization, the Minoans, from 2700 to 1420 BC. Knossos, now home to one of the most visited archaeological sites in Greece, is considered to be the oldest city in Europe. After Minoans, Crete was ruled by Mycenaean civilization, Rome, Byzantine Empire, Andalusian Arabs, the Venetian Republic and the Ottoman Empire. In 1898 Crete achieved independence from Ottoman empire and became formal Cretan State and in December 1913, it became part of Greece.

Crete is known to have a unique poetry form called mantinada. These are mostly improvised, short rhyming poems and mostly performed with the Cretan music instrument lyra. Famous and nine times Nobel prize nominated writer Nikos Kazantzakis was born in Crete. The island is the birthplace of Eleftherios Venizelos, leader of Greek national liberation movement, renaissance painter El Greco and famous opera singer Nana Mouskori as well. Also according to Greek mythology, Zeus was born on Crete.

Crete is mostly a mountainous island and characterized by the high mountain range crossing from west to east. The highest point of the island is at Idi mountain with 2456 metres in elevation. Through the west, Lefka mountain reaches 2452 metres and to the east the Dikti Mountains reach to 2148 metres in elevation. Those mountains

Figure 3.2: Famous Minoan Palace in Knossos, Crete

are rising above the high upland plains of Nida, Omalos and also by several gorges like the famous Samaria Gorge. Northern coast is gradually slopped and it has many natural harbours and coastal places, where the major places like Chania, Rethymno and Irakleio are located. Along the south-central part, the Mesara Plain extends and it is the major expanse of Crete's flatlands with 29 km. Crete also has six small rivers, springs, one natural lake called Kournas and also many artificial lakes.

Figure 3.3: Arkalochori view from South Wikipedia

Arkalochori, a town in Crete where the earthquake sequence that is subject to this thesis occurred, is located 33km south of Heraklion city, near the center of Heraklion

Prefecture, at an altitude of 400 and it has around 11000 population of the municipal unit. It lies on the western edge of the Minoa Pediada plain. The municipal unit has an area of 237.589 squared km.

Arkalochori is a small town and people living there are mostly engaged in agriculture, commerce and arts. The main land products in the area are olive oil and olives, raisins, grapes and few cereals. There is a well known bazaar held every Saturday and it attracts the people from Iraklion and Lassithi.The town is relatively new so there is almost no traditional architecture. Most of the houses are made of masonry. There is an archaeological site of a Minoan sacred cave and it is a well known touristic attraction.

## 3.2 Seismicity in Crete

Crete is known to have high level shallow and intermediate-depth seismicity. The reason of this is that, it is in central part of the Hellenic Arch and Trench system where lithospheric plates of Africa and Eurasia converge and former bends and subducts under the the later. Most of the events have depth less than 25-30 kilometers. As shown in Fig 3.4 and mentioned by Caputo et Al., close to the Hellenic trench south of Crete, the available fault plane solutions indicate a NNE–SSW direction of compression, but within the island and its surroundings E(SE)–W(NW) and roughly N–S extensions associated with ruptures along normal and oblique-slip faults prevail.

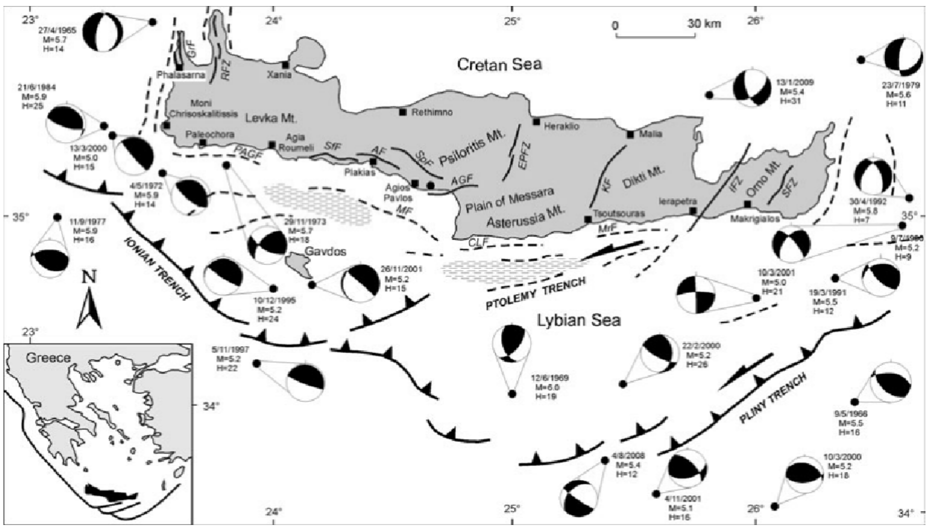


Figure 3.4: Seismotectonic map of Crete by Caputo et Al. (?)

Island has some historical earthquakes showing magnitude more than 8 in the history. There occured an eathquake with around 8.5 Mw in the Eastern Mediterranian and epicenter of this earthquake is assumed as Crete. This earthquake is also the largest record ever in Greece. In this earthquake nearly all towns or Crete are known to be destroyed with a lot of causalties. This earthquake was also followed by a tsunami that killed thousands of people on the southern and eastern coasts of the Mediterranean, Libya, Alexandria, and the Nile Delta. Another devastating historical earthquake in the region happened at 1303, with an estimated magnitude of 8.0. Also in 1856 another earthquake with an estimated Mw 7.7-8.3 has occurred in Heraklion. This earthquake was felt at a very wide area from Sicily to North Africa. Almost 500 people were reported to die. This earthquake is known as an intermediate depth earthquake with a 60-100 kilometers depth and epicenter was the northern coast of Crete.

As mentioned above, Crete is affected by shallow or intermediate-depth type earthquakes. Intermediate depth ones are felt at a wider range as in 1856 earthquake. Shallow ones are felt in smaller areas and a good example of these ones is the subject of this thesis, 2021 Mw 5.9 Arkalochori earthquake sequence with a recorded very high 0.80 g vertical PGA (ITSAK, 2021). This earthquake sequence will also be mentioned detailed in the next subsection.

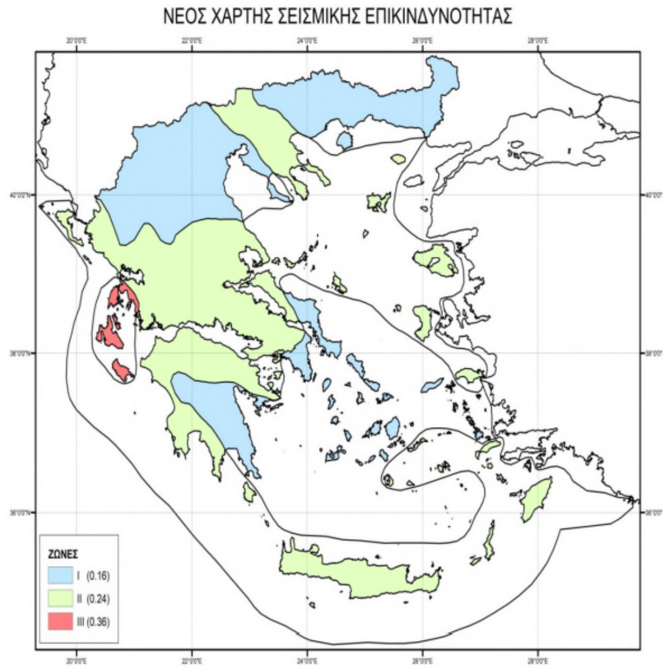


Figure 3.5: Seismic Map of Greece, by Technical Chamber of Greece

In the seismic map of Greece created by the Technical Chamber of Greece, Crete is shown in the Zone 2 with the PGA value of 0.24 g found by 10 % probability of exceedance in 50 years. Also seismic maps created for Greece by other organizations have similar PGA values for most parts of the Crete, which is very low and conflicts the PGA value of horizontal 0.6 g recorded in this earthquake. One aim of this thesis is also to find the reason of this difference between the real data and the estimation.

Also Figure 3.6, which was taken from ETAM report on the sequence, gives us idea about seismicity in the Arkalochori region directly. In this figure earthquakes from June 2021 till the main shock are shown in red in their epicenters. Blue colors are the seismic sequence from 27 September 2021 till May 2022. Grey colors are the seismicity around Arkalochori from 1960s to June 2021. By checking this figure we can say that this is a new active seismic zone which needs more attention.

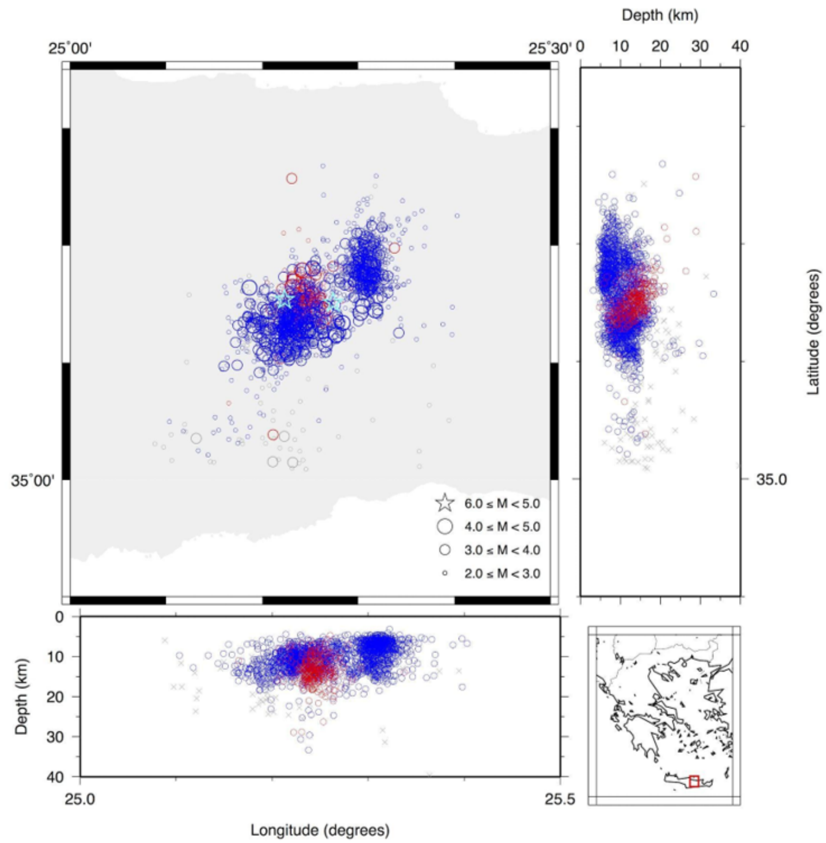


Figure 3.6: Distribution of aftershock epicenters for magnitudes above l2.0, according to the GI/EAA list. Earthquakes from June 2021 to the ML5.8 mainshock are shown in red. The seismic sequence from 9/27/2021 to May 2022 is shown in blue. Seismicity around Arkalochori from the 1960s to June 2021 is shown in grey. Figure is from ETAM report on Arkalochori sequence

## 3.3 Arkalochori Earthquake Sequence in 2021 and the Damage Caused by it

On 27 September 2021 06:17 UTC around Arkalochori (25 km distance to Heraklion, Crete), a strong and shallow earthquake with 5.8 ML and 5.9 MW (according to records of National Observatory of Athens, NOA) occurred. According to the moment tensor solution of NOA, earthquake had a depth of 6.4 km. ARK1 station, which was almost at 2.735 km of epicentral distance to the event, recorded a large 0.8 g vertical component of ground acceleration.

This mainshock was a part of earthquake swarm started in 4 June 2021 (MW = 4.6). Largest foreshock had an MW of 4.8 at 24 July. One day after the main event, there was a strong aftershock with MW 5.1 (NOA) with a depth of 4.7 km. This aftershock had a severe intensity and caused collapse in some already damaged structures. At all, there were more than 10 aftershock events which were larger than 4.0 MW. All aftershocks were grouped as southern and northern clusters and most damage was in the region of the most extensive southern cluster. Also all the foreshocks and aftershocks bigger than MW 4.0 were in southern cluster. Figure 3.7 shows the moment tensors of the two leagest events.

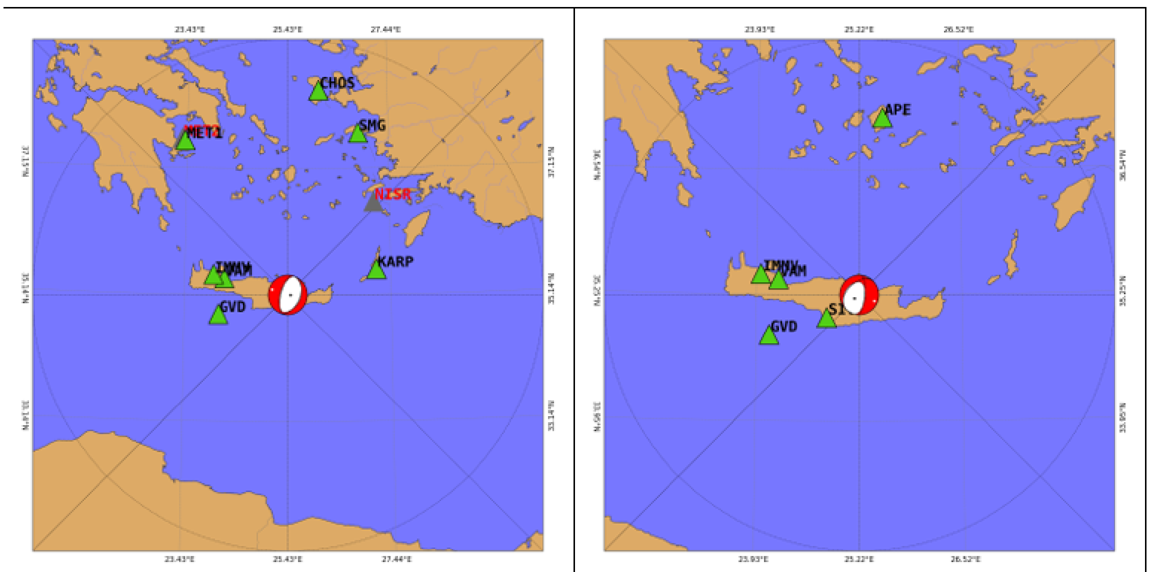


| 5.8 ML, N35.1430 E25.2690 Depth=10.4 km<br>Mechanism: 5.9 Mw, Mo=8.663e+17 Nm,<br>Strike/Dip/Rake: 25°/33°/-81° | 5.3 ML, N35.1457 E25.2232 Depth=10.7 km<br>Mechanism: 5.1 Mw, Mo= 4.635e+16 Nm,<br>Strike/Dip/Rake: 5°/64°/-112° |
|---|---|

Figure 3.7: Moment tensors of the main shock and the largest aftershock, from ETAM report on the sequence

There was one casualty and 20 injuries after this earthquake. More than 5000 structures, which makes the 80 % of Arkalochori got damaged during the sequence with various levels. Town Kato Poulies was nearly all collapsed, only 2 homes remained intact. All the other houses were collapsed or had a big risk to collapse. Situation was not so different in other close towns and villages. Here you can find a few damage photos taken by me during a field trip to the region after the main event.

Figure 3.8: Damage photos from the Arkalochori earthquake site trip

In the earthquake region, most of the structures were buildings made of stones and bricks with load bearing masonry walls and almost all of these structures were built by following a seismic code. Also there were buildings with reinforced concrete frames and infill walls. These ones were constructed according to the provisions. Damage was mainly on the structures built with load bearing masonry walls. Collapse or near collapse rate among these was very high. Reinforced concrete structures were less damaged.

Figure 3.9: Damage photos from the Arkalochori earthquake site trip

## 3.4 Data Set Used and the Recording Stations in Crete

The aim of this thesis is to investigate the local site effects on the Cretan seismic stations and to find out how the most common used ground motion prediction equations for shallow crustal regions work compared to real data so huge amount of data from all Cretan stations were used to make the analysis. Total of data set includes almost 8500 time histories (all 3 components for each event) from 20 seismometers and 8 accelerometers in Crete and Gavdos. These time histories are from the events happened between 2012-2022 with minimum Mw 4.0 and maximum epicentral distance of 300 km. All this data was used to find out H/V Fourier and spectral ratios. Total number of events per station and the date range of the data can be found in Table 3.2.

For the GMPE comparisons, another subset of data from this data set was used. For this reason first, 6 largest events from the 2021 Arkalochori Earthquake sequence till 2022 were selected. Normally in 20/07/2021 , and two times in 21/10/2021 there were events with Ml 4.5 in the sequence but since Mw of these events were smaller than 4.5, they were also not used. Events used for analyses are the main shock, largest aftershock, one 4.6 Mw, two 4.5 Mw and one 4.4 Mw events as shown in the table 3.1 below.

| Event No | Origin Date | Origin Time | Mw | Depth (km) |
|---|---|---|---|---|
| 1 | 27/09/2021 | 6:17:24 | 5.9 | 10.4 |
| 2 | 28/09/2021 | 4:48:06 | 5.1 | 4.7 |
| 3 | 27/09/2021 | 11:02:26 | 4.6 | 3.0 |
| 4 | 27/09/2021 | 8:21:57 | 4.5 | 12.1 |
| 5 | 28/09/2021 | 15:13:15 | 4.5 | 13.6 |
| 6 | 28/09/2021 | 7:30:45 | 4.4 | 14.2 |

Table 3.1: Events used from the Arkalochori earthquake sequence for the detailed analysis of stations

As mentioned above, used data for the analyses are the recordings from total of 20 seismometers and 8 accelerometers from all Crete and also Gavdos. These stations belong to three different networks.

First of these networks is National Observatory of Athens Seismic Network, International Federation of Digital Seismograph Networks, doi: 10.7914/SN/HL. This network is the nationwide network of Greece and mission of HL is to provide accurate and timely data for seismic monitoring and research of the Southeastern Mediterranean region. In this research CRE1, CRE3, GVD, IACM, IDI, IMMV, KSTE, NPS, SIVA, VAM and ZKR stations of Crete were analyzed and they all belong to HL Network.

Second network to have analyzed stations in this thesis is Seismological Network of Crete (HC), International Federation of Digital Seismograph Networks, doi: 10.7914/SN/HC. The HC network is operated by Institute of Physics of the Earth's Interior and Geohazards, UNESCO Chair on Solid Earth Physics and Geohazards

Risk Reduction, Hellenic Mediterranean University Research Center (former Technological Educational Institute of Crete) (2006) and it was set to monitor the seismic activity in front of the Hellenic Arc. RODP, CHAN, KNDR, KNSS, GVDS, IPPL, KSTE, PFKS and STIA stations in Crete region belongs to this network and they were also analyzed.

There are also stations from ITSAK strong motion network, International Federation of Digital Seismograph Networks, doi: 10.7914/SN/HI. This HI network is operated by Institute of Engineering Seismology Earthquake Engineering (ITSAK) (1981). It is a nationwide network in Greece with more than 200 stations. Stations analyzed from ITSAK network are ARK1 and SIT2.

Digital object identifier (doi) information of all three networks were taken from Evangelidis et al, 2021.

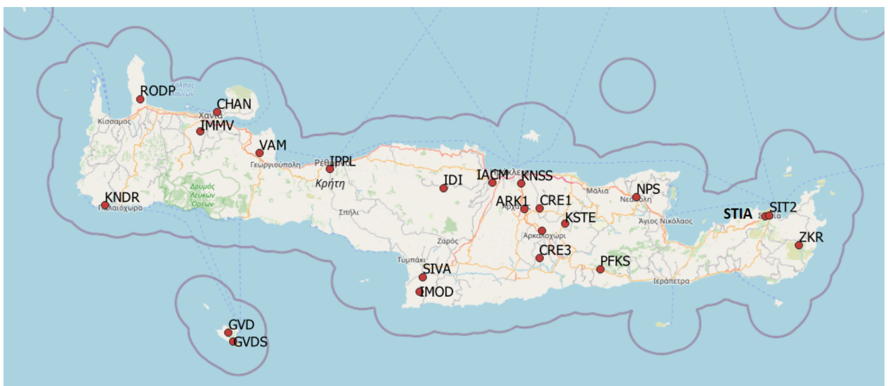


Figure 3.10: Map of Crete created with the Stations of Study created on Qgis

Name and exact location of the stations analysed on this research can be seen on the map above. Among these stations GVDS, IACM, IMMV, KSTE, SIVA and ZKR have both seismometers (HH) and accelerometers (HN) installed, SIT2 has accelerometer and rest of the stations have seismometer.

Data from all the stations were used for both H/V Fourier and H/V spectral ratio analysis. For the distance scaling graphs, since only data from above mentioned earthquakes from Arkalochori sequence was used, stations to record the data accurately, with no error or clip etc. were limited so only 15 stations were analyzed. These stations will be mentioned in the data analysis chapter.

| Station Name | Channel | Network | Number of Earthquakes | Date Range |
|---|---|---|---|---|
| ARK1 | HN | HI | 2 | Mw 5.9-MW 5.1 |
| CHAN | HH | HC | 142 | 2014-2022 |
| CRE1 | HH | HL | 69 | 2021-2022 |
| CRE3 | HH | HL | 57 | 2021-2022 |
| GVD | HH | HL | 151 | 2021-2022 |
| GVD | HN | HL | 87 | 2017-2022 |
| GVDS | HN | HC | 62 | 2016-2022 |
| IACM | HH | HL | 75 | 2017-2022 |
| IACM | HN | HL | 85 | 2017-2022 |
| IDI | HH | HL | 179 | 2012-2022 |
| IMMV | HH | HL | 143 | 2012-2022 |
| IMMV | HN | HL | 146 | 2012-2022 |
| IMOD | HH | HC | 44 | 2020-2022 |
| IPPL | HH | HC | 19 | 2020-2022 |
| KNDR | HH | HC | 120 | 2014-2022 |
| KNSS | HH | HC | 138 | 2020-2022 |
| KSTE | HH | HL | 20 | 2021-2022 |
| KSTE | HN | HL | 20 | 2021-2022 |
| NPS | HH | HL | 166 | 2012-2022 |
| PFKS | HH | HC | 137 | 2020-2022 |
| RODP | HH | HC | 80 | 2015-2022 |
| SIT2 | HN | HI | 175 | 2013-2022 |
| SIVA | HH | HL | 46 | 2012-2022 |
| SIVA | HN | HL | 43 | 2012-2022 |
| STIA | HH | HC | 98 | 2015-2022 |
| VAM | HH | HL | 189 | 2012-2022 |
| ZKR | HH | HL | 187 | 2012-2022 |
| ZKR | HN | HL | 110 | 2012-2022 |

Table 3.2: Total amount of data used and the date range of events per station (Total number of events = 2770)

All the data used was in SAC (Seismic Analysis Code) format except the data from ARK1 station. SAC files were made into SAC after downloading from the EIDA node in miniseed format. Data from ARK1 was in ascii format. Since ITSAK only shared the main shock's and the largest aftershock's data with the public from ARK1 station, only 2 events were used for that one. Rest of the data from the other stations were also publicly shared and they were provided by National Observatory of Athens.

## 3.5 Effect of Earthquake Sequence on the Gravestones in Cretan Cemeteries

After the Arkalochori earthquake sequence, in mid-November 2021 (around 50 days after the main shock) I had a chance to join a site investigation trip to Crete. During that trip we made a visit to the cemeteries of Arkalochori with Dr. Olga-Joan Ktenidou and took photos of gravestones and headstones to investigate the possible trajectory of the ground motion by checking how they rotated.

Figure 3.11: Photos of rotated gravestones after Arkalochori earthquake sequence

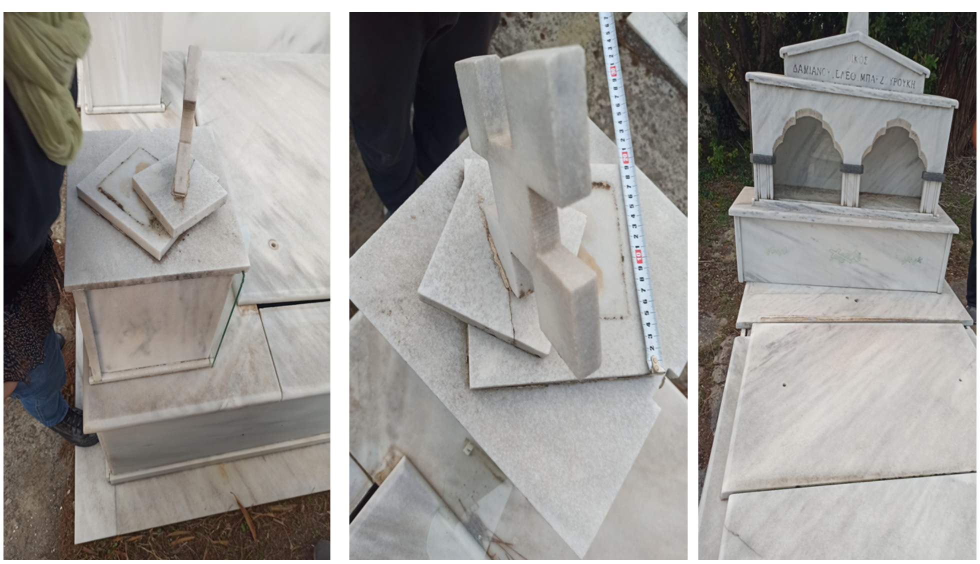

Figure 3.12: Photos of rotated headstone and smaller objects

A lot of rotated gravestones and headstones as in Figure 3.11 were measured in 3.13 different graveyards and then after the trip rotation angles were calculated and directions (CW or CCW) were noted. Also figure 3.12 shows examples from the rotated headstone and smaller objects.

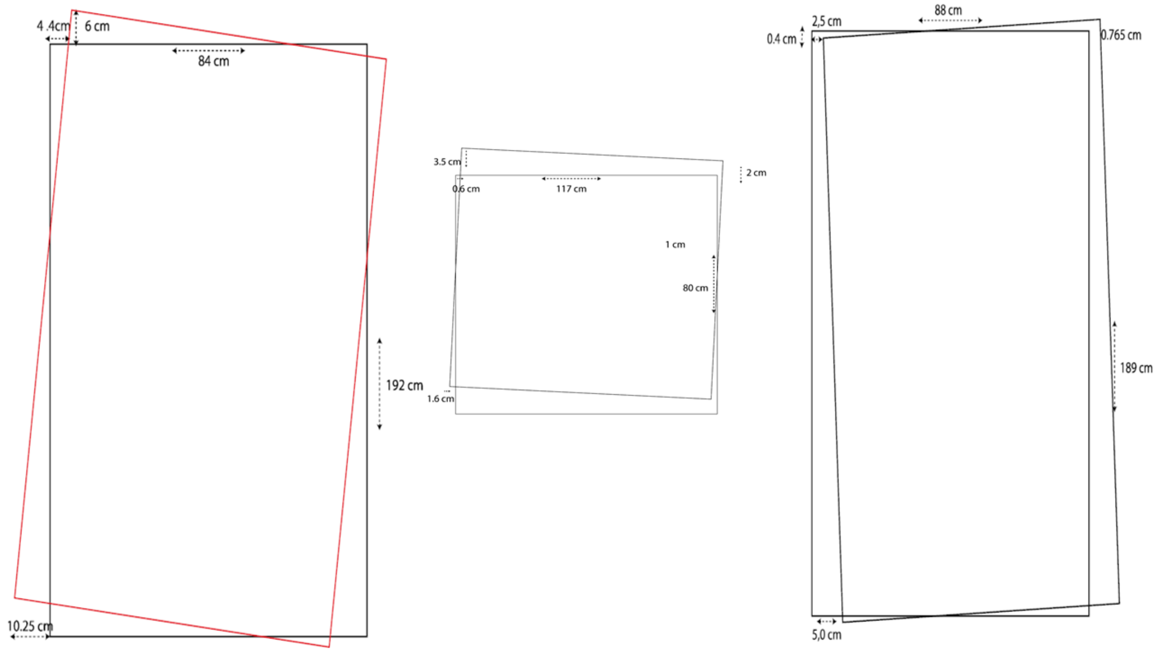


Figure 3.13: Drawings with measurements made for the three gravestones on Figure 3.10

Also all the measured graveyards were pinned from Google Earth as shown in Figure 3.11 to check along with the rotations and try to estimate a path. There were many examples of graves next to each other one of which rotated clockwise and the other counter clockwise. There was also no difference discerned in the vertical (downlift) or horizontal (eastward) displacement observed near the cemetery area after the earthquake according to the HUA Earth Observation Team (I. Parcharidis, personal communication, 26/02/2022). There was no correlation between the rotation of the gravestones so ground motion path could not be predicted. Unfortunately we did not have recordings from the cemeteries themselves that could help understand the difference in ground motion between them. Also there were a lot of unknown variables to do dynamic analysis so no further study on this part was made.


Figure 3.14: Map of the rotated and measured graves

# Chapter 4

# DATA ANALYSIS

## 4.1 Signal Processing

As already mentioned in the previous chapter, for the H/V analysis of all stations, a huge data set of almost 10000 time histories from all the station were used. First step of the thesis was to do signal processing one by one for all the time histories to find the lowest and highest usable frequencies per station. This process was done on Matlab.

First, by using the code for each station all the time histories were opened and noise corridor, start of P waves, start of S waves and end of S waves were picked from Z, N and E components of each event. P waves are faster than S waves and they arrive the station earlier than the S waves so they are easy to identify. S waves are slower but bigger in amplitude so in general, there is an abrupt change in amplitude when S waves arrive. Also since S waves are slower, frequency in time history lowers. After the S waves slowest surface waves arrive. These waves have less frequency and due to that they produce the largest waves in the long term time history.

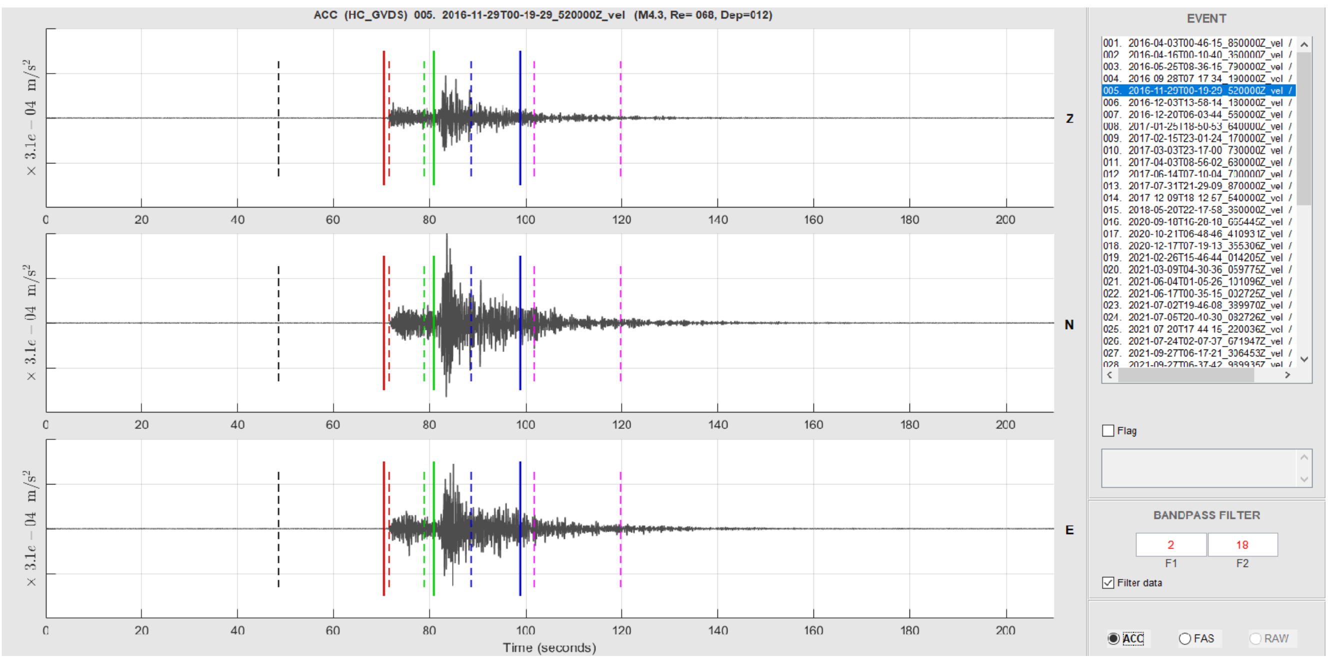


Figure 4.1: Matlab program to find lowest and highest usable frequency, wave picking part

All these were taken into account as noise corridor, P wave arrival, S wave arrival and end of S waves were chosen for all the time histories in the data set. An example of the Matlab program used in the thesis that SAC files are translated into time histories per Z, E and N components and then picking of waves are done is above in the figure. Black line is the start of noise, red line represents the start of P waves, green line is the start of S waves and blue line is the end of S waves.

After the picking of waves, program calculates the Fourier amplitude spectrum of S interval of the earthquake and Fourier spectrum of noise both for N and E

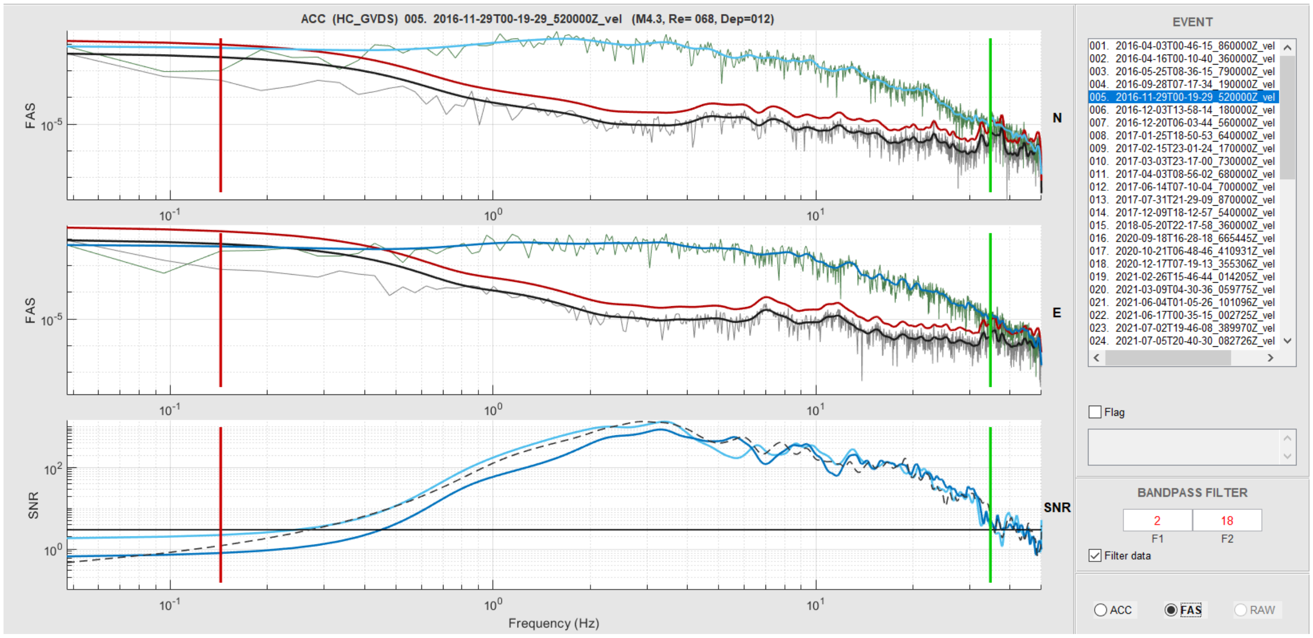


Figure 4.2: Matlab program to find lowest and highest usable frequency, Fourier analysis part

components.

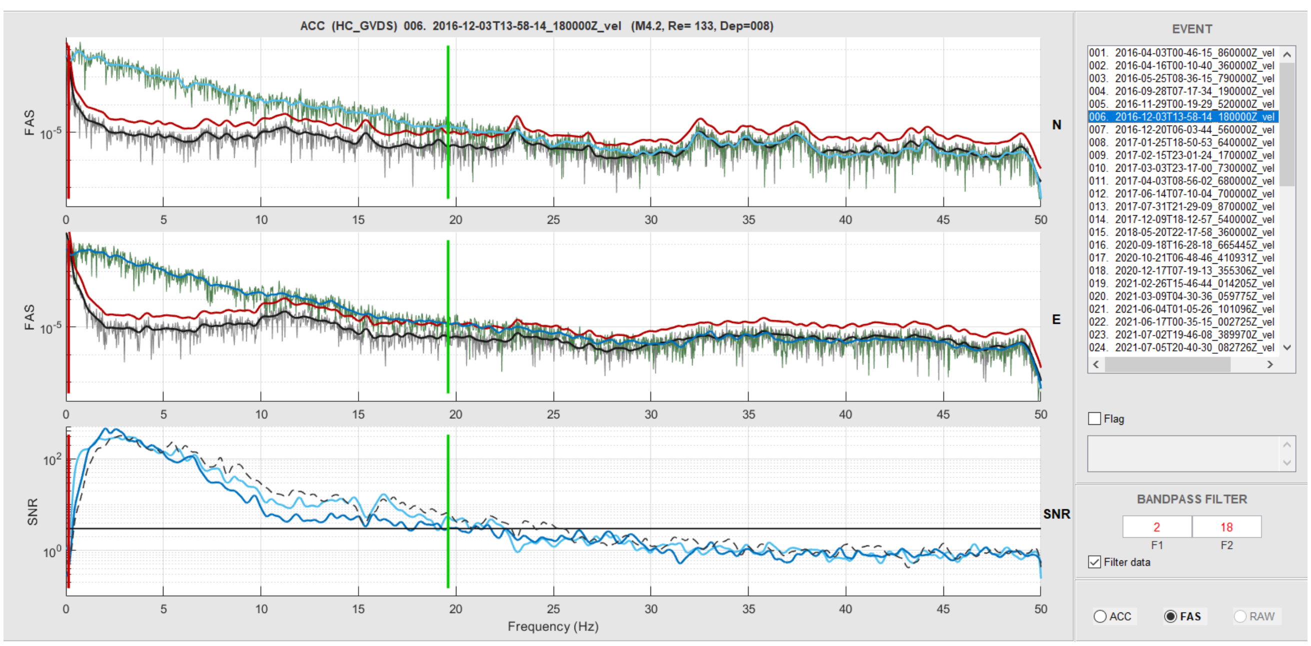


Figure 4.3: Matlab program to find lowest and highest usable frequency, Fourier analysis part

Also by that info, signal to noise ration is calculated. Figure above is an example of log-log representation of N and E Fourier spectrum for the noise and earthquake, also signal to noise ratio. Green smooth line represents the earthquake, red smooth line represents the 3 times noise and black line represents the noise. In SNR, dark blue represents the east, blue represents the N component's signal to noise ratio. Choosing the lowest usable frequency is done from this part. Red line represents the LUF. We choose the LUF when SNR gets bigger than 1 and the envelope starts to increase. To choose HUF, semi log-log representation of the same graphs are used.

Black straight line on SNR horizontal axis is SNR=3 line. Highest usable frequency is chosen when one of N or E SNR falls down to 3.

After finding out the LUF and HUF for all the events from all stations, those values were extracted to Excel and mean and standard deviation of LUF and HUF were calculated for each instrument. To be on the safe side, for LUF, mean plus standard deviation and for HUF, mean minus standard deviation values were used. You can find all the LUF and HUF values per station on table 4.1. Since ARK1 recordings were given already processed and filtered, they were excluded from this signal processing procedure

| Station Name | Channel | LUF (Hz) | HUF (Hz) |
|---|---|---|---|
| CHAN | HH | 0.3 | 5.8 |
| CRE1 | HH | 0.6 | 21.2 |
| CRE3 | HH | 0.5 | 13.7 |
| GVD | HH | 0.2 | 14.8 |
| GVD | HN | 0.3 | 10.2 |
| GVDS | HN | 0.2 | 13.7 |
| IACM | HH | 0.2 | 6.9 |
| IACM | HN | 0.3 | 6.4 |
| IDI | HH | 0.2 | 23.6 |
| IMMV | HH | 0.2 | 17.3 |
| IMMV | HN | 0.3 | 15.3 |
| IMOD | HH | 0.2 | 20.7 |
| IPPL | HH | 0.4 | 7.9 |
| KNDR | HH | 0.2 | 9.2 |
| KNSS | HH | 0.4 | 16.2 |
| KSTE | HH | 0.4 | 17.4 |
| KSTE | HN | 0.4 | 19.8 |
| NPS | HH | 0.2 | 12.3 |
| PFKS | HH | 0.5 | 13.7 |
| RODP | HH | 0.29 | 13.2 |
| SIT2 | HN | 0.47 | 5.1 |
| SIVA | HH | 0.46 | 12.7 |
| SIVA | HN | 0.42 | 12.3 |
| STIA | HH | 0.35 | 10.8 |
| VAM | HH | 0.26 | 12.3 |
| ZKR | HH | 0.33 | 9.6 |
| ZKR | HN | 0.34 | 6.6 |

Table 4.1: Lowest and highest usable frequency values calculated for each station

## 4.2 Acceleration Response Spectra

Acceleration response spectrum gives the maximum acceleration response on a given load function for simple damped single degree of freedom systems. X axis of the spectrum is frequency or period, y axis of the spectrum is acceleration (might change to velocity or displacement due to interest). If one knows the natural frequency of the system, response can be chosen from the spectrum accordingly. Response spectrum concept was explained in detail in the previous chapter.

In this research, PSA from the time histories are calculated with two reasons. First is to find out the PGA and SA(1.0 sec) of the 6 events from the Arkalochori Earthquake sequence to use as the observation values on the residual analysis. Second reason is to create H/V peak spectral acceleration ratio profiles. Reason to do both analyses will be explained in next sections of this chapter.

Response spectra for both reasons were calculated using Matlab software. Method used to calculate response spectra was Newmark-Hall approach. To do that, SAC files were first imported as time histories and then by using Newmark approach response spectra were calculated by an already written code. An example of a response spectrum of a time history from IMOD..HH station created by the Matlab code using Newmark approach is as below;

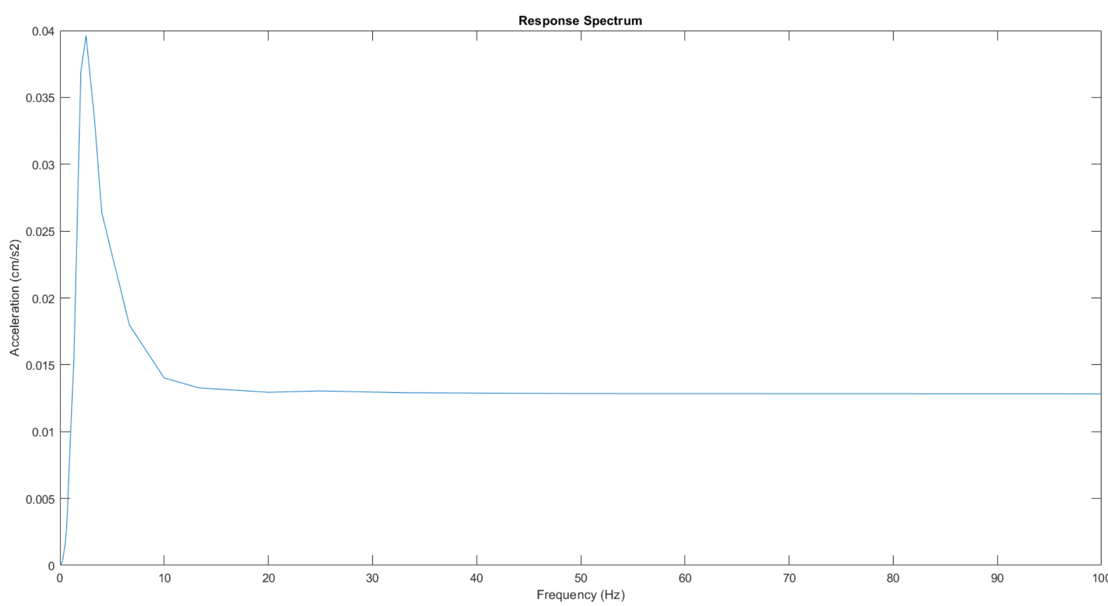


Figure 4.4: A response spectrum of a time history from IMOD..HH station, created by Matlab code

## 4.3 H/V Spectral Ratio (HVSR)

H/V spectral ratio (HVSR) is a technique used to estimate the site effects without needing a reference site. This method is based on two general assumption. First one is that the waves travel equally on the bedrock so H/V on bedrock is 1. Second assumption is that when the waves travel from the bedrock through the soil to the surface, amplitude of vertical component remains the same with a transfer function of 1 so vertical component is the same on bedrock and on the ground. But the horizontal component mostly enlargens due to how 'soft' the soil between the bedrock and ground is so H/V tells us the amplification in between. And the frequency that corresponds to that maximum amplification is known as the resonant frequency of the site.

First way of HVSR is the ratio of the Fourier amplitude of horizontal motion to the vertical one. First people to work on HVSR technique were Nogoshi & Igarashi (1971), and then Nakamura (1989). They related the peak frequency to the resonance frequency of the site. Later on, Lermo & Chavez-Garcia 1993 has shown that it is a successful approach to use the method to identify the resonance frequency of soft sediments.

In this thesis, after signal processing of all time histories, again by using Matlab software HVSR Fourier analysis for every station was done.

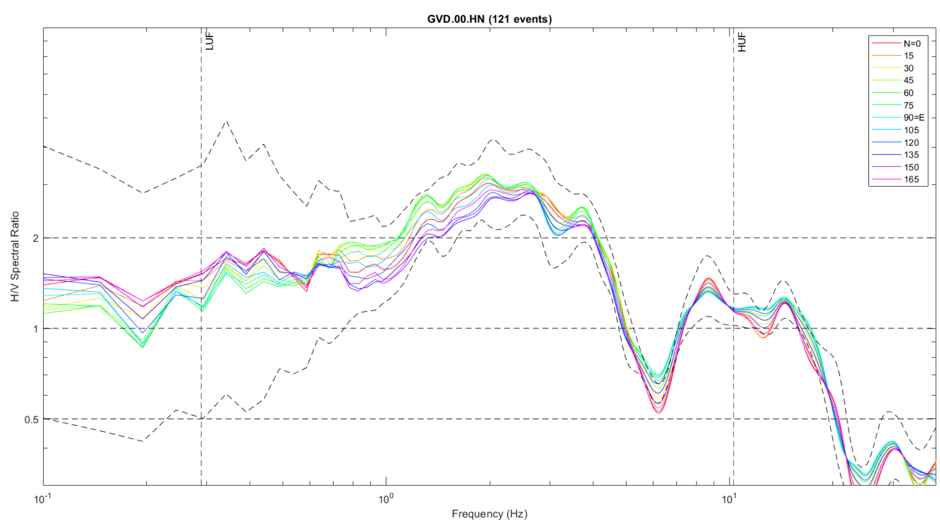


Figure 4.5: H/V Fourier Profile for GVD.00.HN

Main code was provided by Dr. Olga-Joan Ktenidou, which was used in her research "Directional dependence of site effects observed near a basin edge at Aegion, Greece" in 2015. Code was modified to get the related results with this thesis. Mainly, code first transforms SAC files into readable time histories for all three components. Then all the components are rotated with 15 degrees intervals from 0 degree until 180 degrees. Reason of this is to find out the directional dependence of the H/V ratios at the end. After rotation of the time histories, Fast Fourier transform is applied to all rotated time histories by applying signal processing and Fourier Analysis Spectra are found. Then by using all the FAS, mean HVSR and standard deviations for all rotated degrees are found. Figure 4.5 is an example of HVSR profile for GVD station by using the Matlab codes.

Using this technique HVSR Fourier profiles were created for all the seismometers and accelerometers separately.

Another technique used to create the HVSR profiles is H/V response spectral ratios. In this technique, ratio of peak spectral acceleration from horizontal components to vertical one is calculated. This was also done by using Matlab. After calculating the response spectra ( so the PSA) as mentioned in previous section, ratios of the absolute PSAs are taken and average ratios and standard deviations per frequency is calculated.

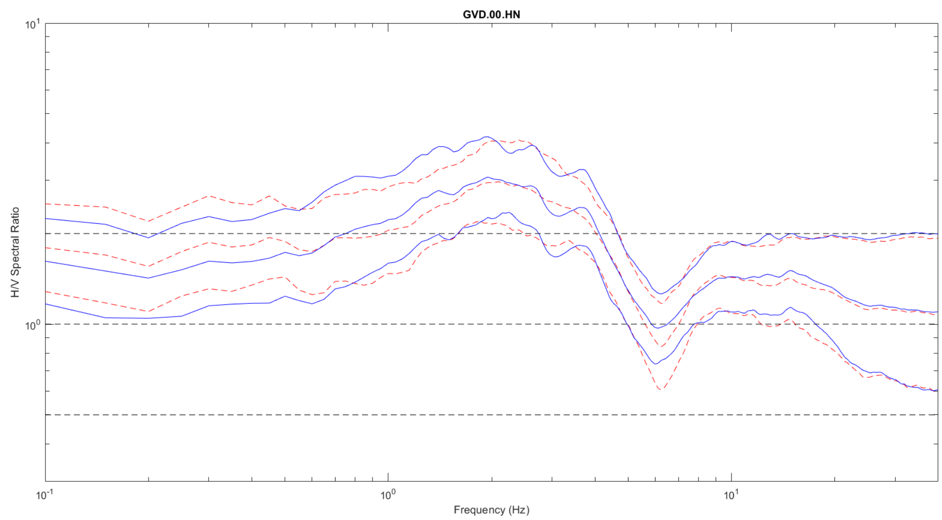


Figure 4.6: H/V PSA Profile for GVD.00.HN

An example of the H/V PSA profile done by using Matlab codes is in Figure 4.6. This one was created by using all the data in the data set from the seismometer in CHAN station. As it can be seen on the H/V PSA profile, result is more smooth compared to Fourier one but there is a main disadvantage of this technique.

If we check the single degree of freedom transfer function per frequencies on Figure 4.7 by Bora et Al 2016, in high frequency response, low frequencies and high frequencies are mixed so H/V PSA does not give accurate result on high frequencies. If we check Figure 4.5 and 4.6 this can easily be observed as after 7-8 Hz H/V PSA gets less detailed and shows another result than Fourier. By taking this into account, even though H/V PSA profiles were also created for each station, only H/V Fourier amplification graphs were used in the results.

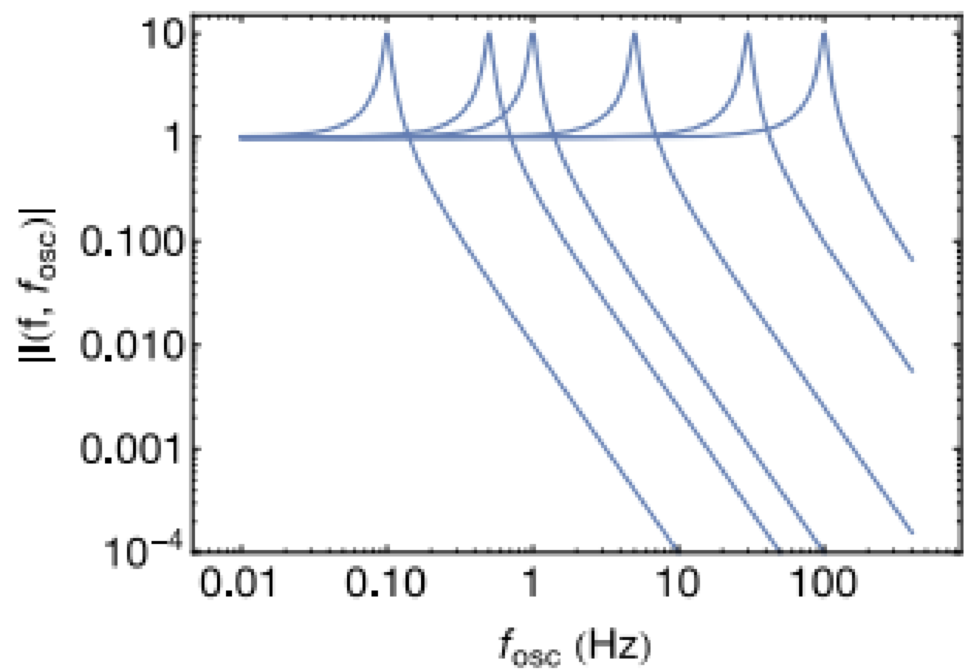


Figure 4.7: Single degree of freedom oscillator transfer function at different oscillator frequencies by Bora et al 2016

## 4.4 Distance Scaling and Residual Analysis and the GMPEs Used for both

Distance scaling is a good way to find out how the strong motions attenuate with distance for a GMPE at a specific magnitude. It is a also good to compare several GMPEs at the same time. To get the most accurate and correct predictions, site, distance and rupture parameters need to be defined. Outcome of a distance scaling is intensity measure type requested on y axis (PGA, SA(1.0 sec) etc.) and the distance parameter on the y axis (rjb, rrup, rhypo etc.). Rupture distance is the shortest distance from the site to the rupture surface and Joyner-Boore distance is the shortest distance to the surface projection of the rupture from the site. Figure 4.8 by Kaklamanos et Al. 2011 shows these distance parameters.

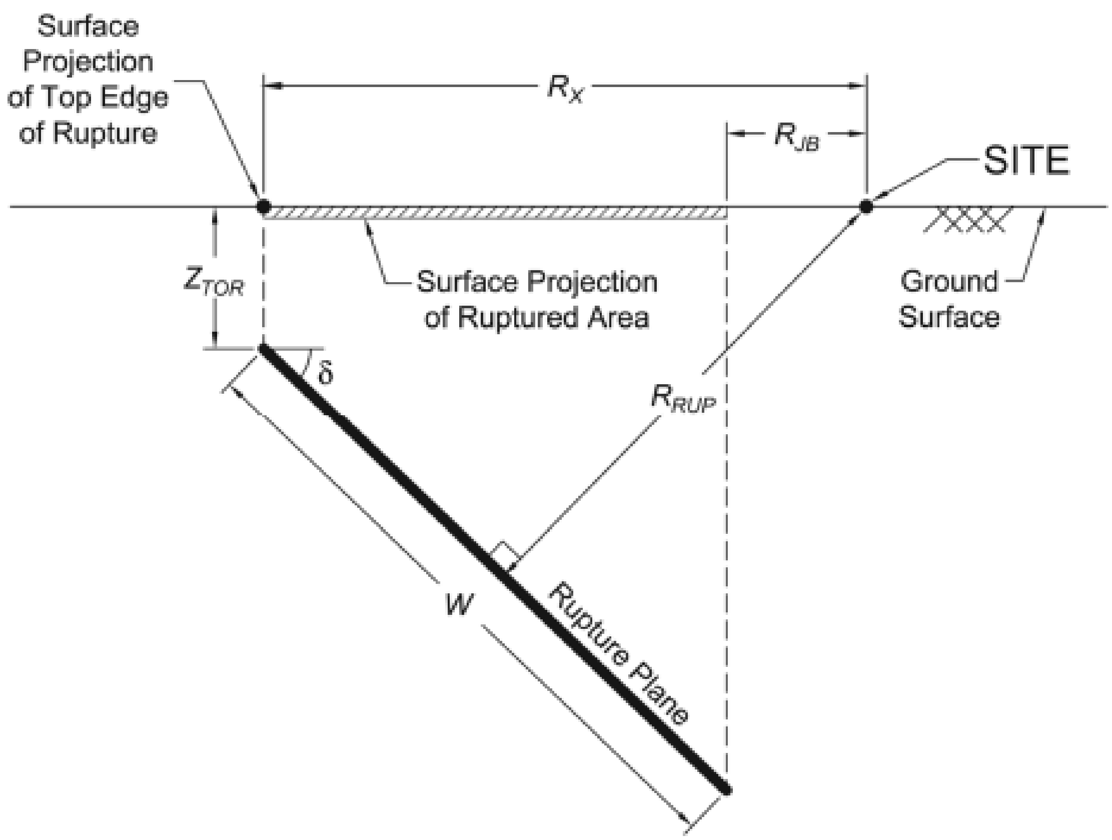


Figure 4.8: GMPE distance parameters by Kaklamanos et al, 2021

Also an example of distance scaling graph with for several intensity measure types (IMTs) and with different GMPEs is in the Figure 4.9.

In general, residuals are made to compare models with observations, basically by subtracting the model from the observation. It is done to check how the predicted

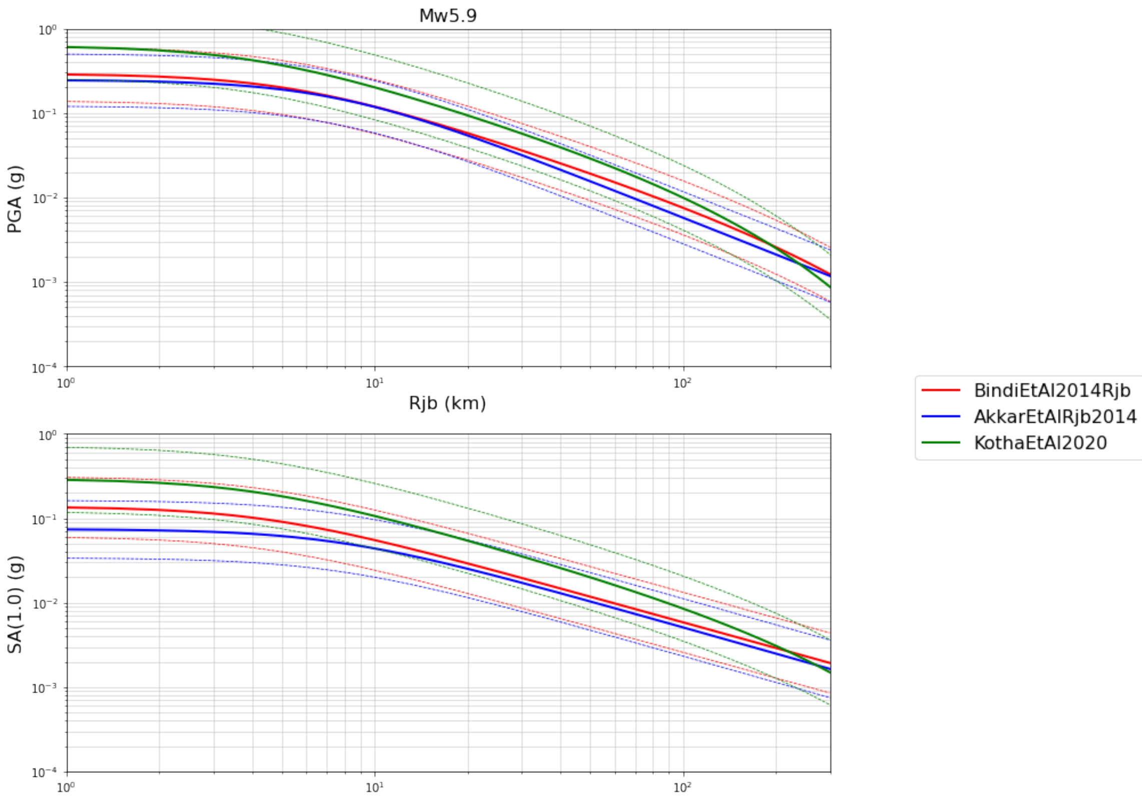


Figure 4.9: Example of a distance scaling graph for several GMPEs and different IMTs

result is close to the real value so it is an important asset to understand the precision of the predictions. In its application to ground motions, GMPE predictions are subtracted from the real ground motion events and this analysis can be used in several ways starting from understanding the GMPE accuracy, accuracy of parameters used to calculate GMPEs, station analysis etc. In the figure 4.10, you can see an example of GMPE residuals with several parameters calculated for Abrahamson et Al,2014 GMPE. It was calculated using the data of the Arkalochori earthquake sequence, but not used since it was out of purpose.

To do both analyses first step was to choose correct GMPEs to use. GMPEs are mostly defined for a specific tectonic region type. In this case, since the region of the sequence is active shallow crustal zone, GMPEs to select were supposed to be defined for this type of tectonic region. To have variety of GMPEs, well known 3 GMPEs from Next Generation Attenuation Models (NGA-West) which use rupture distance as the main distance parameter and 3 well known GMPEs from European researchers which use Joyner-Boore distance were chosen. GMPEs used in the thesis can be found in the table 4.2 and related research papers of them were added to the references. All the specific requirements like required rupture, site, distance parameters were checked from the related papers and Openquake and used accordingly during the calculations.

After choosing the GMPEs, observations from stations that has Arkalochori earth-

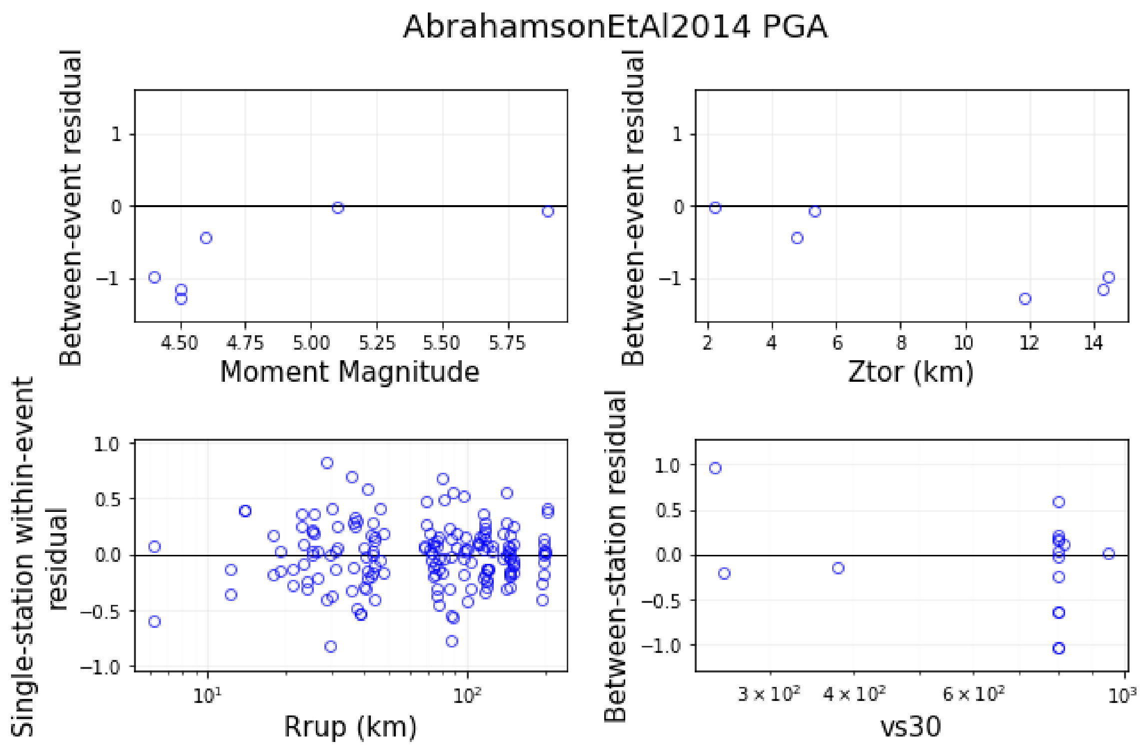


Figure 4.10: Example of GMPE residuals with several parameters

| GMPE Name | Tectonic Region Type | Distance Parameter |
|---|---|---|
| Abrahamson Et Al. 2014 | Active Shallow Crustal | rrup |
| Campbell & Bozorgnia 2014 | Active Shallow Crustal | rrup |
| Chiou & Youngs 2014 | Active Shallow Crustal | rrup |
| Akkar et Al. 2014 | Active Shallow Crustal | rjb |
| Bindi et Al. 2014 | Active Shallow Crustal | rjb |
| Kotha et Al. 2016 | Active Shallow Crustal | rjb |

Table 4.2: GMPEs used in Distance Scaling and Residual Analyses

quake sequence data were added to distance scaling graphs with these GMPEs to see the difference between the observation and prediction on a graph. To do this, Ground Motion Prediction Equations-Strong Motion Tool Kit (gmpe-smtk) of Openquake software was used. This is a Python based tool, tool was used on Jupyter Notebooks. To get the graphs, necessary libraries were imported, then from Openquake hazardlib, GMPEs were imported. Then input parameters like the GMPEs, moment magnitude, intensity measure type that we want the results for defined. Next step was to define the rupture parameters (location, depth, strike, dip,rake) according to the specific event. Based on the site classification, Vs30 was also used as 400 m/s or 800 m/s. Also based on the GMPE, distance parameters, rrup or rjb was used as distance parameter. Next step was to add the observations on distance scaling graphs.

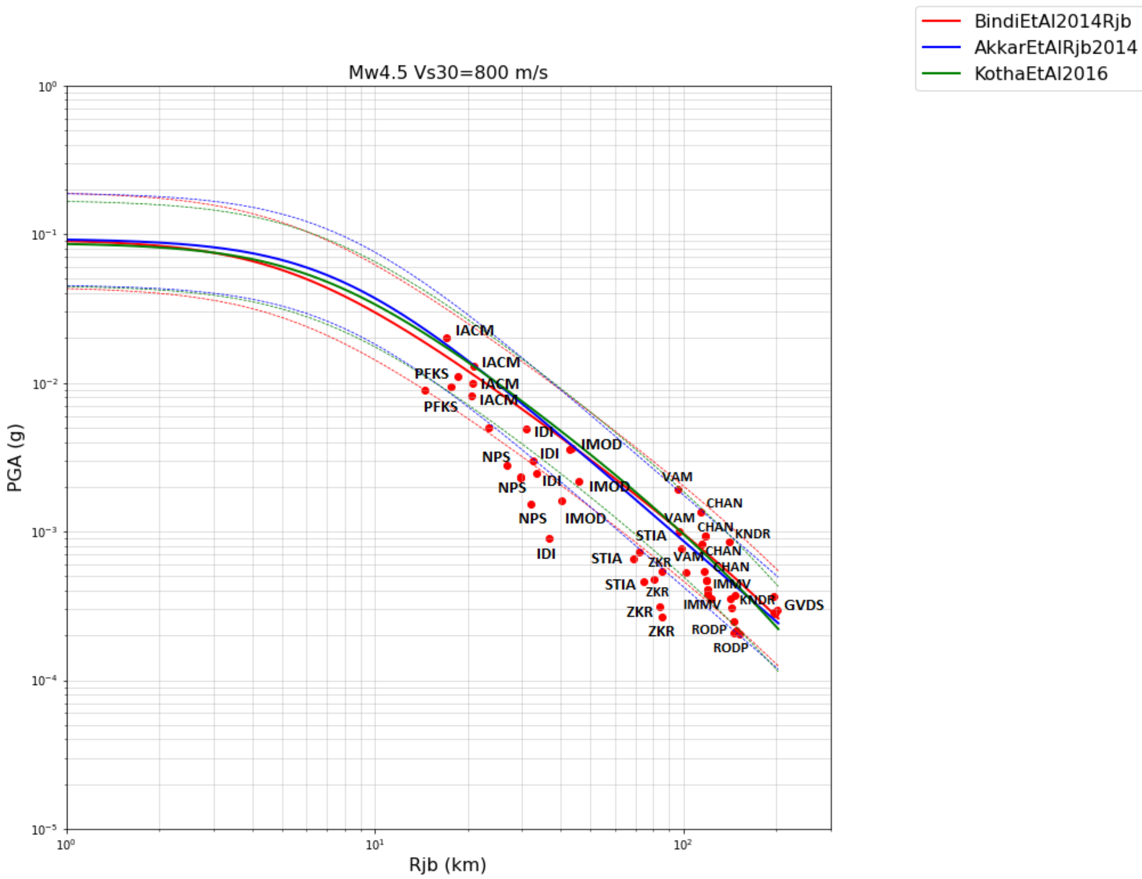


Figure 4.11: Example of distance scaling graph with real events created on Openquake

As mentioned in the previous sections, response spectra for both horizontal components were calculated by Matlab by using the time histories from each station. To use in the comparison, with SRSS (square root of sum of squares) method, for each event resultant of two components (for PGA or SA(1.0 sec)) were calculated. Required distance parameters for event-site combinations were rupture distance and Joyner-Boore distance. To calculate rupture distance, formulas from the paper 'Estimating Unknown Input Parameters when Implementing the NGA Ground-Motion Prediction Equations in Engineering Practice' by Kaklamanos et Al. 2011 was used. An example of distance scaling graph created on Openquake gmpe-smtk tool with real events on it is shown on Figure 4.11.

Till this point, HVSR for each station and also distance scaling graphs with real events were created. Next step was to do residual analysis for each station to find out the overall station performance.

To do this, GMPE predictions (with rrup or rjb accordingly) were exported to Excel for all magnitudes (Mw 5.9-4.6-4.5-4.4) for both Vs30=800 m/s and Vs30=400 m/s and both PGA and SA(1.0 sec). Then on Excel, Then ln residuals were calculated

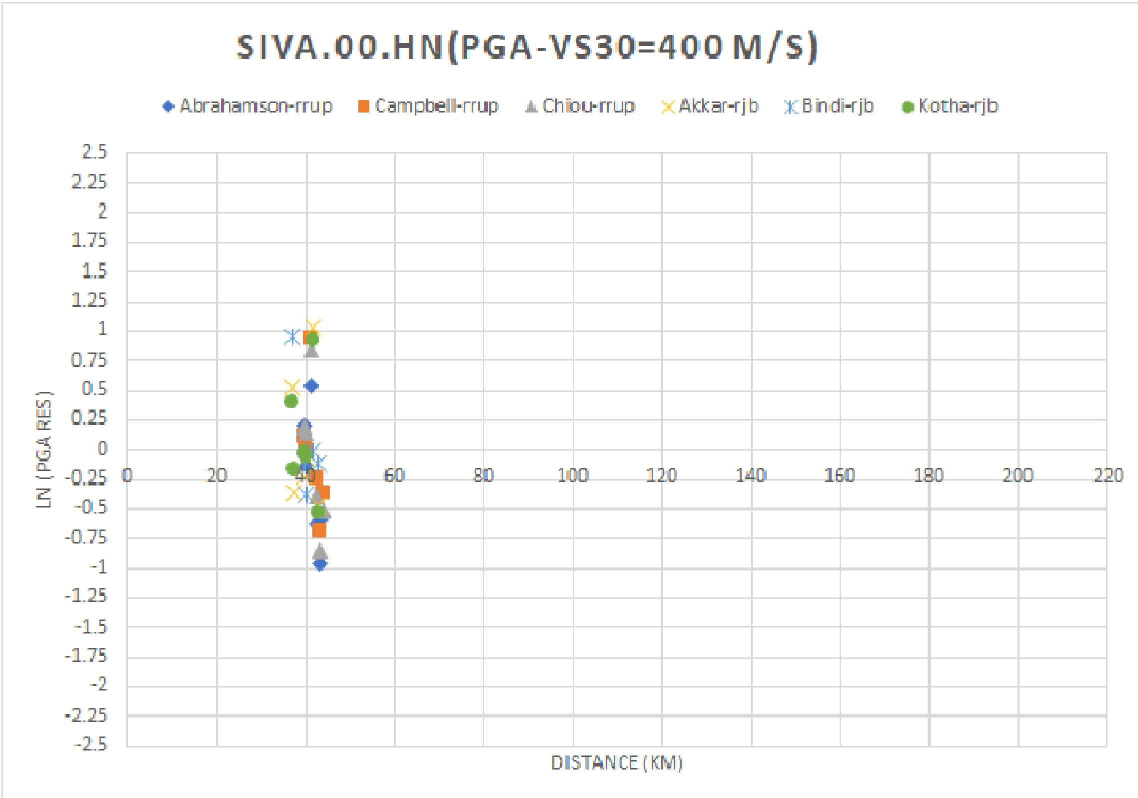


Figure 4.12: Example of residuals for station SIVA

for each station according to the measured or inferred Vs30 and for both Sa(1.0 sec) and PGA. An example of residuals created on Excel is shown on Figure 4.12. On that example, ln (natural logarithm) of predictions for each GMPE is subtracted from the ln of corresponding real event data from SIVA.OO.HN. Since we have 6 events and 6 different GMPEs, 36 residual points are calculated and plotted according to their distance.

As mentioned on the example, Y axis is calculated as ln (observation) - ln (prediction) and x axis is the distance (rjb or rrup in km). Using ln (residuals) instead was to correct the non-linearity in both x and y axis caused by nonlinear regression and also to correct the error issues on y axis.

All these results from HVSR profiles, distance scaling graphs and residuals are analyzed in the next chapter.

# Chapter 5

# ANALYSIS OF THE RESULTS

## 5.1 H/V Fourier Analysis Combined with GMPE Residuals for Stations with Arkalochori Sequence Data

### 5.1.1 Stations with Strong Amplification

#### ARK1..HN

ARK1..HN is an accelerometer station operated by ITSAK and it is located in the center of Arkalochori. It is the closest station to the 2021 Arkalochori earthquake sequence. From this station, ITSAK shared only the main shock's and Mw=5.3 aftershock's data with the public so H/V and the GMPE residuals were calculated by only using these 2 events from the sequence but one would wish to have more than 5 or even 10. Since because there were no more recordings available, the ratio was tentatively computer with 2. On the ITSAK report after the earthquake, ITSAK shared that the site was classified as between Eurocode Type A and B. By using this information, Vs30 for the site was used as 800 m/s on the GMPEs but to make a comparison, 400 m/s option was also calculated.

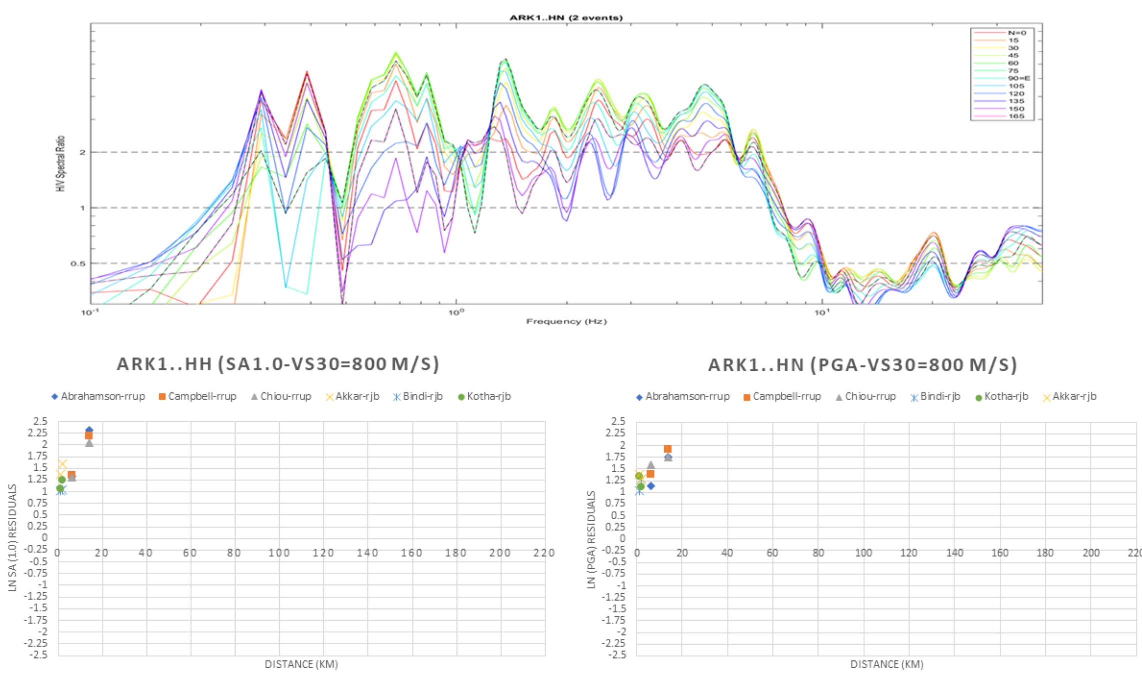


Figure 5.1: ARK1..HN H/V and Residuals with Vs30=800 m/s

Results of the H/V Fourier combined with GMPE residuals for PGA and SA(1.0 sec) for Vs30=800 m/s is as shown above. Since H/V was created only with 2 data, it looks like it has huge directional sensitivity on the graph but we need more data to understand about it so it is not valid. Still, it gives idea about the predominant periods and the amplifications in different frequencies. For instance, there is amplification between 2 to 6.5 between the frequencies 0.5 Hz to 1 Hz and it makes the peak 6.5 at the frequency 0.7 Hz and this might be counted as a possible predominant frequency for the site. Also it reaches again up to 6 at 1.5 Hz. There is strong amplification up to 7 Hz in different ranges.

For this station an H/V amplification graph was created by also ITSAK on the sequence report at 2021 as below.

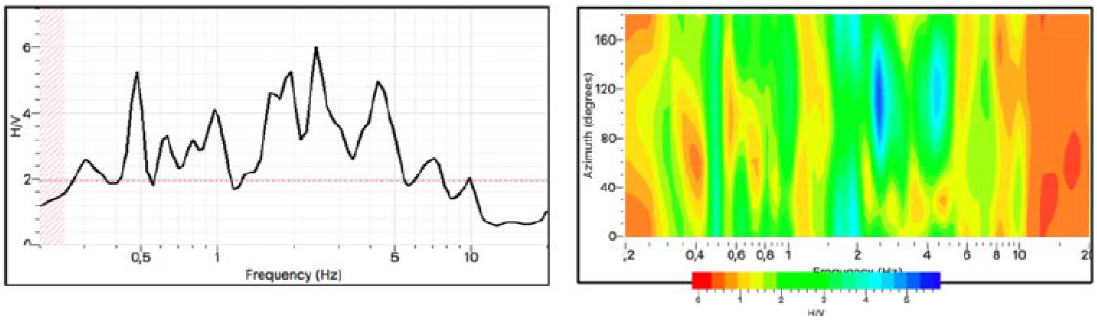


Figure 5.2: H/V - Frequency graph created by ITSAK for the Arkalochori sequence report 2021

It can clearly be seen that both of the H/V amplifications act the same way with strong amplification in ranges from 03-0.5 Hz till 7 Hz. Then in both H/V amplification graphss, in higher frequencies no or little amplification starts.

Also by checking the GMPE residuals we can again get the same feeling of strong amplification in the station. ARK1 is known to be a Eurocode type A-B profile as mentioned on ITSAK report so normally there should be no or very little amplification due to rock profile. By this information, GMPE predictions were calculated with Vs30=800 m/s. PGA residuals are between 1 to 1.9 and averaged around 1.4 and SA (1.0 sec) residuals are between 1 to 2.3 and averages around 1.5. H/V shows strong amplification around 1.0 Hz also it is still amplifying till a high frequency 7 Hz. We do not know PGA's frequency but this might explain it as well. Here we can also understand that GMPEs are underestimating the site and the amplification coming from an A or B profile might not be enough to define the site. To see if using a Vs30=400 m/s closer to Type C, GMPE residuals were also calculated this way and the result was like in the figure below.

For Vs30=400 m/s, residuals for SA (1.0 sec) is between 0.45 to 2 and with an average around 1. It is lower than 1.5 average of Vs30=800 m/s but there is still strong underestimation with Vs30=400 m/s. For PGA, minimum is 0.92 and 1.66 and average is around 1.3. GMPEs underestimate the PGA with Vs30 as well. We can conclude that a profile between type A and B might not be correct and the site might be between type B and C with both results.

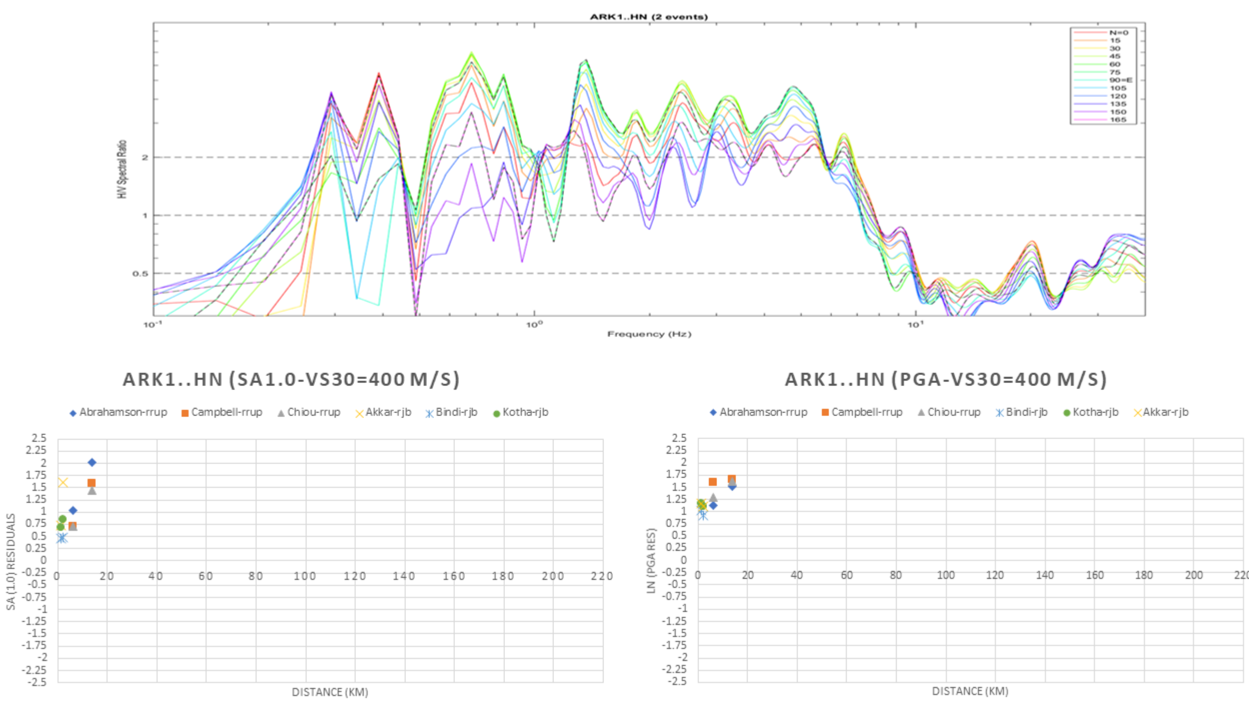


Figure 5.3: ARK1..HN H/V and Residuals with Vs30=400 m/s

**IACM..HN**

This station has both accelerometer and seismoter operated by by National Observatory of Athens and it is in the Hellenic Seismic Network (HL) and it is located in Heraklio, Crete. According to ESM Database, station has Vs30 of 815 m/s which is type A. Amplification is not expected on the site with this information but H/V amplification graphs and residuals tell otherwise. Observations for this site are from the accelerometer but H/V amplification graphs were created with data from both accelerometer and seismometer. Also residuals were calculated with both Vs30=800 m/s and Vs30=400 m/s to compare.

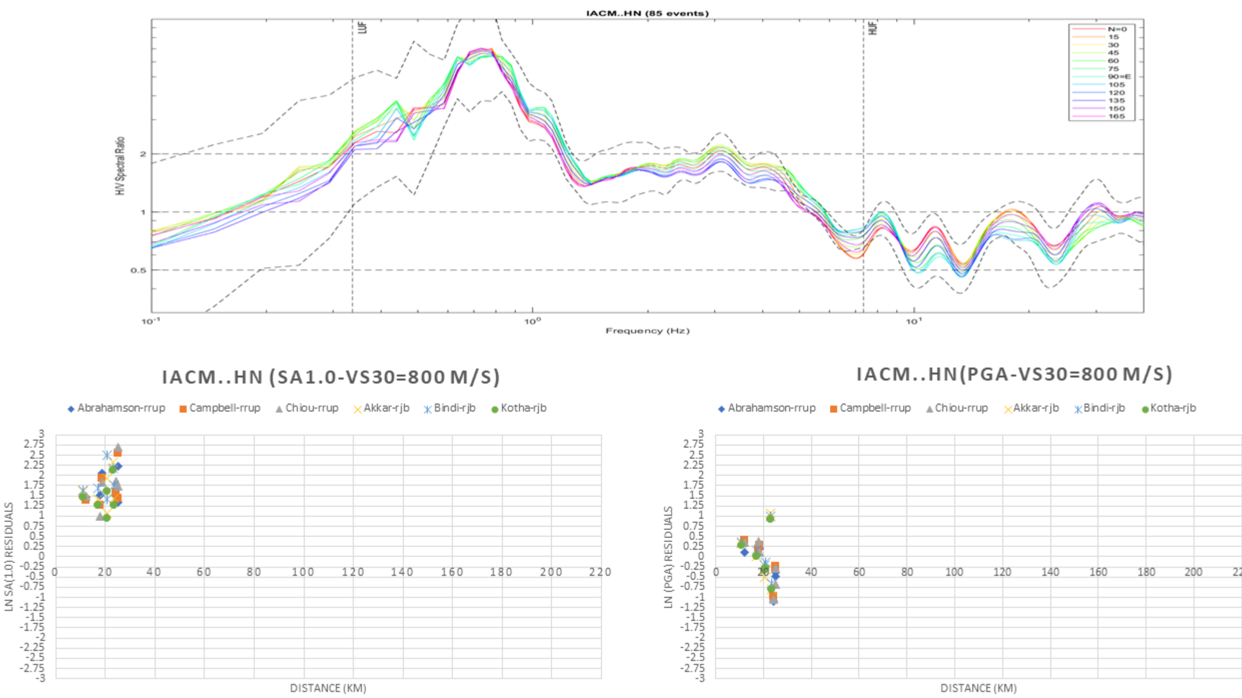


Figure 5.4: IACM..HN H/V and Residuals with Vs30=800 m/s

H/V amplification graph created by accelerometer data has a strong amplification between 0.5-1.2 Hz. Amplitude is around 3 for 0.5 Hz, then it goes up to 7 around 0.6-0.7 Hz (predominant frequency) and goes down to 3 again around 1.2 Hz and then becomes flat and remains between 1.2-6 Hz and keeps gets between 0.5-1 in higher frequencies. Since Vs30=815 m/s according to ESM Database we expect the amplitude to remain between 0.5-2 normally. This type of H/V amplification is closer to be a type C. Also residuals calculated with Vs30=800 m/s supports this. Residuals for PGA are between -1.1 and 1.1 and averaged close to zero. This is expected since H/V amplification is between 0.5-2 amplitude for high frequencies. But SA(1.0 sec) residuals, which is included in the strong amplification frequency range of H/V , are between 1 to 2.75 and average around 1.5, which means GMPEs are underestimating with Vs30=800 m/s and there is much more amplification than expected. To get a better idea on this, residuals were also calculate with Vs30=400 m/s as well.

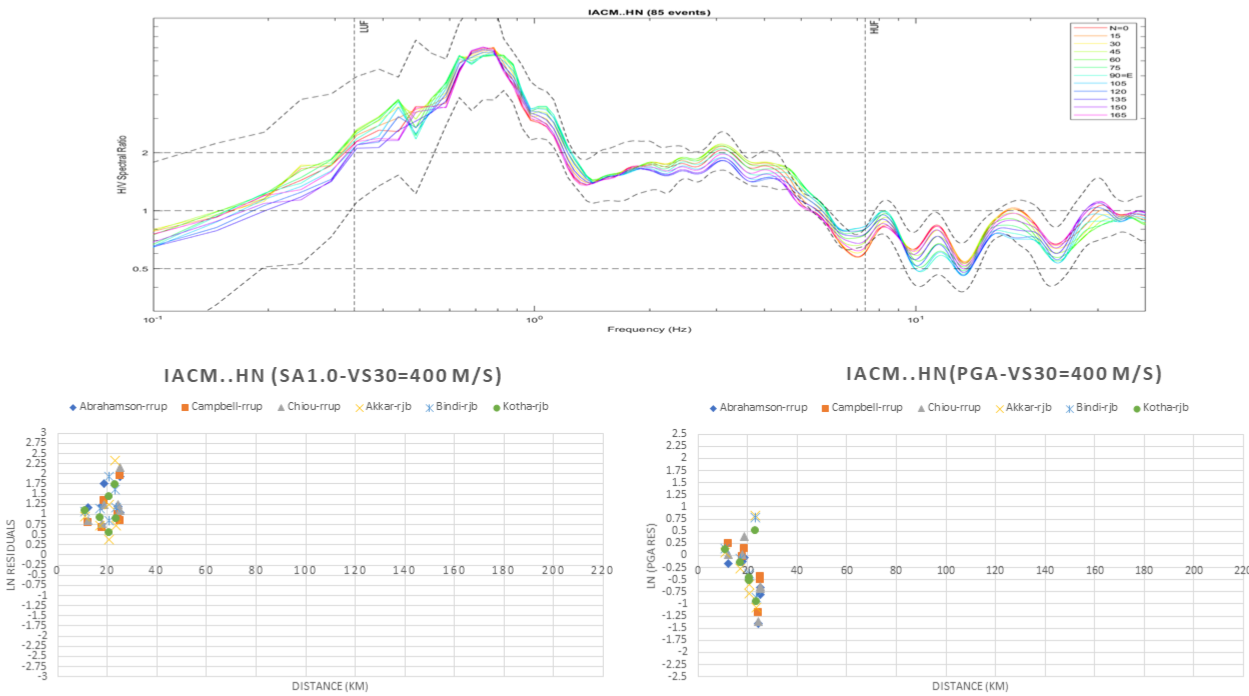


Figure 5.5: IACM..HN H/V and Residuals with Vs30=400 m/s

Residuals with Vs30=400 m/s are lower than Vs30=800 m/s as expected but still for SA(1.0) they are between 0.3 to 2.3 and averaged around 1.3. This result tells us that GMPEs are still failing to predict the amplification on the site with Vs30=400 m/s so this also makes the possibility higher that site is not type A, it is most probably a type C.

Since this site also has a seismometer, even though there is no data from the earthquake sequence, with data of previous events, an H/V amplification graph was created also for IACM..HH. It seems almost identical in character with the H/V amplification graph of IACM..HN so this also supports the conclusion of a type C profile for the site.

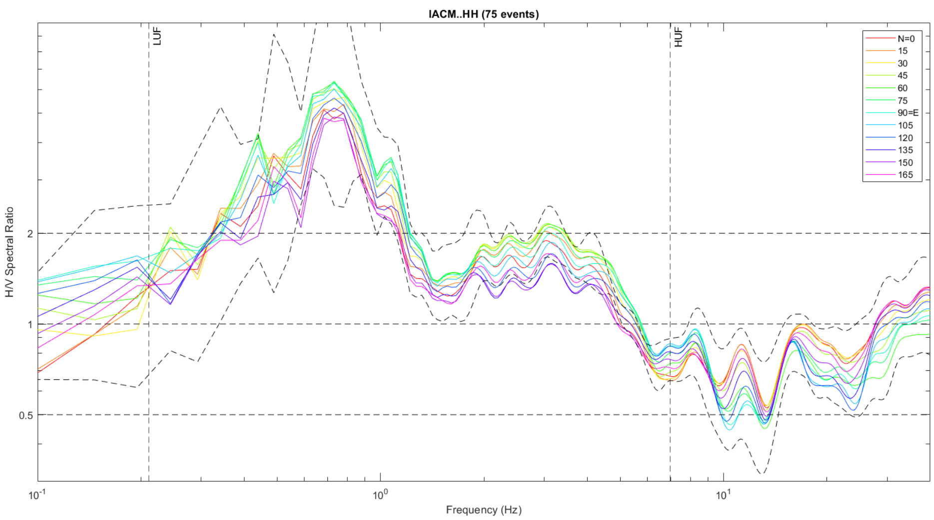


Figure 5.6: H/V Fourier Amplification Graph for IACM..HH

**SIT2..HN**

SIT2 is the only station in this research that just has an accelerometer. Station is operated by ITSAK (HI, ITSAK Strong Motion Network) and located at Town Hall of Siteia, Lasithi. Station is very close to the sea and it has an elevation of 0 meter. Measured Vs30 for the site is told as 378 m/s according to ESM Database so the site is type B and it is closer to type C. With this Vs30, With this Vs30, strong amplification is expected on the site and results of H/V analysis supports this. H/V ratio of the station reaches to 3 at 0.9 Hz and keeps going up till 6-7 amplitude at 1.3-2.5 Hz. Dominant frequency is also in this frequency range. H/V then goes down to 2 at 3 Hz and even to 0.5 at around 4 Hz and shows no amplification for the higher frequencies. This kind of amplification matches with the soil profile B with Vs30=378 m/s.

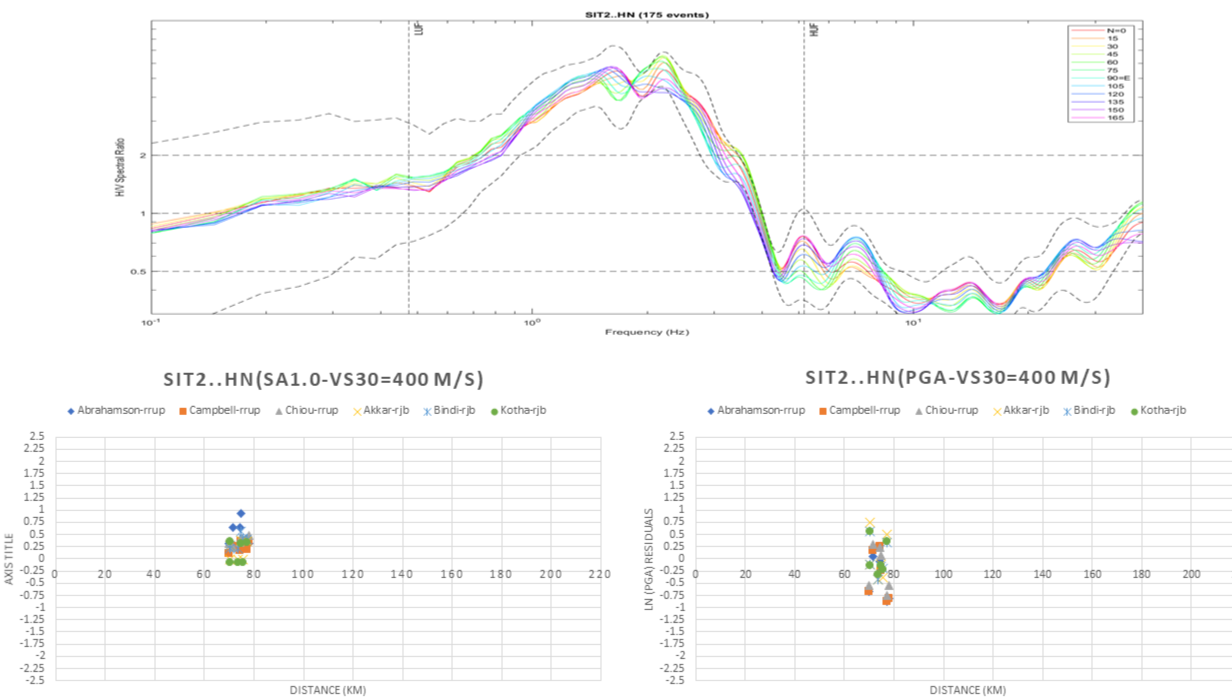


Figure 5.7: SIT2..HN H/V and Residuals with Vs30=400 m/s

Residuals for PGS -0.7 and 0.74 and average is -0.15 so GMPEs are predicting PGA just fine with Vs30=400 m/s. SA (1.0 sec) residuals are between -0.066 and 0.92 and averaged at 0.3. Even though this means observations are a bit higher, GMPE predictions are adequate with this amount of average residual just fine.

**SIVA.00.HN**

SIVA has both accelerometer and seismometer and it is operated by National Observatory of Athens in Hellenic Strong Motion Network, HL, in Sivas, Crete. According to accelnet.gein.noa.gr station has a geology of limestone. ESM Database says Vs30 of the site is 257 m/s and there is a conflict between these. For limestone, we expect little or no amplification but 257 m/s of Vs30 is type C and strong amplification is expected for such a site. H/V amplification graphs for the site were created both by using the data from seismometer and accelerometer but the residual analysis was made only with accelerometer data since there was no data from seismometer for the 6 chosen sequence earthquake. Residuals were calculated with both Vs30=400 m/s and Vs30=800 m/s of GMPE predictions to check which info is more close to be correct.

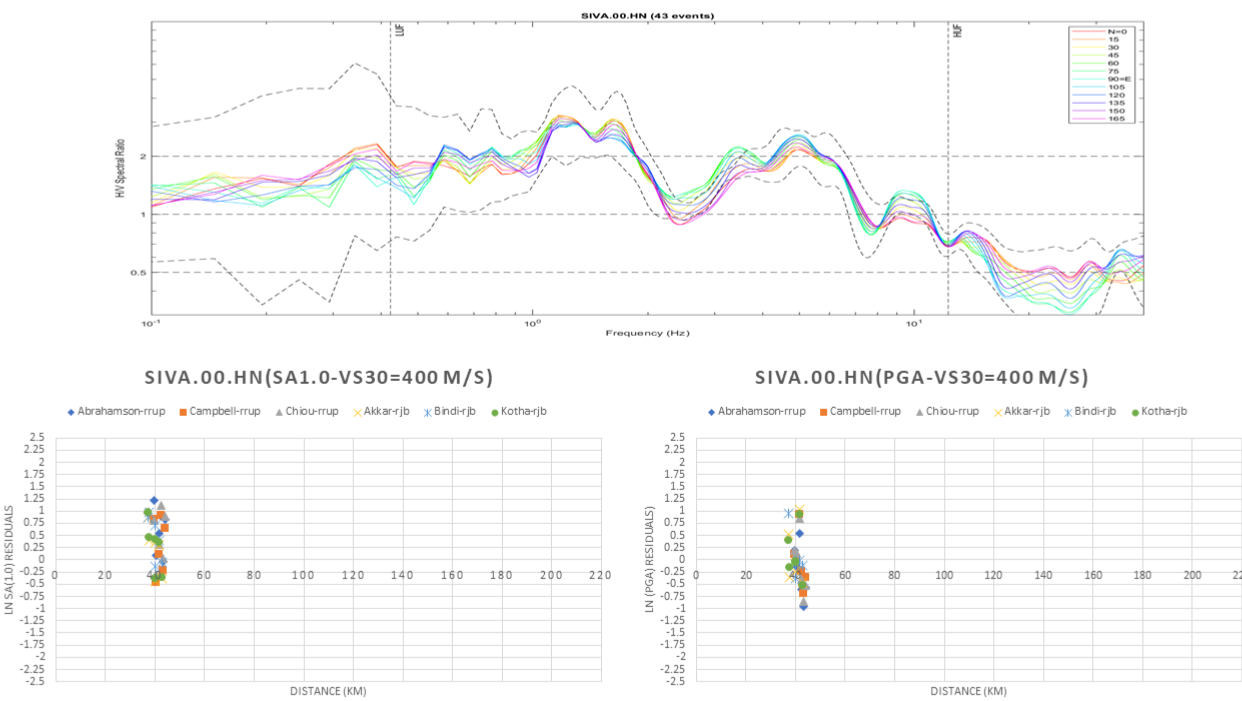


Figure 5.8: SIVA.00.HN H/V and Residuals with Vs30=400 m/s

H/V amplification graph of HN shows amplification between 1-2 Hz and it reaches the maximum 3-3.2 at around 1.2 and 1.7 Hz. This gives us a clue on that site might not be a limestone (rock) profile. Residuals with Vs30=400 m/s are between -0.43 and and 1.21 with 0.37 average. Sa(1.0) is in that amplification region of the amplification graph, even though GMPEs seem to underestimate with Vs30=400 m/s, 0.37 is an acceptable value. PGA residuals are between -0.61 and 1.03. Average residual for PGA is -0.01, which is almost zero so PGA is well predicted with Vs30=400 m/s. This might be explained as PHA is in higher frequencies and H/V goes down in amplitude in higher frequencies.

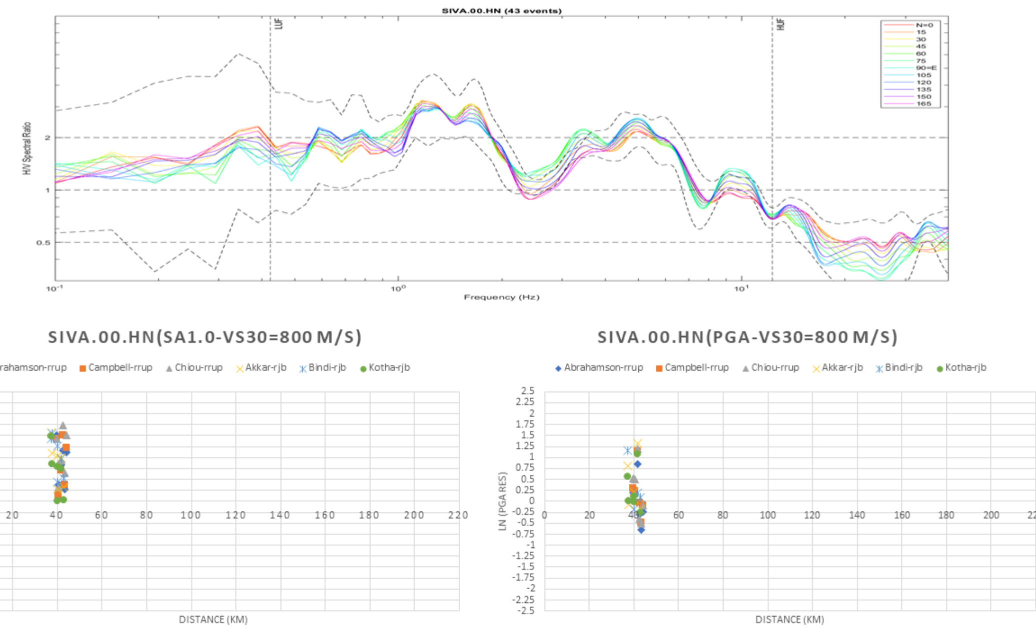


Figure 5.9: SIVA.00.HN H/V and Residuals with Vs30=800 m/s

Residuals for PGA with Vs30=800 m/s seem similar to the one with 400 m/s. It is between -0.75 and 1.25 and averaged at 0.2. This value is higher than 400 m/s residual average but it us expected as since 400 m/s includes more amplification than 800 m/s inside.

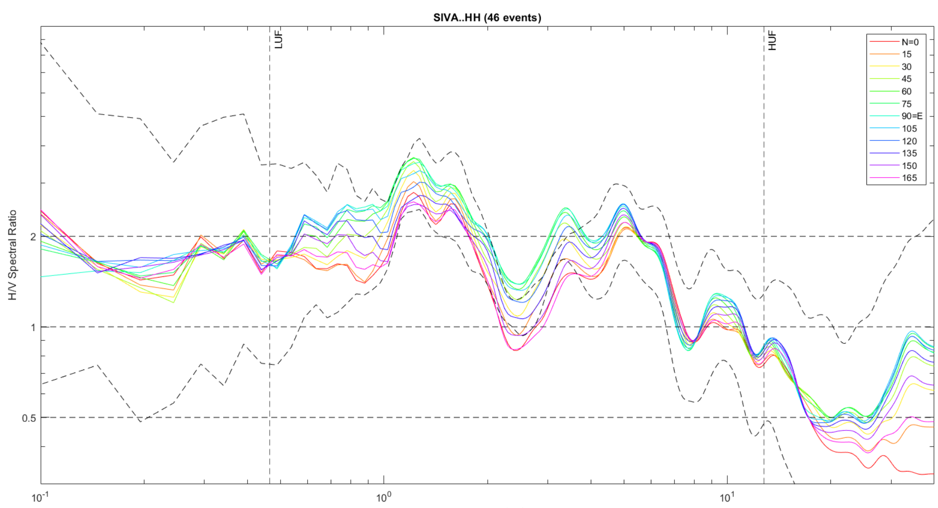


Figure 5.10: H/V Fourier Amplification Graph for SIVA..HH

SA(1.0 sec) residuals are between 0 and 1.75 and averaged around 0.8. This is still less than 1 but still gives us a clue on that 800 m/s Vs30 is not enough to predict accurately as much as 400 m/s so this is another clue that the site is Type C instead of limestone. H/V amplification graph for SIVA..HH from seismometer is almost identical to the one from the accelerometer so this also makes it easier to believe site is more possible to be type C.

### 5.1.2 Reference Stations

**IDI..HH**

IDI..HH is a seismometer operated by National Observatory of Athens and it is in the Hellenic Seismic Network (HL) located in Anogia-Crete. Since it is a seismometer, site is assumed as a rock profile with Vs30=800 m/s so no to low amplification is expected from the site. This Vs30 was also used in all GMPEs for predictions. H/V amplification graph and GMPE residuals calculated using the real data is as below.

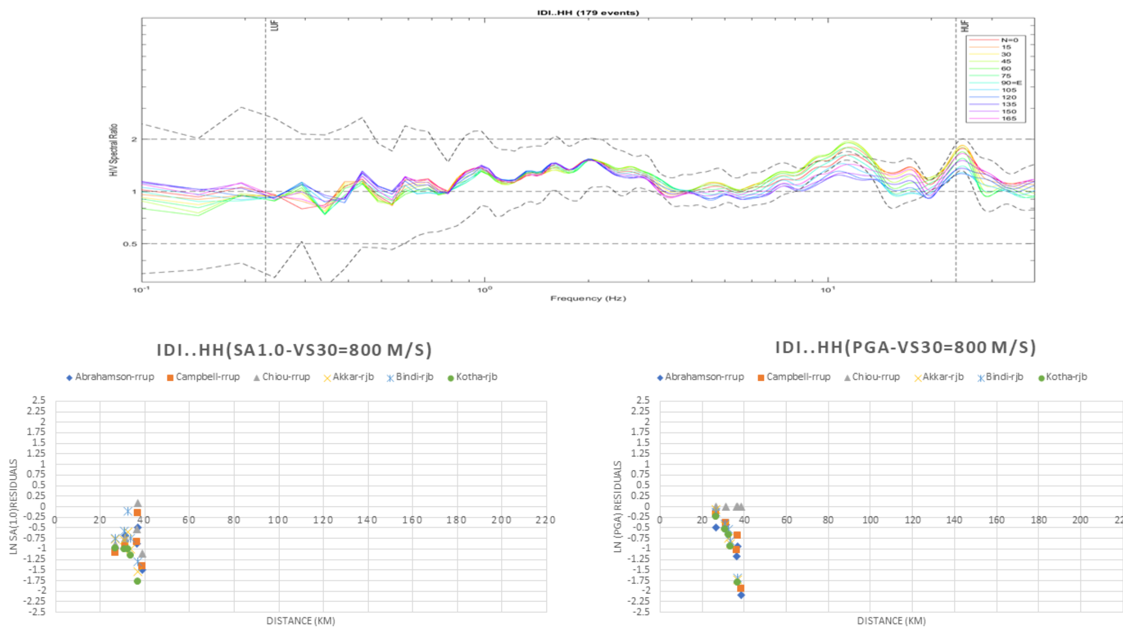


Figure 5.11: H/V and Residuals for IDI..HH

According to this H/V amplification graph since H/V is always around 1 almost for all frequencies, IDI..HH is a perfect reference site with no amplification. Residuals for PGA are between 0 to -2.1 with an average of -0.84 and residuals for SA(1.0) are between 0 to -1.75 with an average of -0.89. This same values of residuals also gives a hint about the flatness of this reference station both in low and high frequencies. We can also say that GMPEs are a bit overpredicting or maybe the site Vs30 is even higher than 800 m/s.

**NPS..HH**

NPS..HH is a seismometer station operated by National Observatory of Athens (HL network) in Neapolis, Crete. Since it is a seismometer, site is assumed as rock profile with Vs30= 800 m/s. According to this assumption, no or very low amplification is expected. By using the data from this station, results for H/V amplification graph and GMPE residuals are as in the figure shown below.

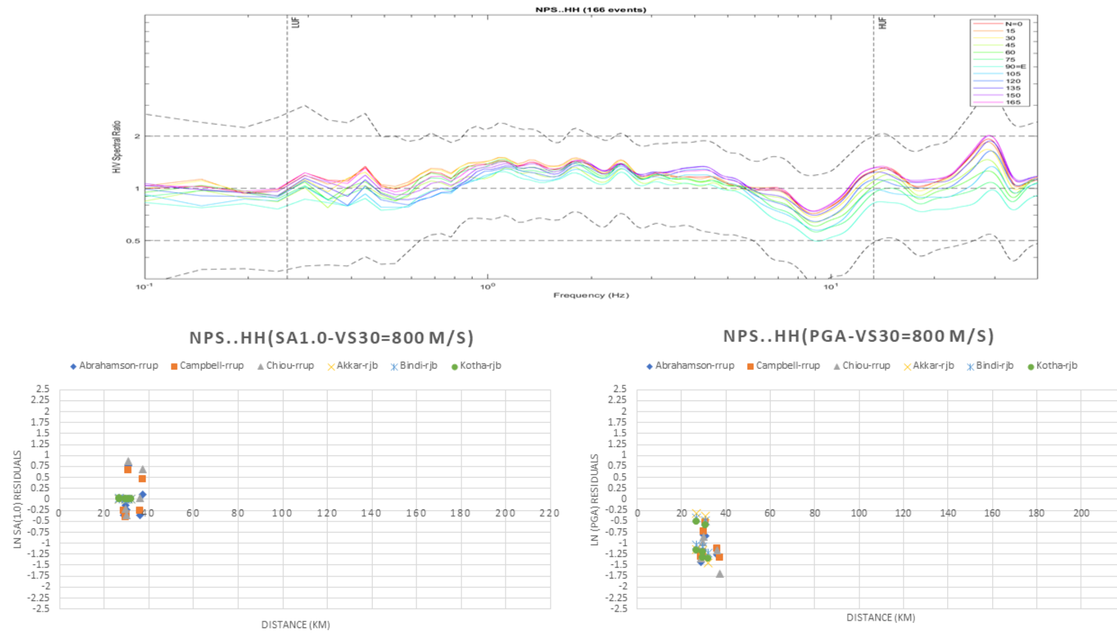


Figure 5.12: H/V and Residuals for NPS..HH

This station also acts as a perfect reference station until 7 Hz since H/V is flat around 1 to 1.4. After 6 Hz there is also directional sensitivity and after 7 Hz there is a small deamplification but till the highest usable frequency, H/V reaches 1 again. SA(1.0 sec) residuals are between -0.77 to 0.97 with an average of 0.01 which means models are predicting the SA(1.0) adequately. For PGA, residuals are between -0.31 to -1.69 and the average is around -1. It can be said that models might overpredicting the PGA a bit, but since it might be located in higher frequencies a certain comment cannot be made.

**VAM..HH**

This station is a seismometer located in Vamos, Crete and operated by National Observatory of Athens. There is no measured Vs30 for the site but since it is a seismometer, it is assumed as a rock profile and Vs30 = 800 m/s was used for GMPE predictions. With this assumption none or little amplification is expected on the site.

H/V amplification graph of the station is mostly flat and between 1 and 2 so the station can also be used as a good reference station. Around 0.4-0.5, 1, 5 and 7 Hz amplification reaches the marginal value of 2. Like all the other reference stations, since there is almost no amplification, we can not talk about a predominant period for the site. Also there is directional sensitivity between 4-10 Hz but this also does not move the amplification out of 1 or 2 H/V ratio. SA(1.0) residuals are between -0.44 to 1.61 and averaged around 0.6. At SA(1.0) H/V also reaches to marginal 2 value, which is larger than most of the other steady frequencies so this small underestimation of GMPEs can be explained with this. For PGA, minimum residual is -0.92 and

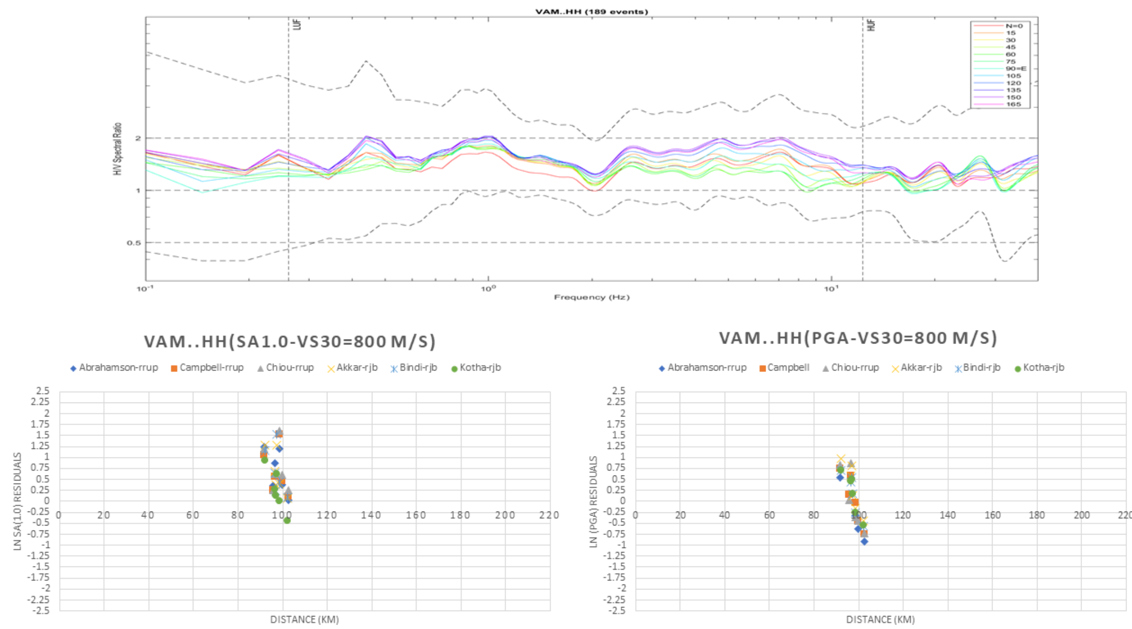


Figure 5.13: H/V and Residuals for VAM..HH

maximum is 0.97. There are various residuals dispersed in between but averaged at 0.1 so it can be said that GMPEs are predicting PGA adequately.

**RODP..HH**

This station is also a seismometer located in Rodopos, Crete. It is counted as a rock profile with Vs30=800 m/s like the other seismometer operating stations. It belongs to the network HC, Seismological Network of Crete. This station was also classified as a reference station according to the analysis results in the below figure.

H/V amplification graph is almost flat and always between 1 and 2 from the lowest usable frequency 0.287 Hz till highest usable frequency 13.05 Hz so this makes it a good reference station. There is no directional sensitivity. H/V's peak is in between 1.3 Hz to 3 Hz with an H/V close 1.7-1.8, which is close to the borderline but still does not count as an amplification. Around 13 Hz H/V reaches to 2 and with higher frequencies some amplification is observed but since the highest usable frequency was calculated as 13.05 after signal processing, those frequencies cannot be trusted. PGA residuals are dispersed between -1.1 and 1.15 and averaged at almost zero (0.02) so GMPEs can be considered to estimate PGA with Vs30=800 m/s. SA(1.0 sec) residuals are all above zero except one value of -0.44 and highest residual is 1.61. Average is 0.61. This means that there is a bit higher amplification for SA(1.0 sec) than the models average prediction. This can not be explained by H/V amplification graph since it shows almost no amplification in this period.

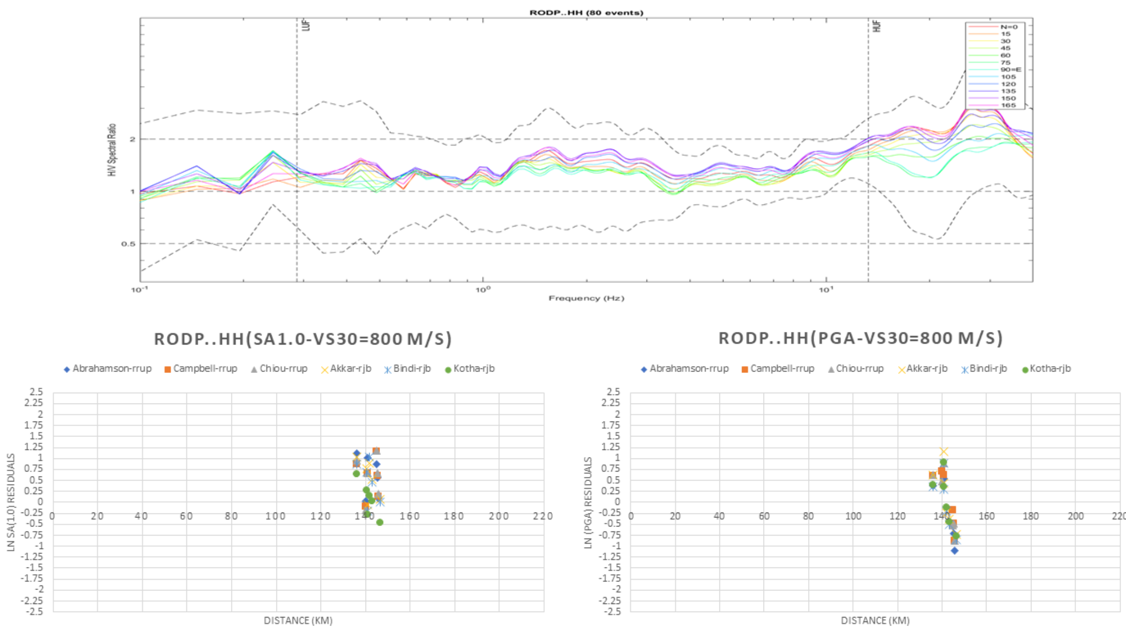


Figure 5.14: H/V and Residuals for VAM..HH

### 5.1.3 Stations with Flat H/V Ratio which Decreases with Higher Frequencies

**CHAN..HH**

This station is in Seismological Network of Crete (HC) and it has a seismometer operated by Technological Educational Institute of Crete. It is located in Chania, Crete. Considering the seismometer set up, site is assumed to have a rock profile with Vs30 = 800 m/s in the GMPE predictions.

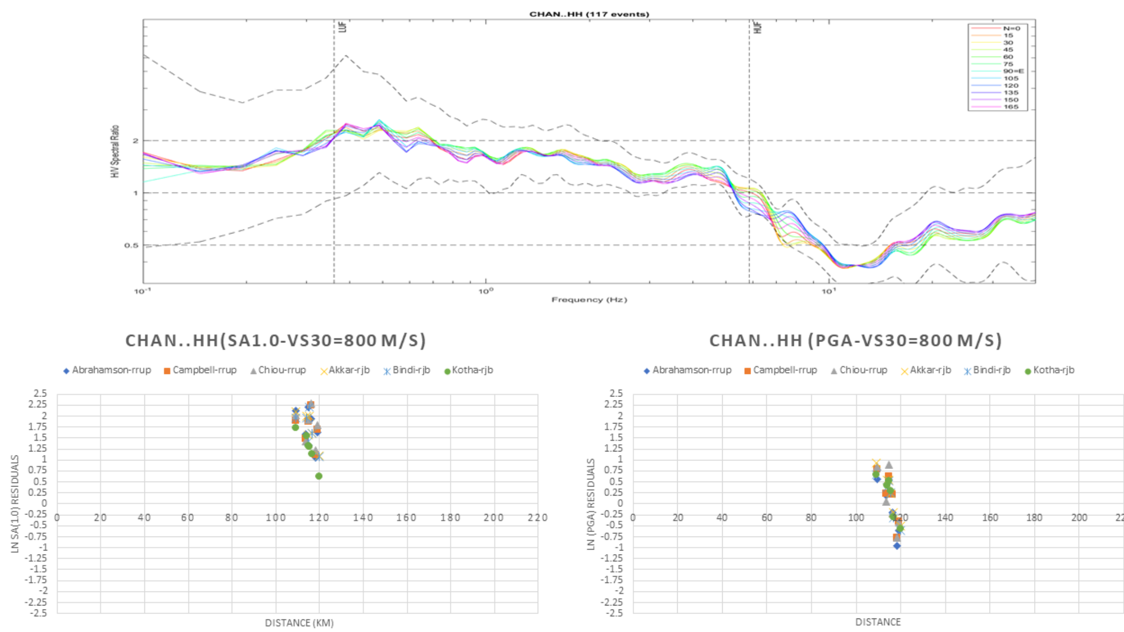


Figure 5.15: H/V and Residuals for CHAN..HH

As shown in the figure, H/V amplification graph has a flat amplification a bit larger than 2 starting from 0.4 Hz till 0.7 Hz and then amplification gradually goes down and reaches to 1 at around highest usable frequency 5.84 Hz.There is no directional sensitivity. PGA residuals are dispersed between -1 and 1 and averaged at 0.1. This shows us that GMPEs can predict the PGA adequately with Vs30 of 800 m/s. SA(1.0) residuals are between 0.64 to 2.2 and averaged around 1.65. With this value of residuals, one would expect higher amplification for SA(1.0) than the amplification around 2 for 1 Hz on the H/V, GMPEs are underpredicting.

**KNDR..HH**

KNDR..HH is a seismometer operated by Technological Educational Institute of Crete inside the Seismological Network of Crete (HC). It is located at Paleochora-Chania, Crete. For this station, no or little amplification expected due to the assumed rock profile with only seismometer set up. Vs30 was inferred as 800 m/s in the GMPE predictions for the station. Results after the H/V Fourier and residual analysis for the station are shown below.

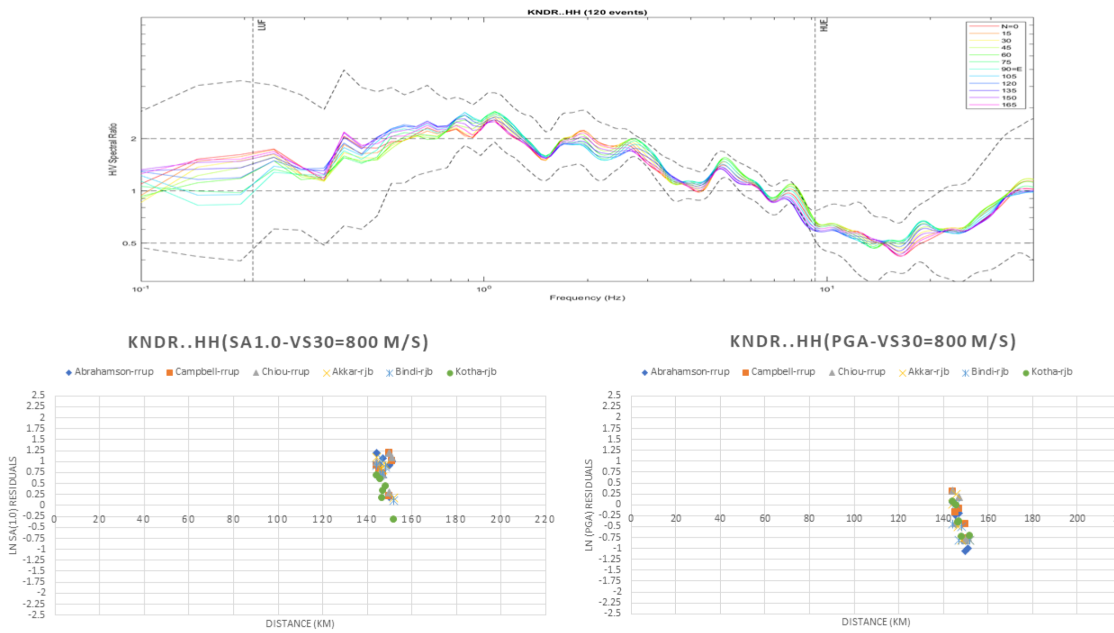


Figure 5.16: H/V Fourier and Residual Results for KNDR..HH

H/V increases to marginal 2 at around 0.4 Hz and is flat until 1.5 Hz between 2-2.5 ratio, then it starts decreasing with higher frequencies. Close the lowest usable frequency 9.3 Hz it reaches 1 and keeps going down 17-18 Hz. Directional sensitivity is very low between LUF and HUF. REsiduals for SA(1.0 sec) are between -0.32 and 1.19 and average value is 0.72. These are acceptable value for GMPE predictions considering the flat small amplification between 0.4 to 1.5 Hz. PGA residuals are between -1.05 to 0.32 and average is -0.4. This also can be explained by the decreasing H/V ratio in higher frequencies where we might seek for the PGA. GMPE predictions are adequate for PGA considering PGA residuals as well.

**IMMV**

This station has both seismometer and accelerometer operated by National Technical University of Athens in the Hellenic Seismic Network (HL).It is located in Iera Moni Varipetrou, Crete. According to the ESM (Engineering Strong Motion) Database station is Eurocode type A with 948 m/s Vs30 value. With this information, we expect no amplification on site.

H/V analysis for the station was done separately from both accelerometer and seismometer data but residual analysis was made only with accelerometer data since there was no data available from the 6 events of the Arkalochori sequence.

H/V ratio seems to reach at maximum of 2 around 0.4 Hz and goes around it till 1.5 Hz but then starts to decrease to around 1 gradually. There is no significant di-

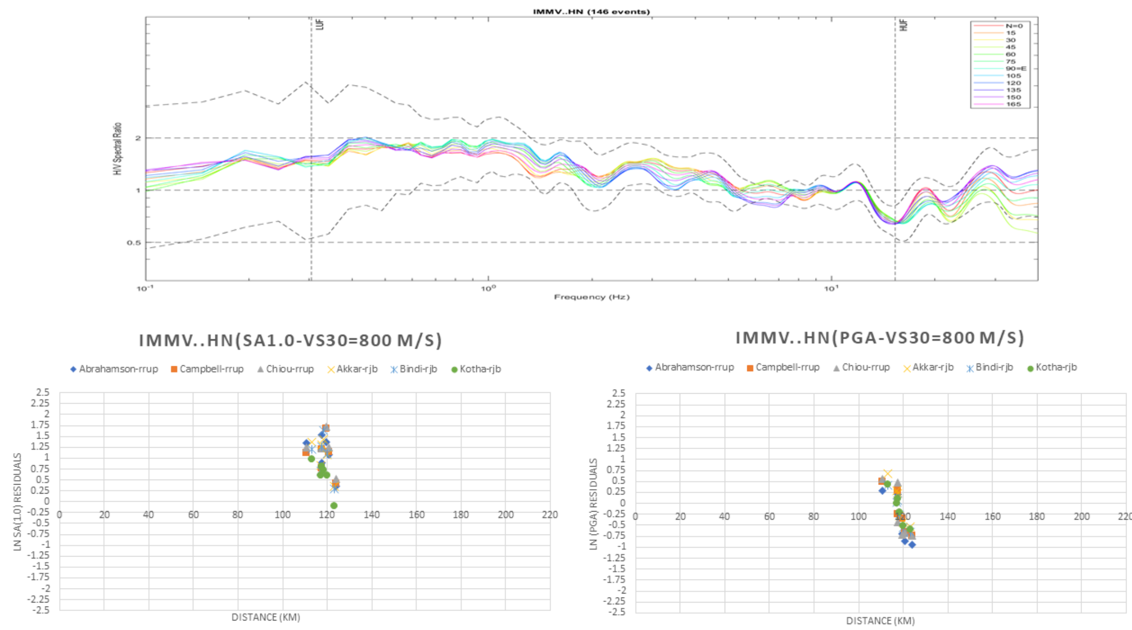


Figure 5.17: H/V Fourier and Residual Results for IMMV..HN

rectional sensitivity. Amplification graph seems to be flat but decreasing with higher frequencies as mentioned in the classification. Since amplification is always around between 1 and 2 starting from LUF and until HUF, we can say that type A classification for the site seems accurate. Residuals for SA(1.0) of IMMV..HN is between -0.1 and 1.72 and average value is 1. Since the site has almost no amplification, this is surprising and we can say that GMPEs are underpredicting the Sa(1.0) even though a lower value than site's Vs30 was used. Using Vs30 as 948 m/s instead of 800 m/s would bring less site effect (amplification) and GMPEs would predict the SA(1.0 sec) even less. For PGA, residuals are between -0.94 and 0.68 and average is -0.19. This can tell us for PGA, GMPE predictions are adequate and even using the 948 m/s instead of 800 m/s can make it more accurate by bringing predictions closer to the observations. This difference in residuals for SA(1.0) to PGA can be explained by the decreasing H/V ratio with the increasing frequencies.

Figure above is the H/V Fourier results for IMMV station by using the data from the seismometer. By comparing both amplification graphs, it is easily seen that they are almost identical and have the same character.

**STIA..HH**

STIA station is another station with only seismometer, located in Sitia Town in Crete. It is operated by Technological Educational Institute of Crete inside the Seismological Network of Crete (HC). It is also assumed as a rock profile with Vs30=800 m/s like the other only seismometer stations, with little or no amplification expectation.

H/V amplification graph of the station does not have significant amplification as

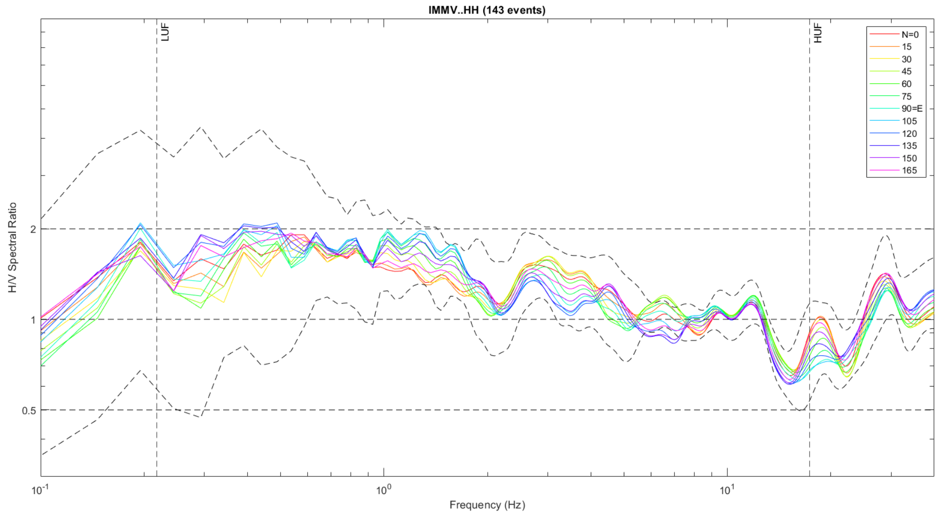


Figure 5.18: H/V Fourier Amplification Graph for IMMV..HH

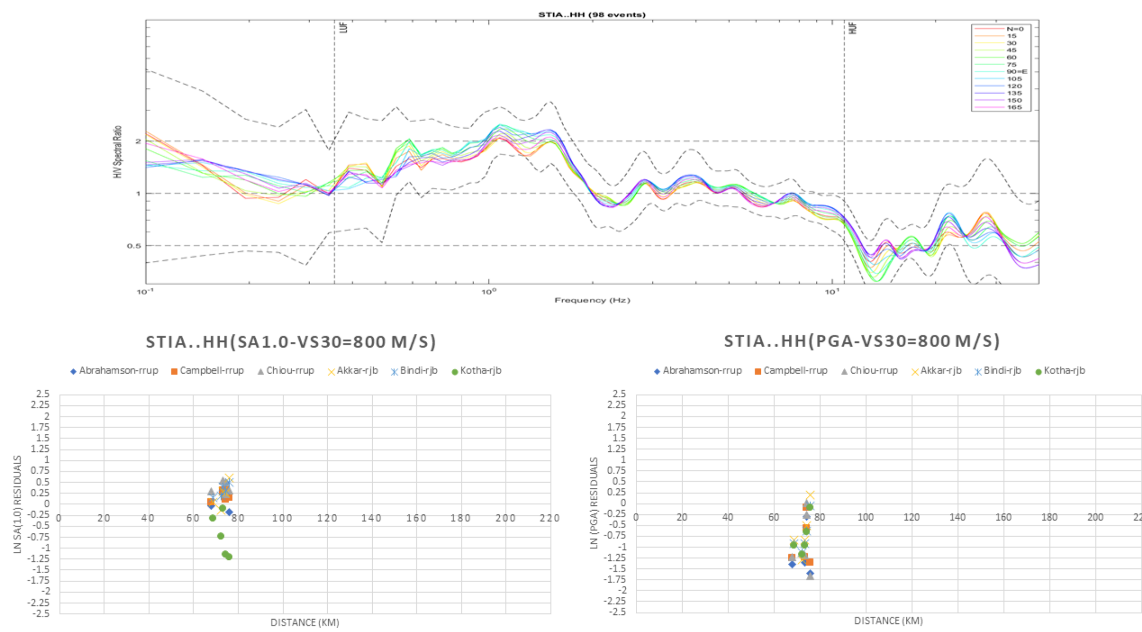


Figure 5.19: H/V Fourier Amplification Graph for IMMV..HH

expected. It is almost flat with a maximum amplification of 2.1-2.2 between 1 Hz to 1.7 Hz but rather than that it is always between 1-2 H/V ratio after 1.7 Hz it is decreasing to 1 at 2 Hz and stays around it till the highest usable frequency 10.8 Hz. It is decreasing again to 0.5 after HUF but since frequencies at that range might not be reliable it is not our concern. Since there is no significant amplification as it remains between 1-2, our rock profile assumption seems correct.

SA(1.0 sec) residuals are between -0.72 and 0.597 and averaged at 0.1. From this result we can say that GMPEs are predicting the SA(1.0) just fine. PGA residuals are between -1.65 to 0.194 averaged at -0.82. This might be explained with the decreasing H/V ratio with the increasing frequencies on the amplification graph but since data might not be reliable after HUF and we are not sure about the PGA's frequency, only know that it is most probably at a high frequency than HUF, this remains as a possibility.

### 5.1.4 Stations with Small Broadband Amplification

**GVDS..HH**

GVDS is a seismometer station in the Gavdos Island, which is located in the south of Crete Island. This station is the most distant station in this assessment and it is operated by Technological Educational Institute of Crete inside the Seismological Network of Crete (HC). Since the only instrument installed is seismometer, we can again assume rock profile for the station with Vs30=800 m/s to use in the GMPE predictions and none to low amplification on the site is expected.

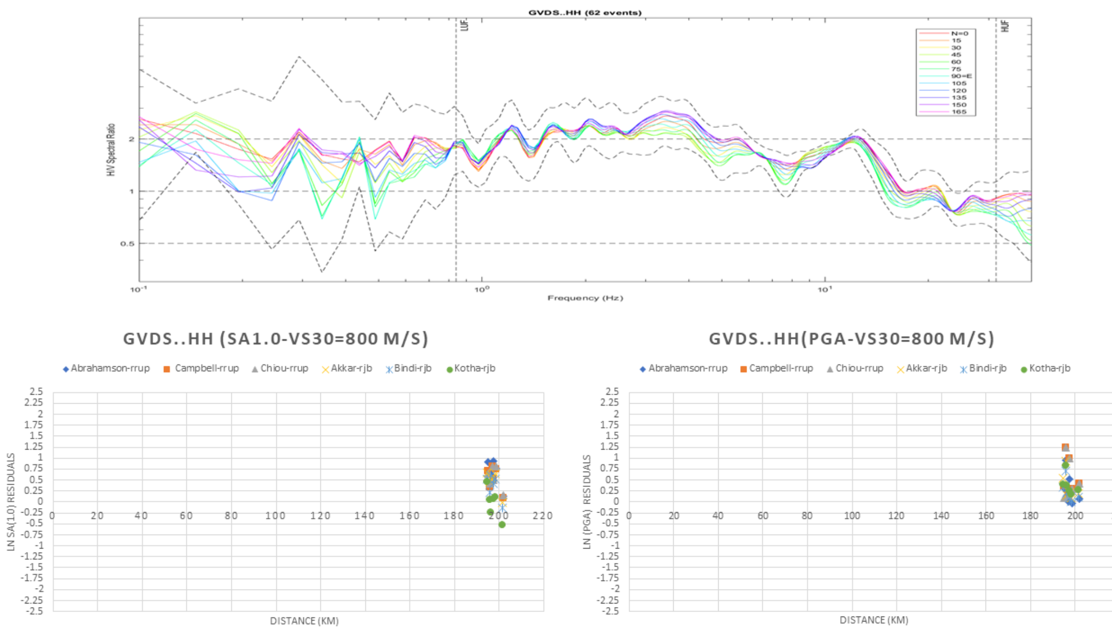


Figure 5.20: H/V and Residuals for GVDS..HH

H/V results show that there is a small broadband amplification between 1.3-5 Hz around 2 to 2.5. After 5 Hz, amplitude lowers but still remains between 0.5 and 2. Such a behaviour is acceptable with the rock profile assumption since the amplification is not that high. SA(1.0 sec) residuals are between -0.53 and 0.93 and average of all residuals is 0.43. PGA residuals are also similar and between -0.03 and 1.24 and the average is 0.39. Since small amplification of 2-2.5 was not reached at 1 Hz yet and also after 5 Hz we see a drop on amplification less than 2 again through the higher frequencies, similar behaviour of SA(1.0) and PGA can be explained. Observations are higher than the models but still since the average of both PGA and SA(1.0) is not that high, GMPEs are predicting the both intensity measures adequately.

**IMOD..HH**

This station is a seismometer operated by Technological Educational Institute of Crete and in the Seismological Network of Crete (HC). Since it is a seismometer it is also assumed as a rock profile with Vs30=800 m/s. It is in Iera Moni Odigitrias, Herakleion, Crete. Considering the seismometer and assumed rock profile, first impression is to expect no to low amplification on the site.

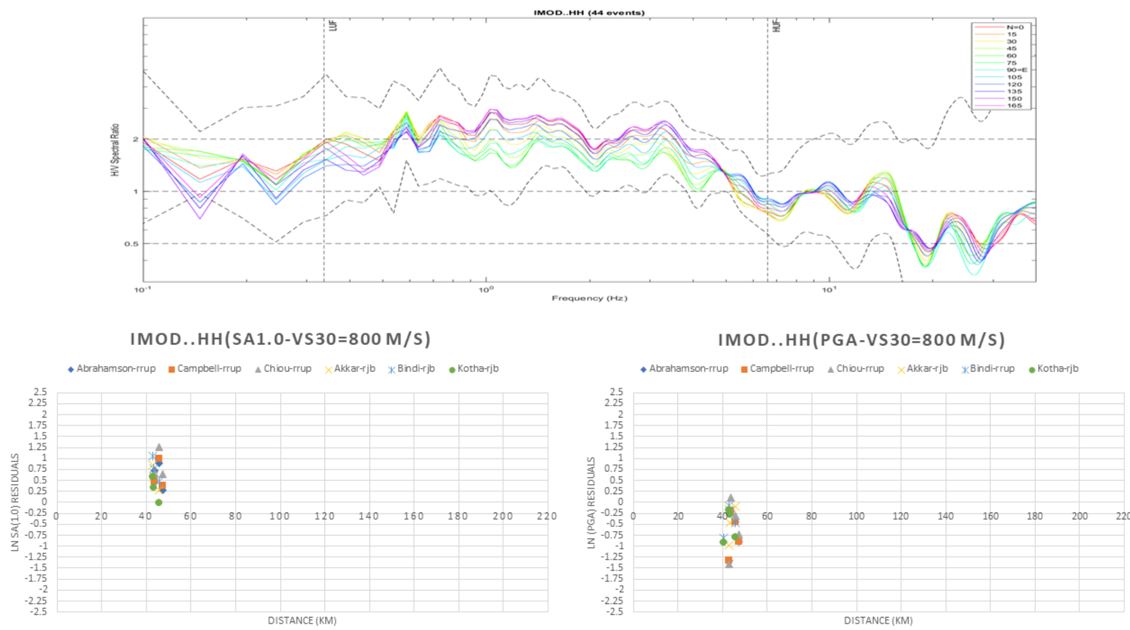


Figure 5.21: H/V and Residuals for CHAN..HH

After checking the created H/V amplification graph for the station, there is small broadband amplification which is 2 to 2.7 between 0.33 Hz and 3.5 Hz and then with higher frequencies this small amplification diminishes to 1 and even less. This is an acceptable amplification behaviour for a rock profile with Vs30=800 m/s, borderline of type B and A. There is an acceptable level of directional sensitivity on the amplification graph as well.Residuals for SA(1.0 sec) are between -0.006 to 1.27 and averaged at 0.62. Small amplification on this assumed rock profile seems to be underestimated by the average of GMPEs. Residuals for PGA are between -1.4 to 0.12 and averaged at -0.53. This can be explained the diminishing of the amplification at the higher frequencies.

**PFKS..HH**

This station is located in Pefkos, Crete and operated by Technological Educational Institute of Crete in the Seismological Network of Crete (HC). It has an operating seismometer and like all the other only seismometer stations, it is assumed to have a rock profile with Vs30=800 m/s. Expected amplification before the analysis is very low. This station does not have usable data from the main shock and the largest aftershock of Mw=5.3 so residual analysis was made with 4 aftershocks of Mw=4.4-4.5 and 4.6. For the H/V analysis 137 events were used and results are both are shown in the figure below.

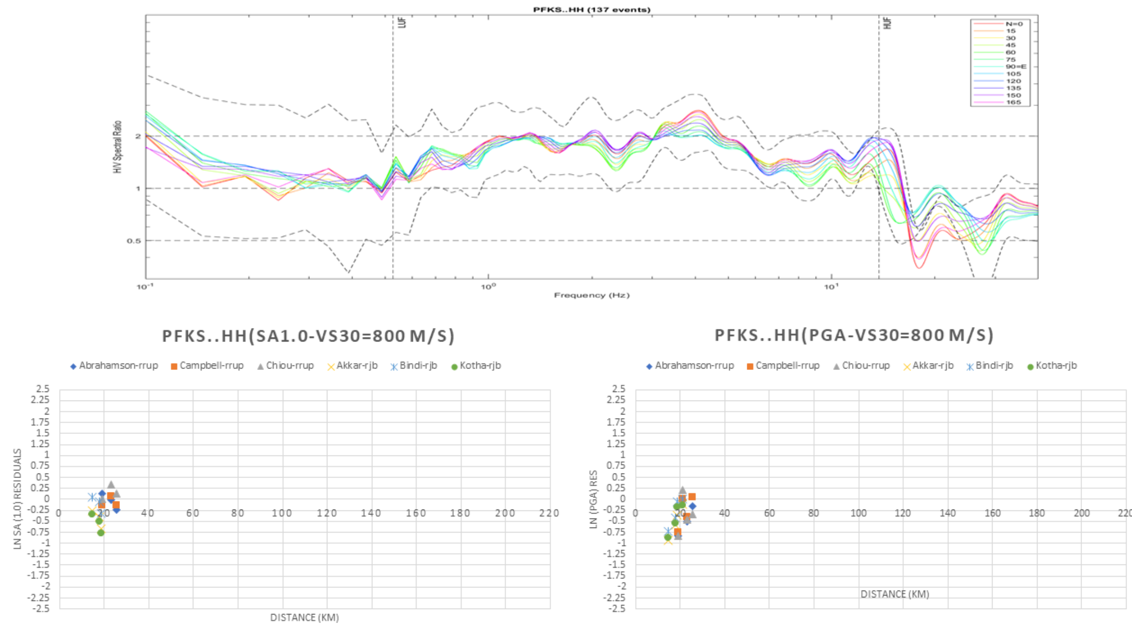


Figure 5.22: H/V and Residuals for PFKS..HH

H/V of the station reaches at 2 around 1 Hz and remains almost flat until 5 Hz. Then it drops around 1.5 Hz and reaches back to 2 at highest usable frequency value 13.7 Hz so we can say the station has a small broadband amplification and this is acceptable for the rock assumption made at the beginning. Residuals for PGA and SA(1.0 sec) shows very similar behavior as well. SA(1.0 sec) residuals are between -0.77 and 0.34, averaged at -0.17 and PGA residuals are between -0.93 and 0.21 and averaged at -0.37. From these values, we can conclude that GMPEs are adequate in predicting SA(1.0) and PGA with Vs30=800 m/s. Also we can say that small broadband amplification might keep going through the higher frequencies which include PGA.

### 5.1.5 Station with a Likely Error in Sensor or Metadata

**ZKR**

This station is operated by National Observatory of Athens and it is located in Zakros, Crete. It has both seismometer and accelerometer. In the data set provided, there is data from both instruments both from the 6 earthquakes of the Arkalochori sequence there was data only from the seismometer. H/V amplification graphs were created separately for both but for GMPE residuals only seismometer data could be used to investigate the station. In a prepared paper by A. Savvaidis and various researchers in 2013 for Central European Journal of Geosciences, this station was mentioned as Eurocode Type A with a foundation formation of overthrusted limestone. Also Vs30 was mentioned in the same paper as 871 m/s. With this soil profile we do not expect amplification. For the GMPE residuals, Vs30= 800 m/s used both H/V and residual results are on the figure below.

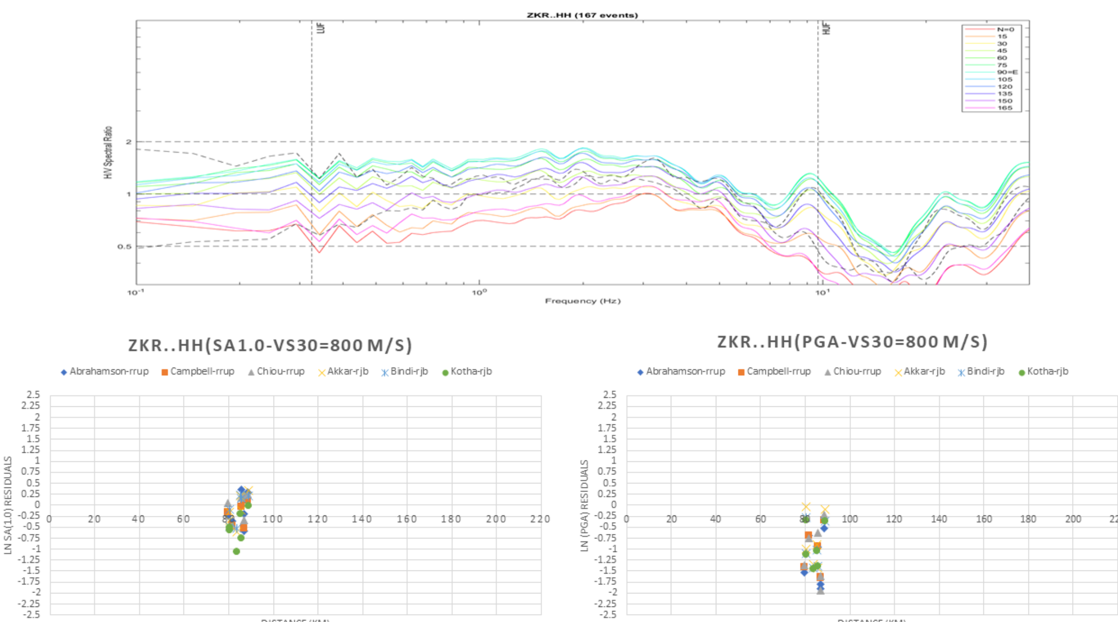


Figure 5.23: H/V and Residuals for ZKR..HH

H/V amplification graph of the seismometer was created by using 167 different events but the result shows a possible sensor error on the station. H/V values goes up in a parallel way in every 15 degrees with a high amount and this can not be explained with directional sensitivity but can be explained with a possible sensor error. Normally when we check the SA(1.0) and PGA residuals made by using the data of this seismometer, we see that observations are well predicted by the GMPEs since measured Vs30 and used value in predictions are close but because of the possible sensor or metadata issue, these observations can not be valid.

If we check the H/V amplification graph created by the data from the accelerom-

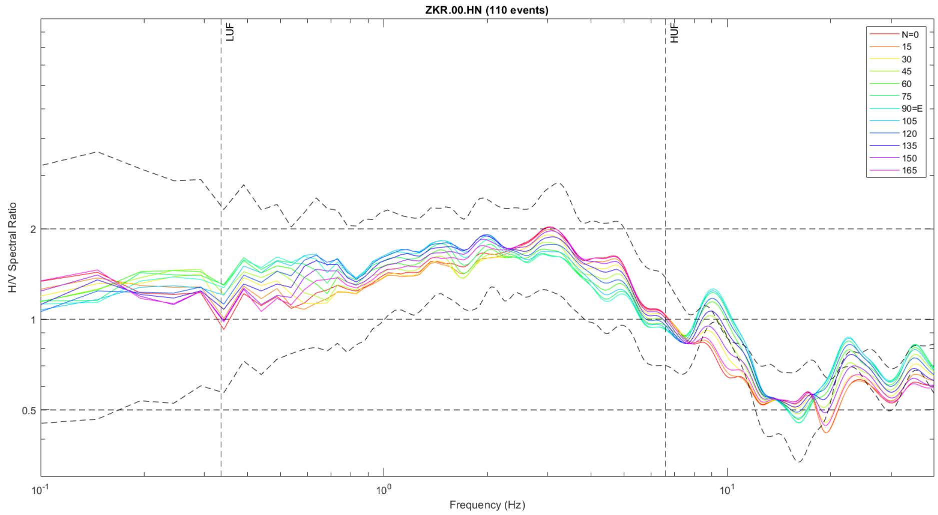


Figure 5.24: H/V and Residuals for ZKR.00.HN

eter, we do not see the same issue and station behaves as a reference station between the 0.33 Hz LUF and 6.6 LUF since the H/V is between 1 and 2. Amplitude makes a peak of 2 at 3-3.5 Hz but which is an acceptable level of amplification for rock sites.

## 5.2 H/V Fourier Analysis Results for Stations with no Arkalochori Sequence Data

**CRE1..HH**

Station is located in Moni Agkarathou, Crete and it is operated by National Observatory of Athens with only seismometer. It is in the Hellenic Seismic Network (HL). It was installed on 28/09/2021, one day after the main shock. Because it is broadbond, this station clipped at the large events chosen from the Arkalochori sequence so it was not used for the residual analysis.

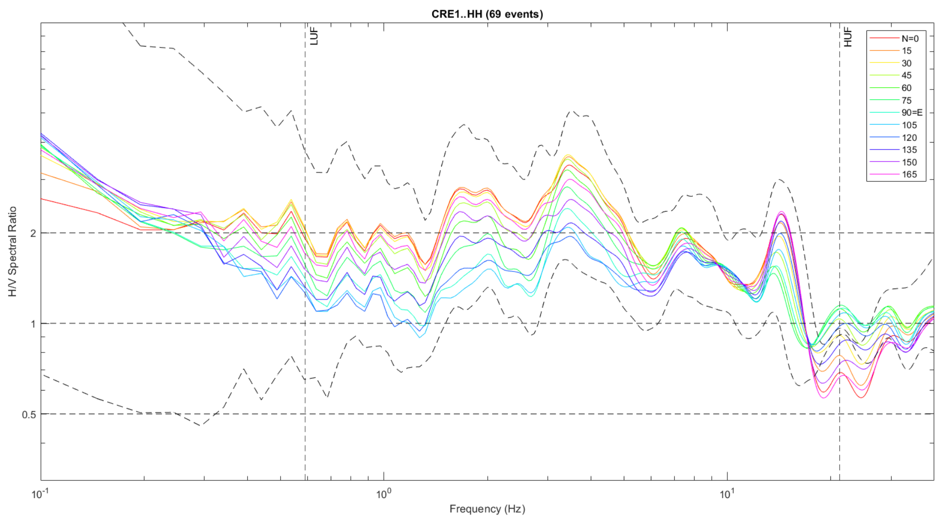


Figure 5.25: H/V amplification graph for CRE1..HH

Station is assumed as a rock site since station is only a seismometer station.There is directional sensitivity in so many frequencies which is not very possible so most probably instrument has a problem and results are not reliable.

**CRE3..HH**

Station is located in Garipa, Crete. It is operated by National Observatory of Athens in the Hellenic Seismic Network (HL). It is a seismometer only station. It was installed on 28/09/2021, one day after the main shock. Station clipped for the events chosen for Arkalochori sequence like CRE1 since it is broadband so residual analysis was not done for it.

Like the other seismometer only stations, soil profile assumed to be rock win the border of Type A and B. Starting from the lowest usable frequency, station seems to have a small broadband amplification around 2 till 4 Hz, then it falls down till 1.5 till the highest usable frequency.

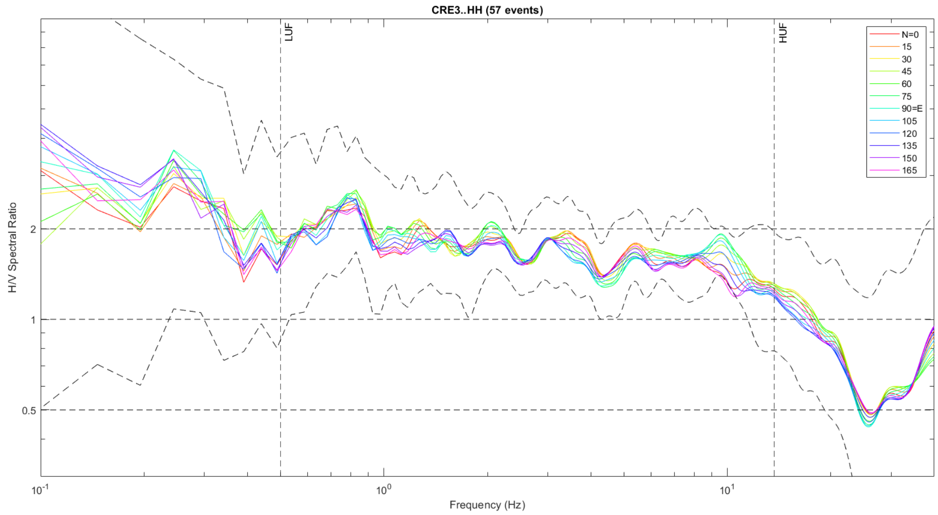


Figure 5.26: H/V amplification graph for CRE3..HH

Since there is small amplification in almost all frequencies (between 1 and 2), assumption of rock soil profile seems valid.

**GVD**

GVD is the only station with GVDS outside the Crete Island and it is located in Gavdos Island. Station is operated by National Observatory of Athens in the Hellenic Seismic Network (HL) and it includes both seismometer and accelerometer.

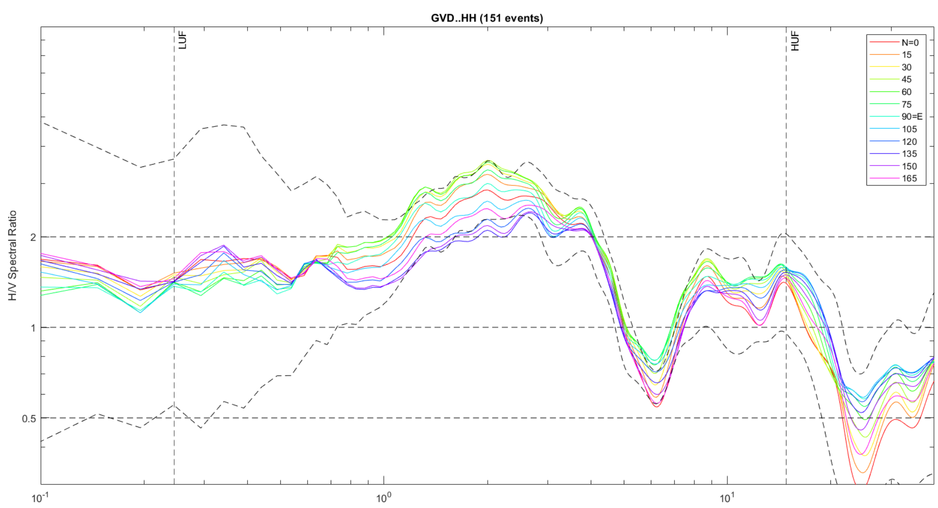


Figure 5.27: H/V Profile for GVD..HH

In ESM database, site is classified as type B with a measured Vs30=427 m/s so amplification is expected on this site. Data from both seismometer and accelerometer were analyzed for this station and results are shown below.HH amplification graph has more directional sensitivity 0.6-3 Hz compared to the HN amplification graph and this can be explained as the seismometers are more sensitive to lower frequencies due to lower sampling rate.

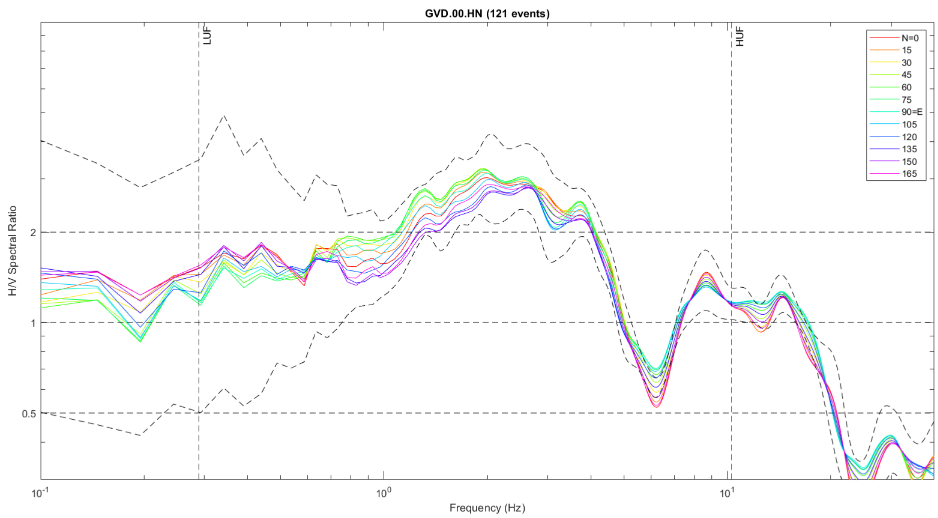


Figure 5.28: H/V amplification graph for GVD.00.HN

Both amplification graphs show similar character and there is amplification around 2.5-3 between 2-3 Hz which gives a clue about the soil type between B and C.

**IMOD..HH**

This is a seismometer station in Iera Moni Odigitrias operated by Technological Educational Institute of Crete in the Seismological Network of Crete (HC). Site is expected to be a rock site due to seismometer.

H/V amplification graph shows directional sensitivity between 0.7 to 5 Hz. Between 0.6-2 there is a broadband amplification between 2.5 to 3, which seems to be high for a rock profile so this gives a clue on that site might have a softer soil profile but this can not be explained just with this H/V analysis.

**IPPL..HH**

Station IPPL is also a seismometer station operated by Technological Educational Institute of Crete in the Seismological Network of Crete (HC). It is located in Tria Monastiria, Rethimno. There is no info about the soil type but it is expected to be rock like the other seismometer stations.

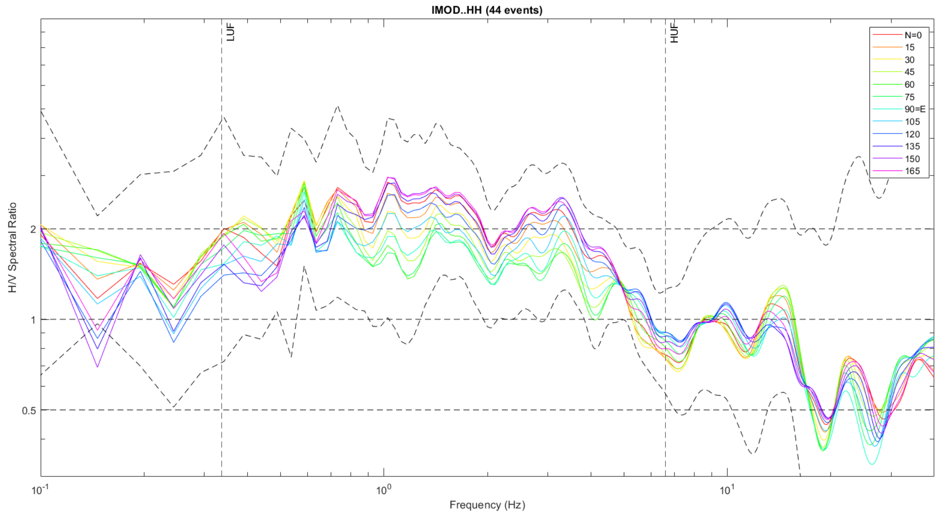


Figure 5.29: H/V and Residuals for IMOD..HH

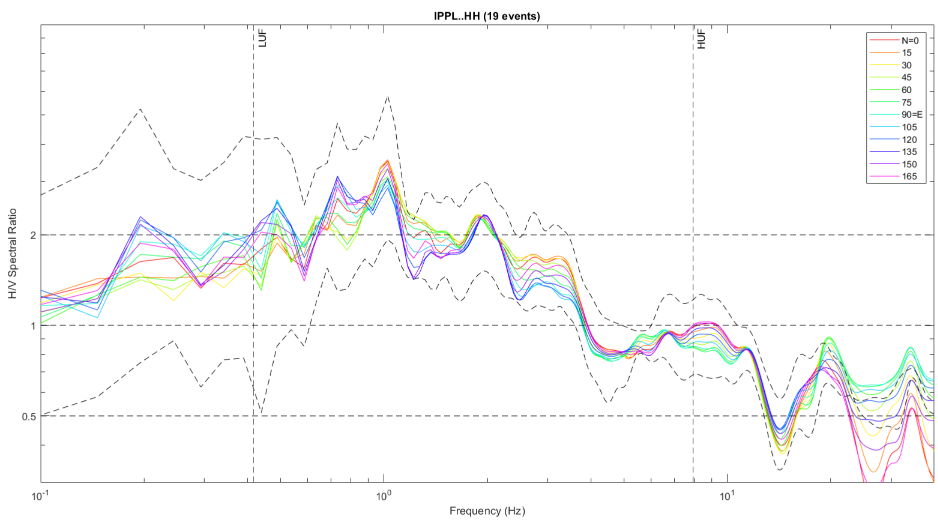


Figure 5.30: H/V and Residuals for IPPL..HH

H/V amplification graph of the station does not act like a rock profile. There is peak amplification of 3.2 at 1 Hz so predominant frequency of the station seems to be 1 Hz. Also amplification range is between 2.5-3.2 between 0.6 to 1.2 Hz. This is not a rock behaviour, it is more close to be between B and C profiles.

**KNSS..HH**

This station is in Knossos, Herakleion and operated by Technological Educational Institute of Crete in the Seismological Network of Crete (HC). As all the other only seismometer stations, site is expected to be rock profile.

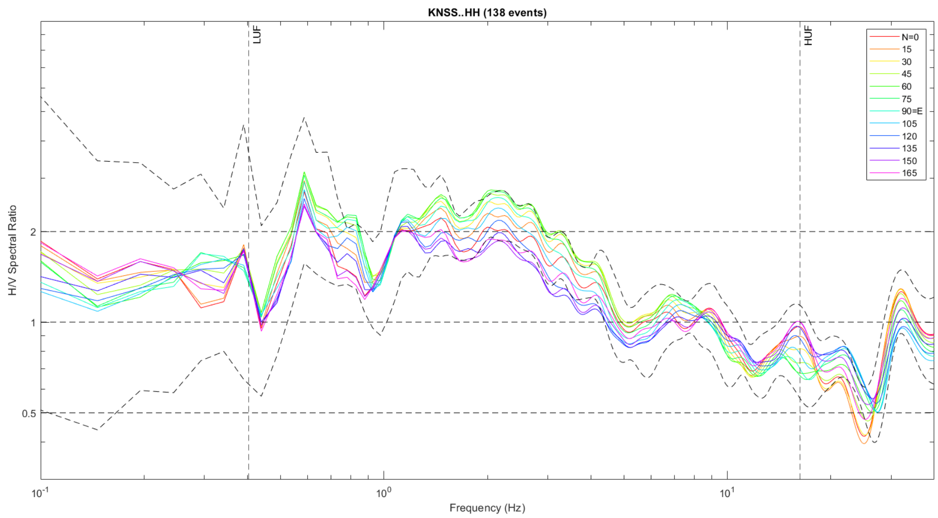


Figure 5.31: H/V and Residuals for KNSS..HH

There is directional sensitivity between 1.1 to 4 Hz. At 0.6 Hz H/V goes up to 3, this might be the predominant frequency for the site. Also between 1-3 Hz, there is small broadband amplification between 2-2.5. Amplification graph seems like a rock as well but the amplification at 0.6 Hz gives a clue on a possible softer soil profile.

**KSTE**

KSTE station is one of the few stations operating with both seismometer and accelerometer. It is located in Kastelli and operated by National Observatory of Athens in the Hellenic Seismic Network (HL). There is no info sbout the soil profile and having both seismometer and accelerometer does not let us make an assumption either. Also this station was installed at 5/11/2021, after the 6 events chosen from the Arkalochori sequence so residual analysis could not be done for it.

The only difference between two amplification graphs are different highest and lowest usable frequency values. HN amplification graph has a higher HUF and smaller LUF values. Since seismometers are more sensitive to lower frequencies LUF was expected to be smaller for HH. There is significant directional sensitivity in both amplification graphs between 5-10 Hz.

Both stations seems to have a very similar, almost identical H/V amplification graphs. Amplitude of amplification is between 0.5-2 in all frequencies so there is none to very low amplification in both amplification graphs. This low to no amplification is a sign of rock profile.

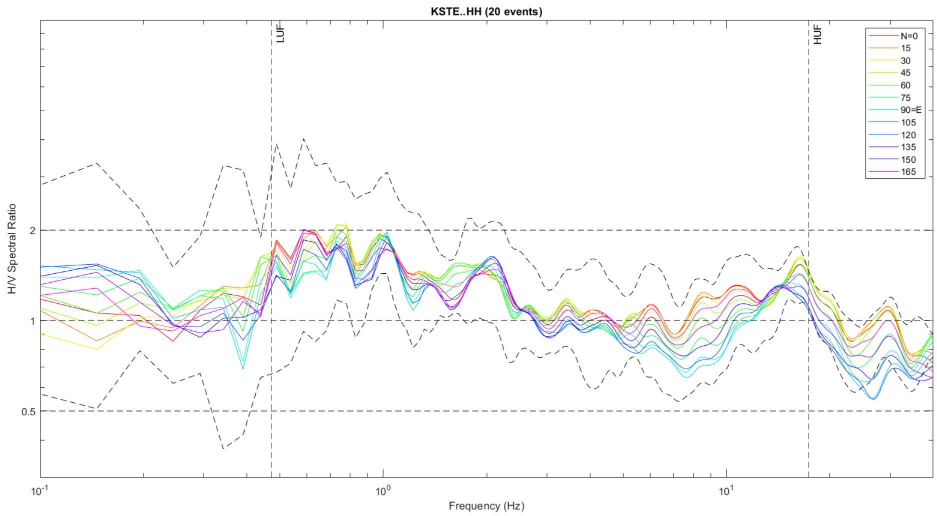


Figure 5.32: H/V and Residuals for KSTE..HH

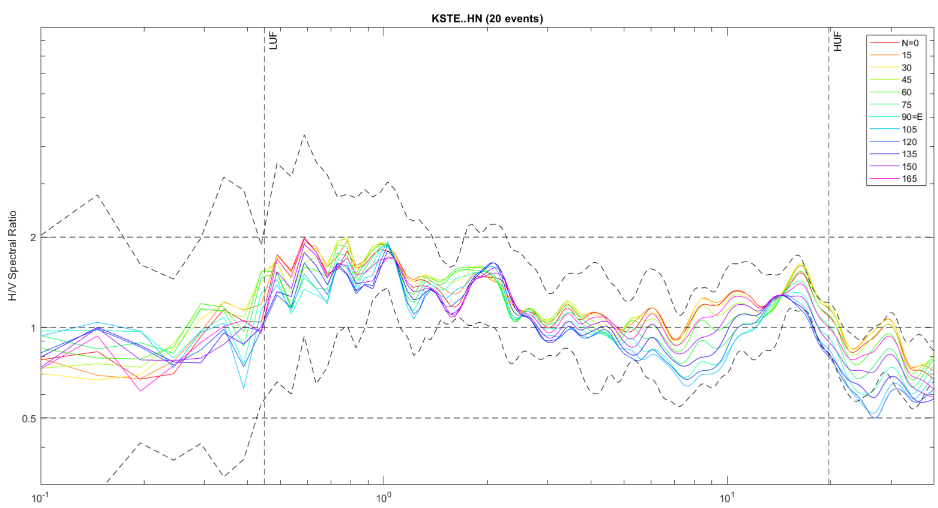


Figure 5.33: H/V and Residuals for KSTE..HN

## 5.3 Distance Scaling

GMPE predictions for all 6 events were already used in in residual analysis to investigate the overall station performance but distance scaling graphs were also created to check GMPE and station behaviour per event. Here scaling graphs were classified in 2 different ways. First of all, GMPEs using rupture distance as distance parameter were shown separately. Also another classification was made according to the event magnitude. In residual analysis all predictions were done with the exact match of magnitude but on distance scaling graphs, events with 4.6, 4.5 and 4.4 Mw were gathered in the same bin of 4.5 Mw. 5.9 and 5.1 Mw were also investigated separately and results are shown in the next subsections. Another classification was made according to the site measured or inferred Vs30. For the sites with only seismometers, Vs30=800 m/s was used. For the sites with measured Vs30 higher than 800 m/s (type A), again Vs30=800 m/s was used. For the sites with a measured Vs30 less than 800 m/s, Vs30=400 m/s was used. Graphs were created for two different intensity measure type, SA(1.0) and PGA.

Since in this thesis subject is to investigate the station behaviour more than the GMPE behaviour, GMPEs will not investigated in detail but the act of observations around the scaling graphs will be explained.

### 5.3.1 Mw=5.9

In the scaling graphs for Vs30=800 m/s Mw=5.9, underestimation of IACM which was discussed on residual analysis is obvious for both GMPEs with rrup and rjb. Observation for the main shock from this station is way outside the +STD curve for SA(1.0) so this also supports the type C profile guess for this station.

Another outlier from this bin is CHAN..HH for SA(1.0) sec for both of rrup and rjb GMPEs. From the H/V and residual analysis, site seems to be a rock site with small or no amplification so this underestimation can not be explained with it. Same observation is

Rest of the stations in this Vs30 group seem to be predicted fine both for PGA and SA(1.0 sec) since they are all inside + and - STD curves of the GMPEs for both distance parameters.

For Vs30=400 m/s graphs, ARK1 is an outlier as expected for H/V and residual results both for rrup and rjb. This station was told to be type A or B by ITSAK in Arkalochori report but both PGA and SA(1.0 sec) but the amplification on site seems could not be predicted even with Vs30=400 m/s both for PGA and SA(1.0 sec). Closest prediction for the site was made by BindiEtAl2014 since it remains in +STD range of it for Sa(1.0 sec) and very close to that for PGA. For SA(1.0 sec) SIVA and SIT2 are also around in +STD range for both rrup and rjb, so predictions with Vs30=400 m/s for these stations seem acceptable.

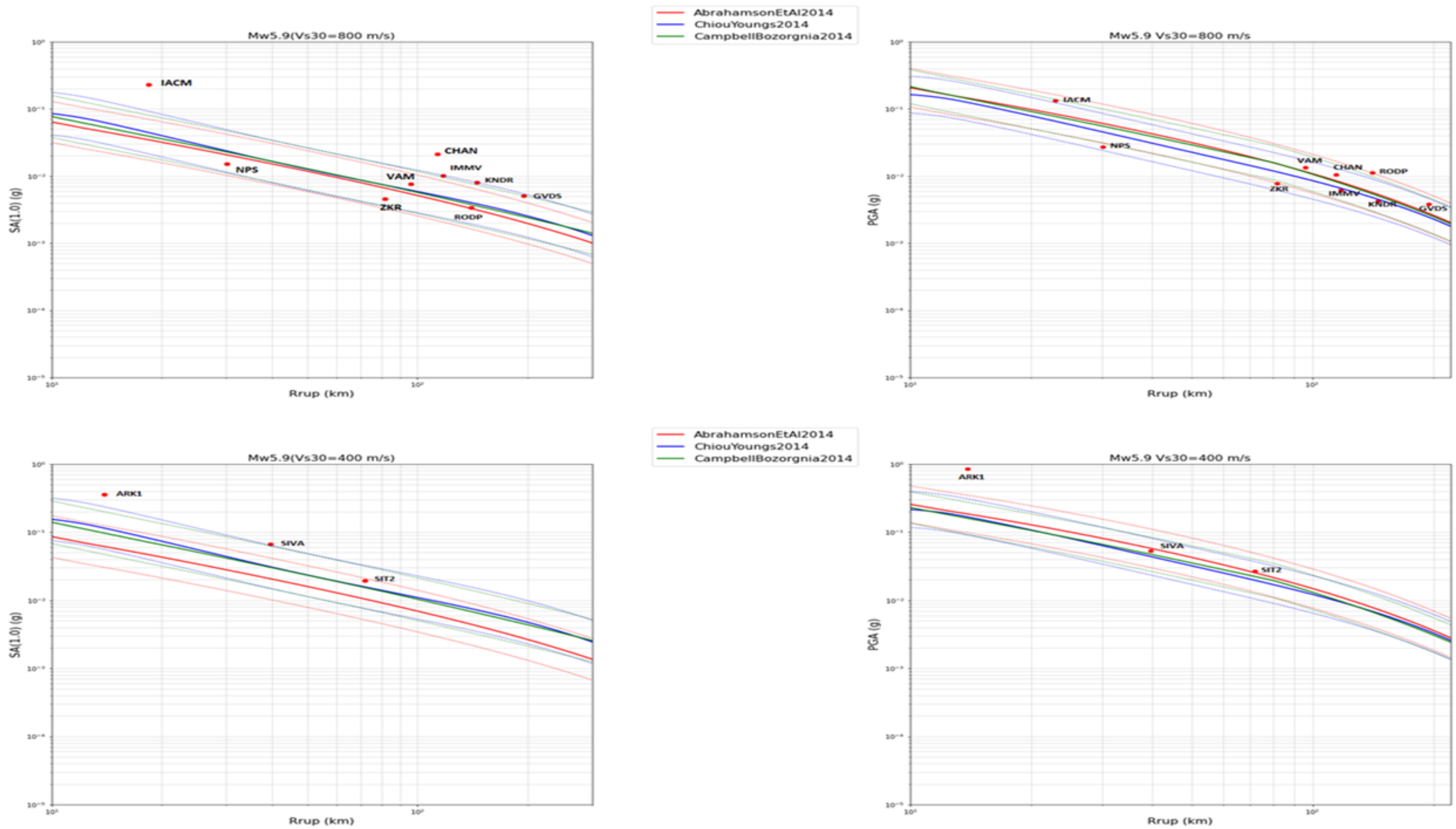


Figure 5.34: Distance Scaling Graphs for for GMPEs using rrup with Mw=5.9 and Vs30=800 m/s and 400 m/s

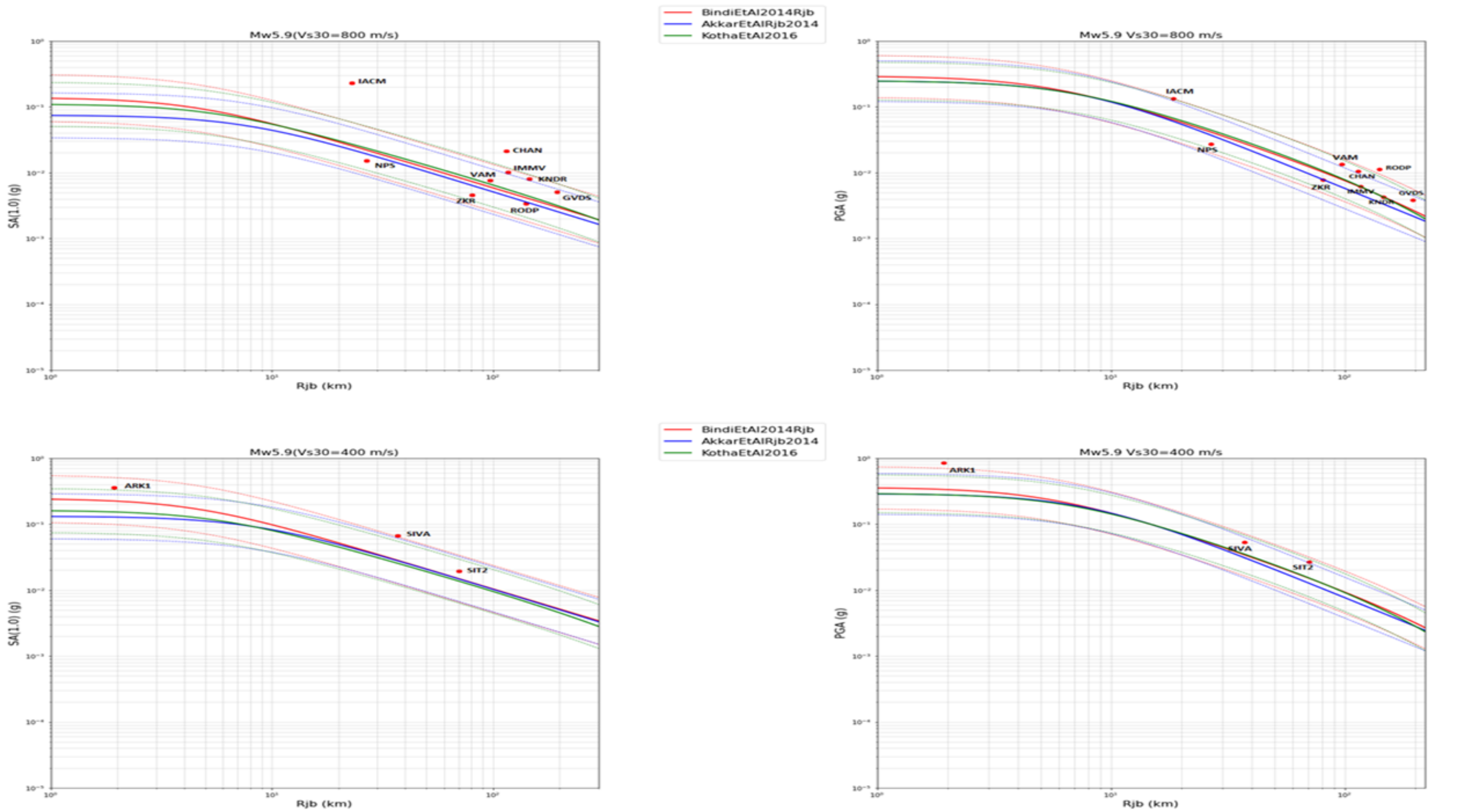


Figure 5.35: Distance Scaling Graphs for for GMPEs using rjb with Mw=5.9 and Vs30=800 m/s and 400 m/s

### 5.3.2 Mw=5.1

In this subsection, distance scaling graphs rrup Vs30=800 m/s and Vs30=400 m/s, rjb Vs30=800 m/s and Vs30=400 m/s were shown separately.

Like in the Mw=5.9 results, observation of IACM..HN for Sa(1.0) seems to be an outlier with a strong underestimation for both rjb and rrup GMPEs so this also supports the claims of the other results on the station.

Again, CHAN..HH observation is an outlier for SA(1.0 sec) in both rrup and rjb graphs and this underestimation cannot be explained with H/V amplification graph of the station since it does not seem to have a significant amplification on that for 1 Hz frequency.

Also IMMV and VAM for rjb GMPEs, IMMV, VAM, RODP and KNDR for rrup GMPEs are slighty out of the +STD range. This small underestimation of SA(1.0) was discussed in the overall station analysis and compensated by the overall station performance.

For the stations in Vs30=400 m/s group, ARK1 is again an outlier for PGA as expected from the overall analysis. This SA(1.0 sec) observation is inside +STD range for both rjb and rrup. Rather than that, SIVA and SIT2 observation are predicted adequately by both rjb and rrup GMPEs with the amplification comes from Vs30=400 m/s. Only PGA observation of SIVA.00.HN is slightly outside +STD range of GMPES, rest of the observations are within the range.

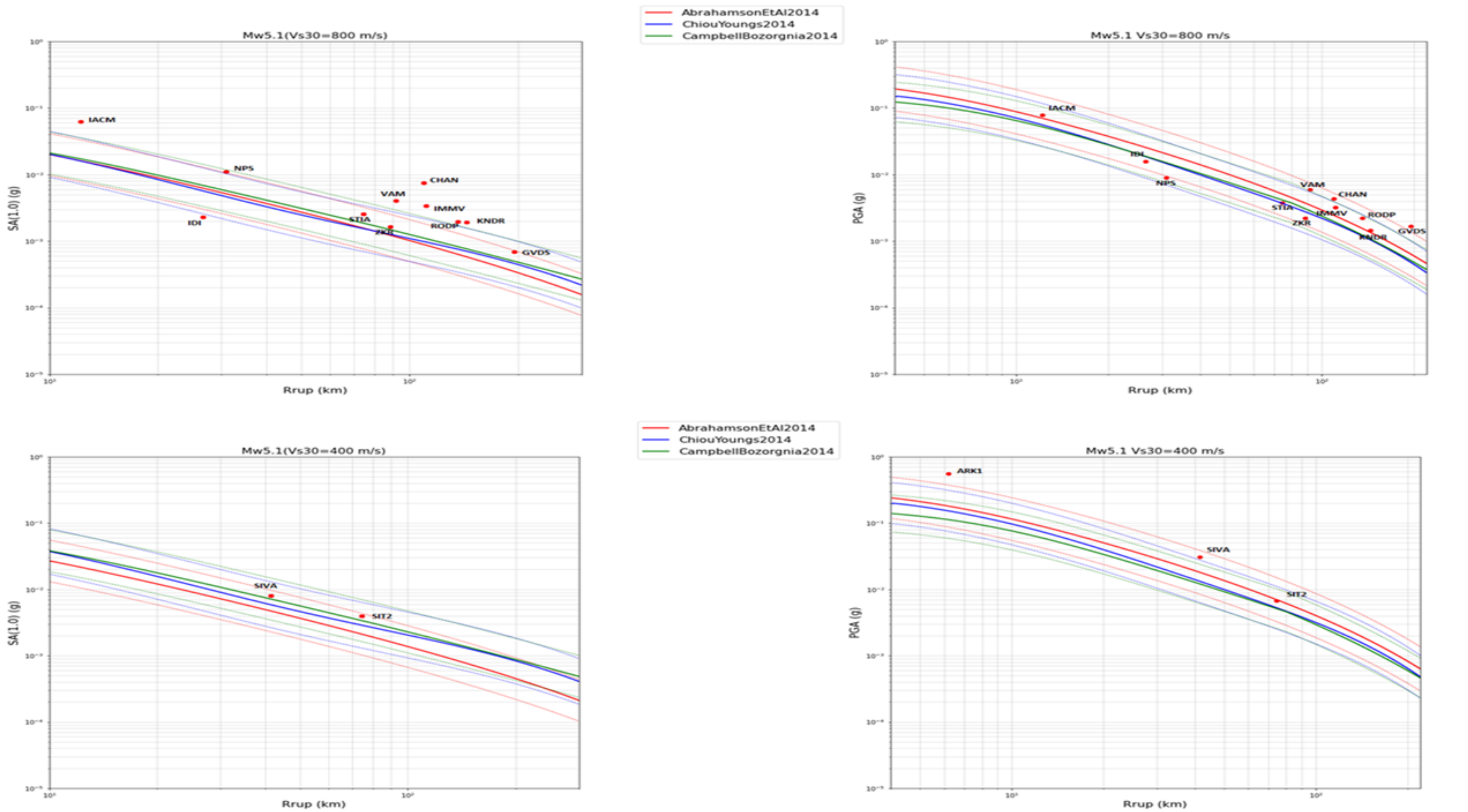


Figure 5.36: Distance Scaling Graphs for for GMPEs using rrup with Mw=5.1 and Vs30=800 m/s and 400 m/s

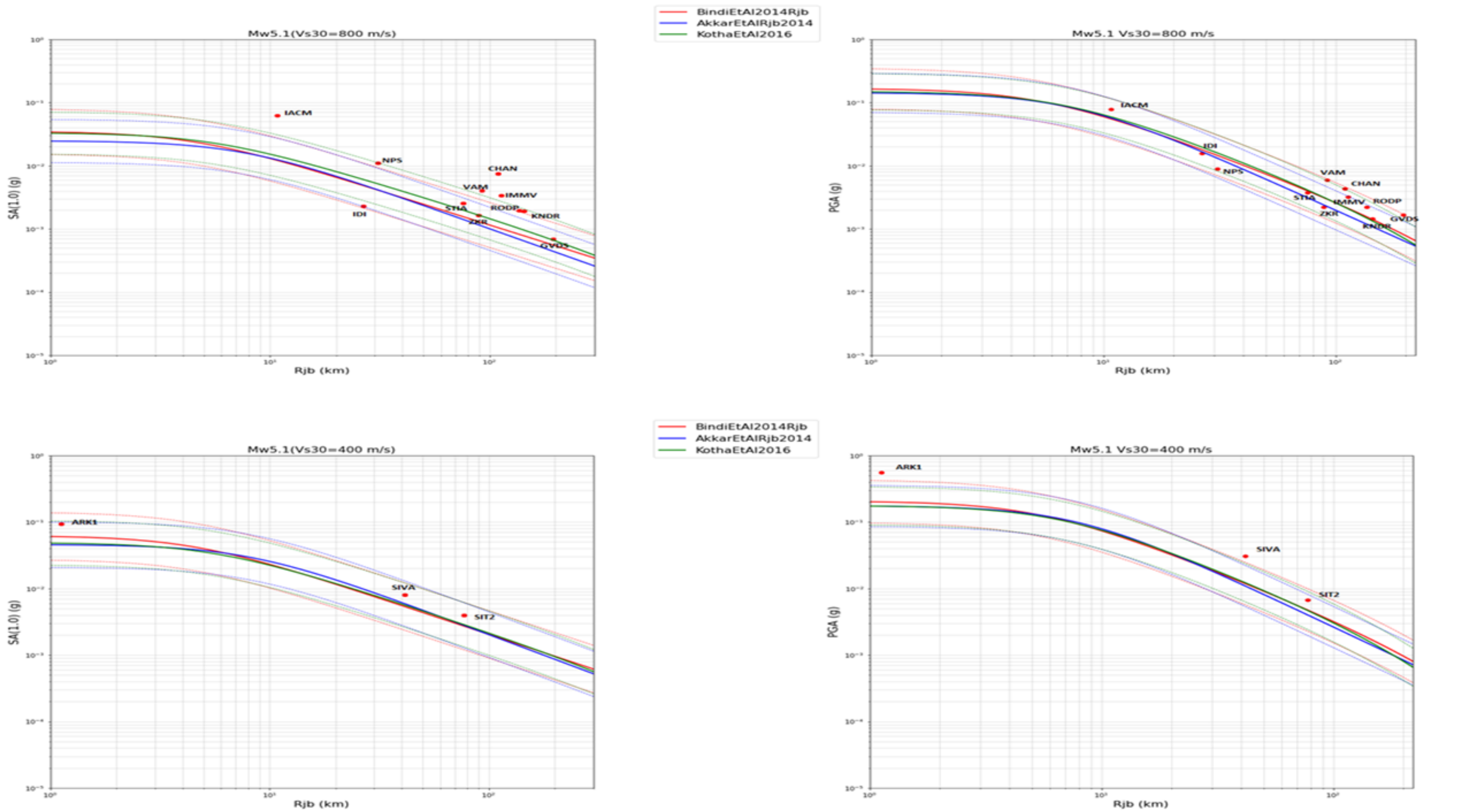


Figure 5.37: Distance Scaling Graphs for for GMPEs using rjb with Mw=5.1 and Vs30=800 m/s and 400 m/s

### 5.3.3 Mw=4.5 bin

Since in the 4.5 bin there are 4 different events for each station, more variety in the results can be observed but the significant ones remain the same.

For instance, IACM seem to have the strongest outliers for SA(1.0 sec) again, although it has events inside the +STD range as well. PGA observations for IACM..HN is all inside the +STD range this time, seem to be predicted fine.

CHAN..HH has also the same results like Mw=5.9 and 5.1. Both SA(1.0) and PGA observations are again outliers. This also tells us that GMPEs are underestimating the station with Vs30=800 m/s although H/V amplification graph does not have significant amplification. IMMV and RODP observations of SA(1.0 sec) for rrup GMPEs and just IMMV observations of SA(1.0 sec) for rjb GMPEs are slightly out of +STD range. This is not expected since the sites are assumed as rock with Vs30=800 m/s but overall station performance seem okay with that underestimation of SA(1.0 sec) since residuals are less than 1 for both. Also IDI..HH has an outlier observation from the same event both for PGA and SA(1.0 sec) but rest of the observations for the station is within the -STD ranges.

For PGA, there is no underpredicted events but 3 stations are overpredicted since the observations from them are outside the -STD curves. These stations are NPS, STIA and ZKR. From the H/V amplification graph of ZKR..HH it was already mentioned that there might be a sensor issue with the station so the observations might not be reliable since there was high directional sensitivity in every frequency. NPS is a good reference station with around 1 H/V ratio almost in all frequencies between LUF and HUF but since we are not aware of the higher frequencies which might include PGA, this overprediction might be caused by that. STIA..HH has a flat H/V amplification graph but ratio goes down to 1 and even less for the higher frequencies where PGA might be so even though it is not certain, the overprediction might be explained with it.

Since ARK1 has data from only two events of Mw5.9 and Mw5.1, distance scaling graphs for Vs30=400 m/s were created with only two stations, SIVA and SIT2. Both PGA and SA(1.0) observations are within the range of mean + and -STD range of rjb and rrup GMPEs so amplification of these stations seem to be predicted adequately for all of them.

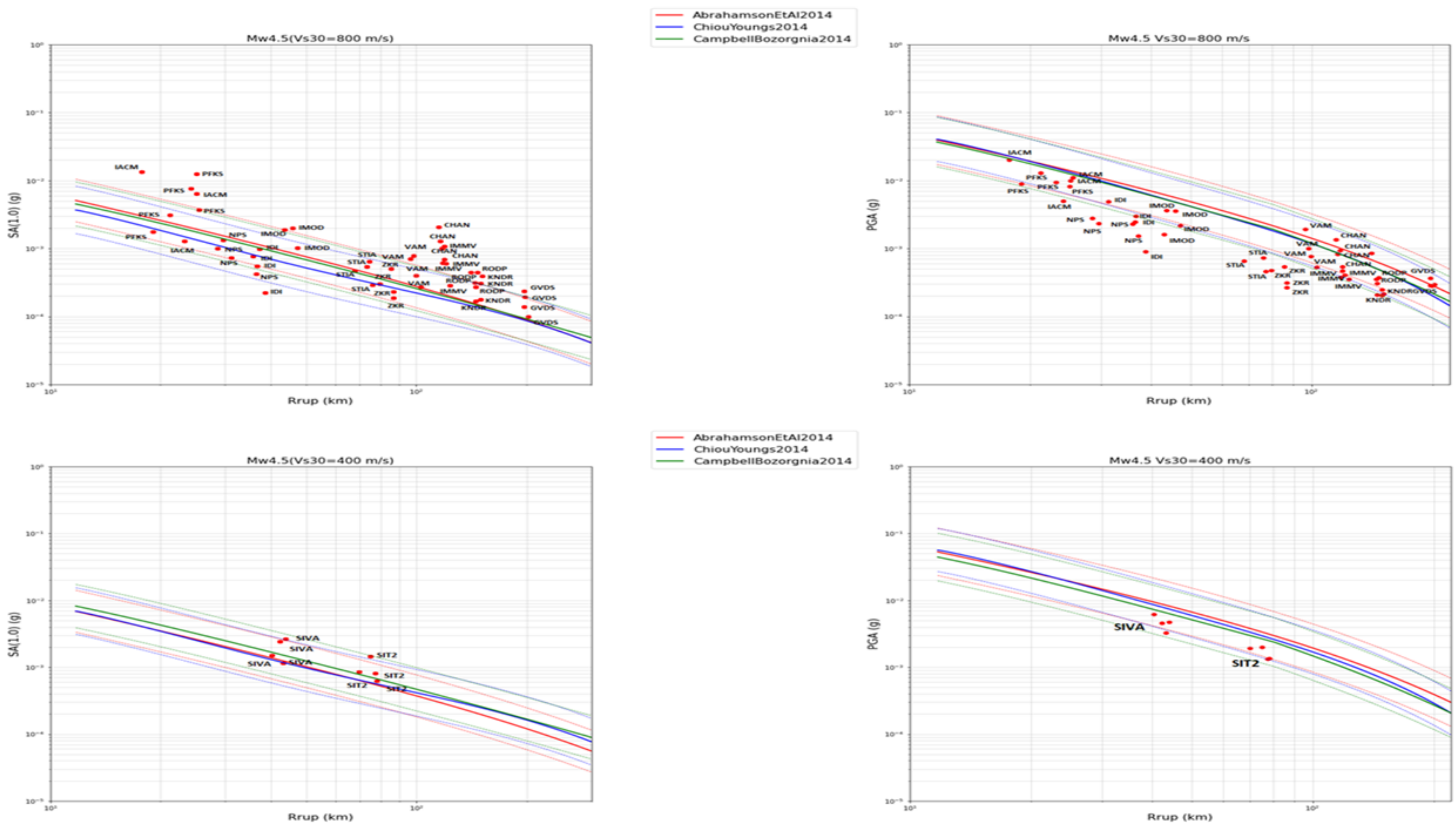


Figure 5.38: Distance Scaling Graphs for for GMPEs using rrup with Mw=4.5 and Vs30=800 m/s and 400 m/s

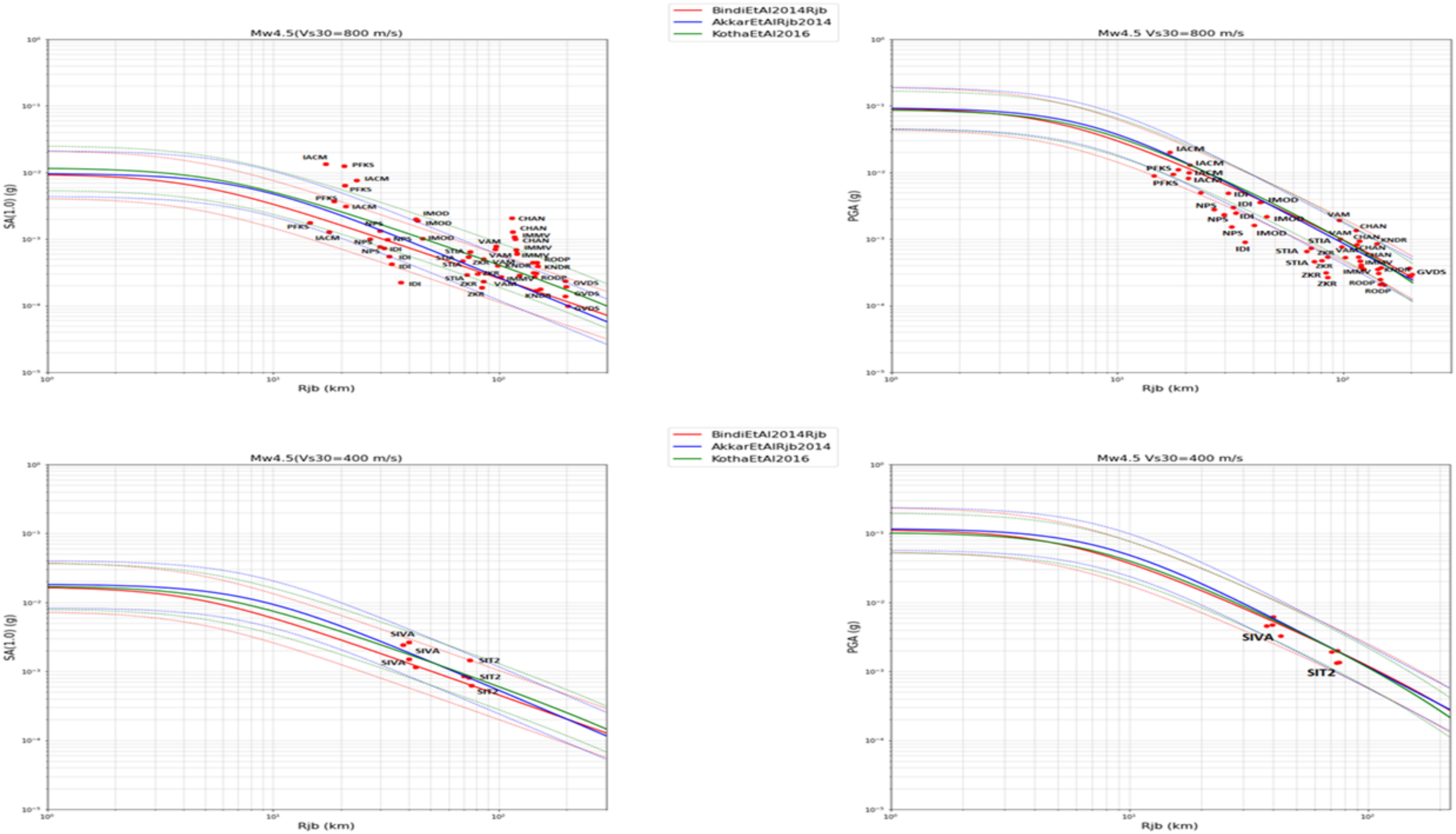


Figure 5.39: Distance Scaling Graphs for for GMPEs using rjb with Mw=4.5 and Vs30=800 m/s and 400 m/s

## Chapter 6

# CONCLUSIONS

In the overall thesis, site effects on Cretan seismic stations were analyzed for 21 Cretan seismic stations. To create the HVSR profiles, data from 20 seismometers and 8 accelerometers were used. For a deeper analysis, main shock (Mw 5.9), largest aftershock (Mw5.1) and 4 more significant aftershocks (between Mw 4.4-4.6) were chosen from 2021 Arkalochori earthquake sequence. These are the largest six events of the sequence till 2022. For these events, there was available data from 16 stations and further analysis was carried out for these 16 stations by calculating residuals of PGA and SA(1.0 sec) by using predictions from 6 different GMPEs. After that, HVSR profiles were combined with GMPE residuals for PGA and SA(1.0 sec) and overall station performance on site effects for each station was analyzed. Average residuals of all stations for PGA and for SA(1.0) can be seen all in Figure 6.1 and 6.2 below. For the distance also average value value was used.

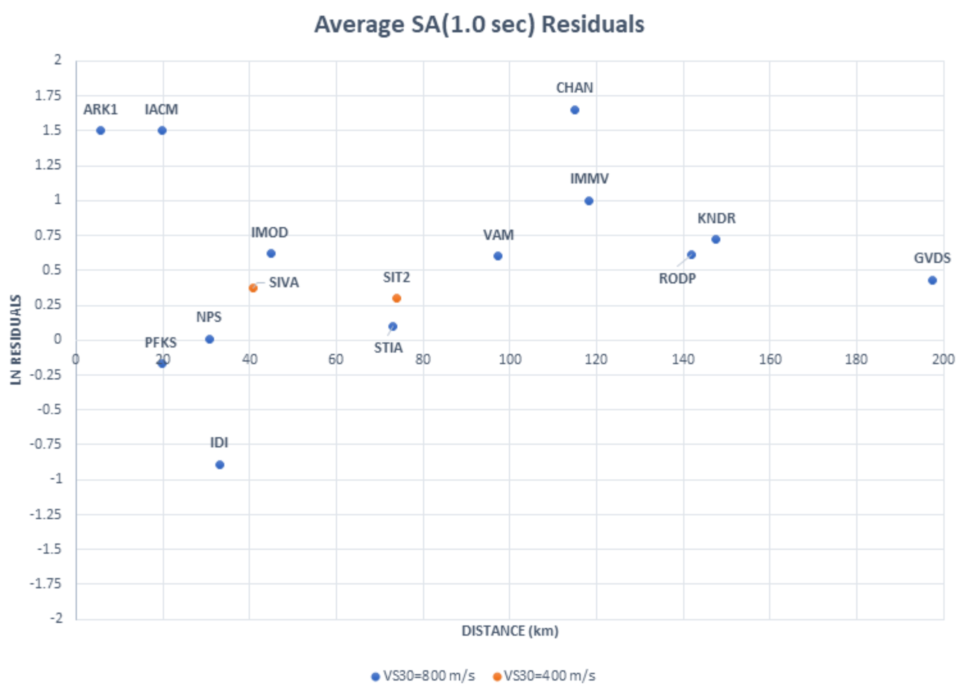


Figure 6.1: PGA Residuals for All Stations

It was found out that there was conflict between the available information on the station soil profile or Vs30 and the analysis results for three stations. First of these stations was IACM. This station was profiled as type A with Vs30=815 m/s so before the analyses no or very low amplification was expected but profile showed strong amplification between 3-7 amplitude starting from 0.5 Hz till 1.2 Hz. Also GMPE residuals for Sa(1.0 sec), which is included in the strong amplification range of HVSR, were very high and averaged at 1.5 for Vs30=800 m/s and 1.3 for Vs30=400 m/s. There were strong underestimation by GMPEs even with Vs30=400 m/s, which is type B but close to type C border of 360 m/s. So for this station I came up with

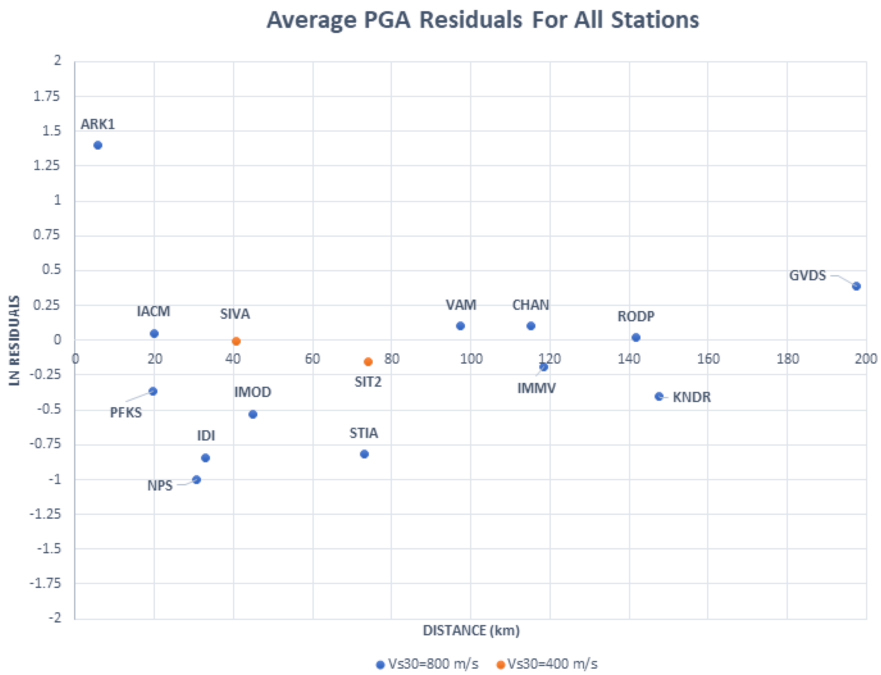


Figure 6.2: SA (1.0 sec) Residuals for All Stations

the conclusion that it might be a type C profile, not type A.

Second conflict was with the station ARK1. ITSAK shared only the main shock and the largest aftershock data from the sequence to the public so only these 2 events were used to create both the HVSR profile and GMPE residuals. After the earthquake sequence, ITSAK shared a report in 2021 and in that report ARK1 station was mentioned as between type A and B, which is a sign for a possible rock profile. But The results for this station showed otherwise. In some frequency ranges, there was amplification up to amplitude 6. Also there was again strong underestimation by GMPEs on SA(1.0 sec) and PGA for both Vs30=800 m/s and Vs30=400 m/s. Residuals went a bit down for Vs30=400 m/s but it was still a strong underestimation so my conclusion on this station was the same as IACM. Site might be a type C (maybe B but close to C) for ARK1, not between A and B as mentioned by ITSAK.

Third conflict was on station SIVA. ON the ESM database, station is told to be type C with Vs30=257 m/s. But on the webpage of Hellenic Seismic Network, accelnet.gein.noa.gr , site geology is limestone and for limestone low amplification is expected like profile between A and B. In the HVSR results, station has amplification between 1-2 Hz and it reaches the maximum 3-3.2 at around 1.2 and 1.7 Hz. PGA residuals were predicted fine but for SA (1.0) residual average was 0.8 for Vs30=400 m/s and 0.37 for Vs30=400 m/s. This might show that limestone geography for the station might be wrong but type C information might be correct.

Another interesting result was on station ZKR. Station's H/V profile had directional sensitivity in all frequencies and rotated H/Vs were all like parallel to each other with a distance. There was a possible sensor problem with this station.

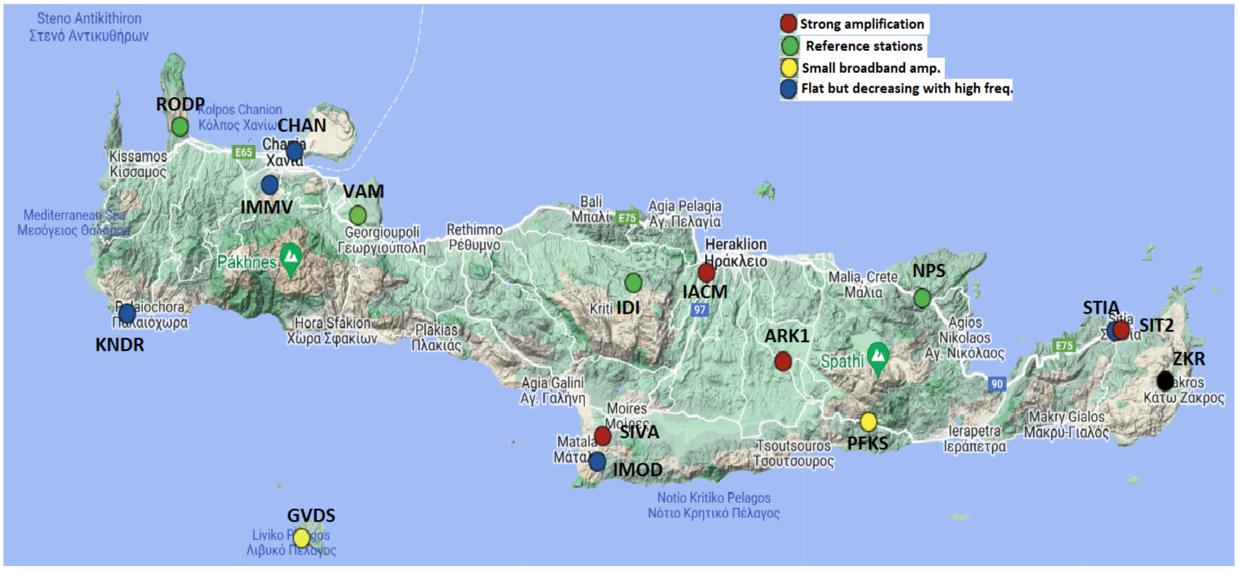


Figure 6.3: Map of Crete with Analyzed Stations including Amplification Classification

After analyzing the HVSR results combined with GMPE residuals, stations were also classified according to their amplification profile. These classifications were strong amplification stations, reference stations, stations with small broadband amplification and stations with flat profile with decreasing amplification in higher frequencies. A Crete map showing the stations on their exact locations and amplification group was created by Google Maps and can be found on Figure 6.1.

First group was the strong amplification. Above mentioned ARK1, IACM, SIVA were one of those stations and station SIT2 was also added to them since it had strong amplification up to 6-7 amplitude at 1.3-2.5 Hz.

Second group was the reference stations. These stations were IDI, NPS, VAM amd RODP and their H/V was around 1 in most of the frequencies and always flat between 1 and 2.

Another classification group was the stations which had small broadband amplification. For these stations, there was a small amplification between 2-2.5 in a range of frequencies. Names of these stations are GVDS and PFKS.

Last group of stations is the flat profiles with no significant or small amplification which still decreases with the higher frequencies. CHAN, IMOD, KNDR, STIA and IMMV are parts of this group. They all have again small amplification between 2-2.5 (max 2 in some) and it decreases as with the increase in frequency between 0.5-1 amplitude.

# Appendix A

# Parameters of the 6 Events of Sequence for the Residual Analysis

| Date | Time | Mw | Strike | Dip | Rake | HypDepth | SiteCode | Channel | Repi(km) | Rhyp(km) | Rjb(km) | Rrup(km) | Rx(km) | PGA (g) | f1.0SA |
|---|---|---|---|---|---|---|---|---|---|---|---|---|---|---|---|
| 27/09/2021 | 6:14:24 | 5.9 | 25 | 33 | -81 | 10.4 | CHAN | HHE | 118.64 | 118.93 | 113.67 | 114.57 | 71.74 | 0.0064 | 0.0110 |
| 27/09/2021 | 6:14:24 | 5.9 | 25 | 33 | -81 | 10.4 | CHAN | HHN | 118.64 | 118.93 | 113.67 | 114.57 | 71.74 | 0.0084 | 0.0182 |
| 27/09/2021 | 6:14:24 | 5.9 | 25 | 33 | -81 | 10.4 | GVDS | HHE | 197.89 | 198.07 | 194.69 | 195.17 | -9.71 | 0.0029 | 0.0046 |
| 27/09/2021 | 6:14:24 | 5.9 | 25 | 33 | -81 | 10.4 | GVDS | HHN | 197.89 | 198.07 | 194.69 | 195.17 | -9.71 | 0.0025 | 0.0021 |
| 27/09/2021 | 6:14:24 | 5.9 | 25 | 33 | -81 | 10.4 | KNDR | HHE | 149.5 | 149.74 | 145.22 | 145.97 | 133.15 | 0.0027 | 0.0036 |
| 27/09/2021 | 6:14:24 | 5.9 | 25 | 33 | -81 | 10.4 | KNDR | HHN | 149.5 | 149.74 | 145.22 | 145.97 | 133.15 | 0.0033 | 0.0071 |
| 27/09/2021 | 6:14:24 | 5.9 | 25 | 33 | -81 | 10.4 | NPS | HHE | 33.63 | 34.66 | 26.77 | 30.1 | 26.15 | 0.0245 | 0.0139 |
| 27/09/2021 | 6:14:24 | 5.9 | 25 | 33 | -81 | 10.4 | NPS | HHN | 33.63 | 34.66 | 26.77 | 30.1 | 26.15 | 0.0112 | 0.0061 |
| 27/09/2021 | 6:14:24 | 5.9 | 25 | 33 | -81 | 10.4 | RODP | HHE | 144.45 | 144.7 | 140.06 | 140.81 | 104.07 | 0.0032 | 0.0024 |
| 27/09/2021 | 6:14:24 | 5.9 | 25 | 33 | -81 | 10.4 | RODP | HHN | 144.45 | 144.7 | 140.06 | 140.81 | 104.07 | 0.0044 | 0.0024 |
| 27/09/2021 | 6:14:24 | 5.9 | 25 | 33 | -81 | 10.4 | VAM | HHE | 101.23 | 101.58 | 95.88 | 96.79 | -64.18 | 0.0104 | 0.0054 |
| 27/09/2021 | 6:14:24 | 5.9 | 25 | 33 | -81 | 10.4 | VAM | HHN | 101.23 | 101.58 | 95.88 | 96.79 | -64.18 | 0.0086 | 0.0055 |
| 27/09/2021 | 6:14:24 | 5.9 | 25 | 33 | -81 | 10.4 | ZKR | HHE | 86.12 | 86.53 | 80.43 | 81.6 | -45.7 | 0.0039 | 0.0027 |
| 27/09/2021 | 6:14:24 | 5.9 | 25 | 33 | -81 | 10.4 | ZKR | HHN | 86.12 | 86.53 | 80.43 | 81.6 | -45.7 | 0.0067 | 0.0037 |
| 27/09/2021 | 6:14:24 | 5.9 | 25 | 33 | -81 | 10.4 | ARK1 | HNE | 2.74 | 8.85 | 1.92 | 13.89 | -0.87 | 0.5953 | 0.2281 |
| 27/09/2021 | 6:14:24 | 5.9 | 25 | 33 | -81 | 10.4 | ARK1 | HNN | 2.74 | 8.85 | 1.87 | 13.89 | -0.84 | 0.5994 | 0.2783 |
| 27/09/2021 | 6:14:24 | 5.9 | 25 | 33 | -81 | 10.4 | SIVA | HNE | 43.78 | 44.58 | 37.15 | 39.61 | 36.92 | 0.043 | 0.0506 |
| 27/09/2021 | 6:14:24 | 5.9 | 25 | 33 | -81 | 10.4 | SIVA | HNN | 43.78 | 44.58 | 37.15 | 39.61 | 36.92 | 0.0304 | 0.0439 |
| 27/09/2021 | 6:14:24 | 5.9 | 25 | 33 | -81 | 10.4 | IACM | HNE | 25.48 | 26.83 | 18.44 | 23.01 | -5.83 | 0.0884 | 0.1641 |
| 27/09/2021 | 6:14:24 | 5.9 | 25 | 33 | -81 | 10.4 | IACM | HNN | 25.48 | 26.83 | 18.44 | 23.01 | -5.83 | 0.0998 | 0.1583 |
| 27/09/2021 | 6:14:24 | 5.9 | 25 | 33 | -81 | 10.4 | SIT2 | HNE | 76.35 | 76.82 | 70.45 | 71.69 | -54.19 | 0.0201 | 0.0120 |
| 27/09/2021 | 6:14:24 | 5.9 | 25 | 33 | -81 | 10.4 | SIT2 | HNN | 76.35 | 76.82 | 70.45 | 71.69 | -54.19 | 0.0174 | 0.0154 |
| 27/09/2021 | 6:14:24 | 5.9 | 25 | 33 | -81 | 10.4 | IMMV | HNE | 121.88 | 122.17 | 116.98 | 117.71 | -79.64 | 0.004 | 0.0063 |
| 27/09/2021 | 6:14:24 | 5.9 | 25 | 33 | -81 | 10.4 | IMMV | HNN | 121.88 | 122.17 | 116.98 | 117.71 | -79.64 | 0.0047 | 0.0079 |
| 28/09/2021 | 4:48:00 | 5.1 | 5 | 64 | -112 | 4.7 | CHAN | HHE | 111.15 | 111.24 | 109.27 | 109.29 | -108.9 | 0.003 | 0.0051 |
| 28/09/2021 | 4:48:00 | 5.1 | 5 | 64 | -112 | 4.7 | CHAN | HHN | 111.15 | 111.24 | 109.27 | 109.29 | -108.9 | 0.0031 | 0.0054 |
| 28/09/2021 | 4:48:00 | 5.1 | 5 | 64 | -112 | 4.7 | IDI | HHE | 30.68 | 31 | 26.51 | 26.6 | -26.22 | 0.0097 | 0.0016 |
| 28/09/2021 | 4:48:00 | 5.1 | 5 | 64 | -112 | 4.7 | IDI | HHN | 30.68 | 31 | 26.51 | 26.6 | -26.22 | 0.0123 | 0.0016 |
| 28/09/2021 | 4:48:00 | 5.1 | 5 | 64 | -112 | 4.7 | GVDS | HHE | 195.21 | 195.26 | 195.72 | 195.73 | -41.61 | 0.0012 | 0.0005 |
| 28/09/2021 | 4:48:00 | 5.1 | 5 | 64 | -112 | 4.7 | GVDS | HHN | 195.21 | 195.26 | 195.72 | 195.73 | -41.61 | 0.0012 | 0.0004 |
| 28/09/2021 | 4:48:00 | 5.1 | 5 | 64 | -112 | 4.7 | KNDR | HHE | 145.07 | 145.13 | 144.15 | 144.17 | -87.4 | 0.001 | 0.0009 |
| 28/09/2021 | 4:48:00 | 5.1 | 5 | 64 | -112 | 4.7 | KNDR | HHN | 145.07 | 145.13 | 144.15 | 144.17 | -87.4 | 0.001 | 0.0017 |
| 28/09/2021 | 4:48:00 | 5.1 | 5 | 64 | -112 | 4.7 | NPS | HHE | 34.97 | 35.24 | 30.91 | 30.92 | -0.47 | 0.0068 | 0.0097 |
| 28/09/2021 | 4:48:00 | 5.1 | 5 | 64 | -112 | 4.7 | NPS | HHN | 34.97 | 35.24 | 30.91 | 30.92 | -0.47 | 0.0058 | 0.0051 |
| 28/09/2021 | 4:48:00 | 5.1 | 5 | 64 | -112 | 4.7 | RODP | HHE | 137.21 | 137.28 | 136.07 | 136.09 | -74.41 | 0.0014 | 0.0012 |
| 28/09/2021 | 4:48:00 | 5.1 | 5 | 64 | -112 | 4.7 | RODP | HHN | 137.21 | 137.28 | 136.07 | 136.09 | -74.41 | 0.0018 | 0.0016 |
| 28/09/2021 | 4:48:00 | 5.1 | 5 | 64 | -112 | 4.7 | STIA | HHE | 78.69 | 78.81 | 75.88 | 74.27 | -70.37 | 0.0027 | 0.0016 |
| 28/09/2021 | 4:48:00 | 5.1 | 5 | 64 | -112 | 4.7 | STIA | HHN | 78.69 | 78.81 | 75.88 | 74.27 | -70.37 | 0.0026 | 0.0020 |
| 28/09/2021 | 4:48:00 | 5.1 | 5 | 64 | -112 | 4.7 | VAM | HHE | 94.52 | 94.62 | 92.16 | 91.52 | 46.16 | 0.0045 | 0.0033 |
| 28/09/2021 | 4:48:00 | 5.1 | 5 | 64 | -112 | 4.7 | VAM | HHN | 94.52 | 94.62 | 92.16 | 91.52 | 46.16 | 0.004 | 0.0023 |
| 28/09/2021 | 4:48:00 | 5.1 | 5 | 64 | -112 | 4.7 | ZKR | HHE | 91.21 | 91.31 | 88.75 | 88.36 | -20.55 | 0.0007 | 0.0008 |
| 28/09/2021 | 4:48:00 | 5.1 | 5 | 64 | -112 | 4.7 | ZKR | HHN | 91.21 | 91.31 | 88.75 | 88.36 | -20.55 | 0.0021 | 0.0014 |
| 28/09/2021 | 4:48:00 | 5.1 | 5 | 64 | -112 | 4.7 | SIVA | HHE | 45.33 | 45.55 | 41.57 | 41.49 | 12 | 0.0135 | 0.0049 |
| 28/09/2021 | 4:48:00 | 5.1 | 5 | 64 | -112 | 4.7 | ARK1 | HNE | 3.72 | 9.2 | 1.12 | 2.26 | 2.23 | 0.4963 | 0.0633 |

**Table A.1 continued from previous page**

| Date | Time | Mw | Strike | Dip | Rake | HypDepth | SiteCode | Channel | Repi(km) | Rhyp(km) | Rjb(km) | Rrup(km) | Rx(km) | PGA (g) | f1.0SA |
|---|---|---|---|---|---|---|---|---|---|---|---|---|---|---|---|
| 28/09/2021 | 4:48:00 | 5.1 | 5 | 64 | -112 | 4.7 | ARK1 | HNN | 3.72 | 9.2 | 1.12 | 2.26 | 2.23 | 0.2549 | 0.0690 |
| 28/09/2021 | 4:48:00 | 5.1 | 5 | 64 | -112 | 4.7 | SIVA | HNE | 45.33 | 45.55 | 41.57 | 41.49 | 12 | 0.0128 | 0.0058 |
| 28/09/2021 | 4:48:00 | 5.1 | 5 | 64 | -112 | 4.7 | SIVA | HNN | 45.33 | 45.55 | 41.57 | 41.49 | 12 | 0.0282 | 0.0055 |
| 28/09/2021 | 4:48:00 | 5.1 | 5 | 64 | -112 | 4.7 | IACM | HNE | 15.38 | 17.53 | 10.77 | 12.21 | -1.61 | 0.049 | 0.0316 |
| 28/09/2021 | 4:48:00 | 5.1 | 5 | 64 | -112 | 4.7 | IACM | HNN | 15.38 | 17.53 | 10.77 | 12.21 | -1.61 | 0.0612 | 0.0532 |
| 28/09/2021 | 4:48:00 | 5.1 | 5 | 64 | -112 | 4.7 | SIT2 | HNE | 80.12 | 80.56 | 77.35 | 74.05 | -74.04 | 0.0049 | 0.0028 |
| 28/09/2021 | 4:48:00 | 5.1 | 5 | 64 | -112 | 4.7 | SIT2 | HNN | 80.12 | 80.56 | 77.35 | 74.05 | -74.04 | 0.0045 | 0.0028 |
| 28/09/2021 | 4:48:00 | 5.1 | 5 | 64 | -112 | 4.7 | IMMV | HNE | 115.06 | 115.37 | 113.29 | 110.31 | 111.7 | 0.0022 | 0.0021 |
| 28/09/2021 | 4:48:00 | 5.1 | 5 | 64 | -112 | 4.7 | IMMV | HNN | 115.06 | 115.37 | 113.29 | 110.31 | 111.7 | 0.0023 | 0.0027 |
| 27/09/2021 | 11:02:24 | 4.6 | 15 | 80 | -93 | 3 | CHAN | HHE | 115.8 | 115.83 | 114.04 | 114.86 | 98.59 | 0.0009 | 0.0012 |
| 27/09/2021 | 11:02:24 | 4.6 | 15 | 80 | -93 | 3 | CHAN | HHN | 115.8 | 115.83 | 114.04 | 114.86 | 98.59 | 0.001 | 0.0016 |
| 27/09/2021 | 11:02:24 | 4.6 | 15 | 80 | -93 | 3 | IDI | HHE | 34.97 | 35.09 | 30.91 | 31.27 | 29.09 | 0.0031 | 0.0004 |
| 27/09/2021 | 11:02:24 | 4.6 | 15 | 80 | -93 | 3 | IDI | HHN | 34.97 | 35.09 | 30.91 | 31.27 | 29.09 | 0.0038 | 0.0006 |
| 27/09/2021 | 11:02:24 | 4.6 | 15 | 80 | -93 | 3 | GVDS | HHE | 196.78 | 196.81 | 197.34 | 197.4 | -173.47 | 0.0003 | 0.0002 |
| 27/09/2021 | 11:02:24 | 4.6 | 15 | 80 | -93 | 3 | GVDS | HHN | 196.78 | 196.81 | 197.34 | 197.4 | -173.47 | 0.0002 | 0.0001 |
| 27/09/2021 | 11:02:24 | 4.6 | 15 | 80 | -93 | 3 | IMOD | HHE | 47.15 | 47.24 | 43.44 | 43.7 | -43.34 | 0.0029 | 0.0016 |
| 27/09/2021 | 11:02:24 | 4.6 | 15 | 80 | -93 | 3 | IMOD | HHN | 47.15 | 47.24 | 43.44 | 43.7 | -43.34 | 0.0022 | 0.0010 |
| 27/09/2021 | 11:02:24 | 4.6 | 15 | 80 | -93 | 3 | KNDR | HHE | 147.74 | 147.77 | 146.9 | 146.98 | -18.28 | 0.0003 | 0.0003 |
| 27/09/2021 | 11:02:24 | 4.6 | 15 | 80 | -93 | 3 | KNDR | HHN | 147.74 | 147.77 | 146.9 | 146.98 | -18.28 | 0.0003 | 0.0003 |
| 27/09/2021 | 8:24:00 | 4.5 | 232 | 63 | -97 | 12.1 | GVDS | HHE | 200.91 | 200.93 | 201.59 | 201.9 | 5.64 | 0.0002 | 0.0001 |
| 27/09/2021 | 8:24:00 | 4.5 | 232 | 63 | -97 | 12.1 | GVDS | HHN | 200.91 | 200.93 | 201.59 | 201.9 | 5.64 | 0.0002 | 0.0001 |
| 27/09/2021 | 11:02:24 | 4.6 | 15 | 80 | -93 | 3 | NPS | HHE | 33.66 | 33.79 | 29.57 | 29.64 | 27.9 | 0.0021 | 0.0012 |
| 27/09/2021 | 11:02:24 | 4.6 | 15 | 80 | -93 | 3 | NPS | HHN | 33.66 | 33.79 | 29.57 | 29.64 | 27.9 | 0.0009 | 0.0006 |
| 27/09/2021 | 11:02:24 | 4.6 | 15 | 80 | -93 | 3 | PFKS | HHE | 25.2 | 25.37 | 20.86 | 21.22 | 11.85 | 0.0097 | 0.0025 |
| 27/09/2021 | 11:02:24 | 4.6 | 15 | 80 | -93 | 3 | PFKS | HHN | 25.2 | 25.37 | 20.86 | 21.22 | 11.85 | 0.0086 | 0.0018 |
| 27/09/2021 | 11:02:24 | 4.6 | 15 | 80 | -93 | 3 | RODP | HHE | 141.72 | 141.75 | 140.7 | 140.78 | -47.2 | 0.0007 | 0.0003 |
| 27/09/2021 | 11:02:24 | 4.6 | 15 | 80 | -93 | 3 | RODP | HHN | 141.72 | 141.75 | 140.7 | 140.78 | -47.2 | 0.0005 | 0.0004 |
| 27/09/2021 | 11:02:24 | 4.6 | 15 | 80 | -93 | 3 | STIA | HHE | 76.09 | 76.15 | 73.21 | 73.19 | 38.77 | 0.0007 | 0.0005 |
| 27/09/2021 | 11:02:24 | 4.6 | 15 | 80 | -93 | 3 | STIA | HHN | 76.09 | 76.15 | 73.21 | 73.19 | 38.77 | 0.0007 | 0.0004 |
| 27/09/2021 | 11:02:24 | 4.6 | 15 | 80 | -93 | 3 | VAM | HHE | 98.64 | 98.68 | 96.4 | 96.52 | -60.72 | 0.0017 | 0.0006 |
| 27/09/2021 | 11:02:24 | 4.6 | 15 | 80 | -93 | 3 | VAM | HHN | 98.64 | 98.68 | 96.4 | 96.52 | -60.72 | 0.001 | 0.0004 |
| 28/09/2021 | 15:07:12 | 4.5 | 31 | 35 | -91 | 13.6 | GVDS | HHE | 197.68 | 197.7 | 198.27 | 198.78 | -29.61 | 0.0002 | 0.0001 |
| 28/09/2021 | 15:07:12 | 4.5 | 31 | 35 | -91 | 13.6 | GVDS | HHN | 197.68 | 197.7 | 198.27 | 198.78 | -29.61 | 0.0002 | 0.0001 |
| 27/09/2021 | 7:26:24 | 4.4 | 4 | 41 | -172 | 14.2 | GVDS | HHE | 195.7 | 195.72 | 196.23 | 197.14 | 30.98 | 0.0002 | 0.0001 |
| 27/09/2021 | 7:26:24 | 4.4 | 4 | 41 | -172 | 14.2 | GVDS | HHN | 195.7 | 195.72 | 196.23 | 197.14 | 30.98 | 0.0002 | 0.0001 |
| 27/09/2021 | 11:02:24 | 4.6 | 15 | 80 | -93 | 3 | SIT2 | HNE | 77.56 | 77.62 | 74.72 | 74.87 | 23.94 | 0.0015 | 0.0009 |
| 27/09/2021 | 11:02:24 | 4.6 | 15 | 80 | -93 | 3 | SIT2 | HNN | 77.56 | 77.62 | 74.72 | 74.87 | 23.94 | 0.0013 | 0.0012 |
| 27/09/2021 | 11:02:24 | 4.6 | 15 | 80 | -93 | 3 | IACM | HNE | 21.55 | 21.75 | 17.11 | 17.76 | 15.65 | 0.0115 | 0.0091 |
| 27/09/2021 | 11:02:24 | 4.6 | 15 | 80 | -93 | 3 | IACM | HNN | 21.55 | 21.75 | 17.11 | 17.76 | 15.65 | 0.0163 | 0.0098 |
| 27/09/2021 | 8:24:00 | 4.5 | 232 | 63 | -97 | 12.1 | CHAN | HHE | 121.49 | 121.52 | 119.9 | 118.17 | 106.26 | 0.0003 | 0.0004 |
| 27/09/2021 | 8:24:00 | 4.5 | 232 | 63 | -97 | 12.1 | CHAN | HHN | 121.49 | 121.52 | 119.9 | 118.17 | 106.26 | 0.0003 | 0.0005 |
| 27/09/2021 | 8:24:00 | 4.5 | 232 | 63 | -97 | 12.1 | IDI | HHE | 40.74 | 40.83 | 36.85 | 38.7 | -36.58 | 0.0006 | 0.0001 |
| 27/09/2021 | 8:24:00 | 4.5 | 232 | 63 | -97 | 12.1 | IDI | HHN | 40.74 | 40.83 | 36.85 | 38.7 | -36.58 | 0.0006 | 0.0002 |

**Table A.1 continued from previous page**

| Date | Time | Mw | Strike | Dip | Rake | HypDepth | SiteCode | Channel | Repi(km) | Rhyp(km) | Rjb(km) | Rrup(km) | Rx(km) | PGA (g) | f1.0SA |
|---|---|---|---|---|---|---|---|---|---|---|---|---|---|---|---|
| 27/09/2021 | 8:24:00 | 4.5 | 232 | 63 | -97 | 12.1 | IACM | HNE | 27.73 | 27.87 | 23.47 | 24.19 | 23.11 | 0.0036 | 0.0030 |
| 27/09/2021 | 8:24:00 | 4.5 | 232 | 63 | -97 | 12.1 | IACM | HNN | 27.73 | 27.87 | 23.47 | 24.19 | 23.11 | 0.0034 | 0.0071 |
| 27/09/2021 | 8:24:00 | 4.5 | 232 | 63 | -97 | 12.1 | IMOD | HHE | 49.41 | 49.49 | 45.77 | 47.27 | -44.55 | 0.0012 | 0.0009 |
| 27/09/2021 | 8:24:00 | 4.5 | 232 | 63 | -97 | 12.1 | IMOD | HHN | 49.41 | 49.49 | 45.77 | 47.27 | -44.55 | 0.0018 | 0.0005 |
| 27/09/2021 | 8:24:00 | 4.5 | 232 | 63 | -97 | 12.1 | KNDR | HHE | 152.53 | 152.55 | 151.82 | 149.92 | 136.24 | 0.0002 | 0.0001 |
| 27/09/2021 | 8:24:00 | 4.5 | 232 | 63 | -97 | 12.1 | KNDR | HHN | 152.53 | 152.55 | 151.82 | 149.92 | 136.24 | 0.0001 | 0.0001 |
| 28/09/2021 | 15:07:12 | 4.5 | 31 | 35 | -91 | 13.6 | IACM | HNE | 25.02 | 25.17 | 20.69 | 25.15 | -11.05 | 0.0069 | 0.0038 |
| 28/09/2021 | 15:07:12 | 4.5 | 31 | 35 | -91 | 13.6 | IACM | HNN | 25.02 | 25.17 | 20.69 | 25.15 | -11.05 | 0.007 | 0.0051 |
| 27/09/2021 | 8:24:00 | 4.5 | 232 | 63 | -97 | 12.1 | NPS | HHE | 30.88 | 31 | 26.71 | 28.58 | -5.52 | 0.0027 | 0.0009 |
| 27/09/2021 | 8:24:00 | 4.5 | 232 | 63 | -97 | 12.1 | NPS | HHN | 30.88 | 31 | 26.71 | 28.58 | -5.52 | 0.0008 | 0.0004 |
| 27/09/2021 | 8:24:00 | 4.5 | 232 | 63 | -97 | 12.1 | PFKS | HHE | 19.05 | 19.24 | 14.54 | 19.03 | 12.08 | 0.0069 | 0.0011 |
| 27/09/2021 | 8:24:00 | 4.5 | 232 | 63 | -97 | 12.1 | PFKS | HHN | 19.05 | 19.24 | 14.54 | 19.03 | 12.08 | 0.0058 | 0.0014 |
| 27/09/2021 | 8:24:00 | 4.5 | 232 | 63 | -97 | 12.1 | RODP | HHE | 147.34 | 147.36 | 146.49 | 145.65 | 74.88 | 0.0001 | 0.0001 |
| 27/09/2021 | 8:24:00 | 4.5 | 232 | 63 | -97 | 12.1 | RODP | HHN | 147.34 | 147.36 | 146.49 | 145.65 | 74.88 | 0.0002 | 0.0001 |
| 27/09/2021 | 8:24:00 | 4.5 | 232 | 63 | -97 | 12.1 | STIA | HHE | 71.85 | 71.9 | 68.84 | 67.84 | -50.38 | 0.0005 | 0.0004 |
| 27/09/2021 | 8:24:00 | 4.5 | 232 | 63 | -97 | 12.1 | STIA | HHN | 71.85 | 71.9 | 68.84 | 67.84 | -50.38 | 0.0005 | 0.0003 |
| 27/09/2021 | 8:24:00 | 4.5 | 232 | 63 | -97 | 12.1 | VAM | HHE | 104.15 | 104.18 | 102.07 | 102.75 | -91.57 | 0.0004 | 0.0002 |
| 27/09/2021 | 8:24:00 | 4.5 | 232 | 63 | -97 | 12.1 | VAM | HHN | 104.15 | 104.18 | 102.07 | 102.75 | -91.57 | 0.0003 | 0.0002 |
| 27/09/2021 | 7:26:24 | 4.4 | 4 | 41 | -172 | 14.2 | IACM | HNE | 24.85 | 24.98 | 20.51 | 25.08 | -20.25 | 0.0059 | 0.0066 |
| 27/09/2021 | 7:26:24 | 4.4 | 4 | 41 | -172 | 14.2 | IACM | HNN | 24.85 | 24.98 | 20.51 | 25.08 | -20.25 | 0.0057 | 0.0106 |
| 27/09/2021 | 11:02:24 | 4.6 | 15 | 80 | -93 | 3 | IMMV | HNE | 119.27 | 119.31 | 117.62 | 117.71 | -96.63 | 0.0006 | 0.0005 |
| 27/09/2021 | 11:02:24 | 4.6 | 15 | 80 | -93 | 3 | IMMV | HNN | 119.27 | 119.31 | 117.62 | 117.71 | -96.63 | 0.0007 | 0.0009 |
| 27/09/2021 | 8:24:00 | 4.5 | 232 | 63 | -97 | 12.1 | SIT2 | HNE | 73.34 | 73.39 | 70.38 | 69.7 | -42.36 | 0.0015 | 0.0007 |
| 27/09/2021 | 8:24:00 | 4.5 | 232 | 63 | -97 | 12.1 | SIT2 | HNN | 73.34 | 73.39 | 70.38 | 69.7 | -42.36 | 0.0012 | 0.0005 |
| 27/09/2021 | 8:24:00 | 4.5 | 232 | 63 | -97 | 12.1 | IMMV | HNE | 124.79 | 124.82 | 123.3 | 123.86 | -107.89 | 0.0002 | 0.0002 |
| 27/09/2021 | 8:24:00 | 4.5 | 232 | 63 | -97 | 12.1 | IMMV | HNN | 124.79 | 124.82 | 123.3 | 123.86 | -107.89 | 0.0003 | 0.0002 |
| 28/09/2021 | 15:07:12 | 4.5 | 31 | 35 | -91 | 13.6 | CHAN | HHE | 118.26 | 118.3 | 116.58 | 119.09 | 83.77 | 0.0004 | 0.0007 |
| 28/09/2021 | 15:07:12 | 4.5 | 31 | 35 | -91 | 13.6 | CHAN | HHN | 118.26 | 118.3 | 116.58 | 119.09 | 83.77 | 0.0004 | 0.0008 |
| 28/09/2021 | 15:07:12 | 4.5 | 31 | 35 | -91 | 13.6 | IDI | HHE | 37.56 | 37.66 | 33.58 | 36.5 | -9.62 | 0.0014 | 0.0003 |
| 28/09/2021 | 15:07:12 | 4.5 | 31 | 35 | -91 | 13.6 | IDI | HHN | 37.56 | 37.66 | 33.58 | 36.5 | -9.62 | 0.0021 | 0.0002 |
| 28/09/2021 | 15:07:12 | 4.5 | 31 | 35 | -91 | 13.6 | IMMV | HNE | 121.53 | 121.56 | 119.94 | 120.79 | -91.85 | 0.0003 | 0.0005 |
| 28/09/2021 | 15:07:12 | 4.5 | 31 | 35 | -91 | 13.6 | IMMV | HNN | 121.53 | 121.56 | 119.94 | 120.79 | -91.85 | 0.0003 | 0.0004 |
| 28/09/2021 | 15:07:12 | 4.5 | 31 | 35 | -91 | 13.6 | IMOD | HHE | 46.58 | 46.66 | 42.86 | 45.87 | 18 | 0.003 | 0.0018 |
| 28/09/2021 | 15:07:12 | 4.5 | 31 | 35 | -91 | 13.6 | IMOD | HHN | 46.58 | 46.66 | 42.86 | 45.87 | 18 | 0.0019 | 0.0008 |
| 28/09/2021 | 15:07:12 | 4.5 | 31 | 35 | -91 | 13.6 | KNDR | HHE | 149.23 | 149.25 | 148.43 | 151.13 | 128.02 | 0.0002 | 0.0002 |
| 28/09/2021 | 15:07:12 | 4.5 | 31 | 35 | -91 | 13.6 | KNDR | HHN | 149.23 | 149.25 | 148.43 | 151.13 | 128.02 | 0.0001 | 0.0003 |
| 27/09/2021 | 7:26:24 | 4.4 | 4 | 41 | -172 | 14.2 | IMMV | HNE | 120.18 | 120.21 | 118.56 | 119.43 | -11.28 | 0.0004 | 0.0005 |
| 27/09/2021 | 7:26:24 | 4.4 | 4 | 41 | -172 | 14.2 | IMMV | HNN | 120.18 | 120.21 | 118.56 | 119.43 | -11.28 | 0.0003 | 0.0005 |
| 28/09/2021 | 15:07:12 | 4.5 | 31 | 35 | -91 | 13.6 | NPS | HHE | 33.7 | 33.81 | 29.61 | 35.85 | 17.94 | 0.0022 | 0.0007 |
| 28/09/2021 | 15:07:12 | 4.5 | 31 | 35 | -91 | 13.6 | NPS | HHN | 33.7 | 33.81 | 29.61 | 35.85 | 17.94 | 0.0008 | 0.0002 |
| 28/09/2021 | 15:07:12 | 4.5 | 31 | 35 | -91 | 13.6 | PFKS | HHE | 22.04 | 22.21 | 17.61 | 23.23 | -6.25 | 0.0072 | 0.0009 |
| 28/09/2021 | 15:07:12 | 4.5 | 31 | 35 | -91 | 13.6 | PFKS | HHN | 22.04 | 22.21 | 17.61 | 23.23 | -6.25 | 0.0061 | 0.0009 |
| 28/09/2021 | 15:07:12 | 4.5 | 31 | 35 | -91 | 13.6 | RODP | HHE | 144.09 | 144.12 | 143.15 | 145.4 | 96.19 | 0.0002 | 0.0001 |

**Table A.1 continued from previous page**

| Date | Time | Mw | Strike | Dip | Rake | HypDepth | SiteCode | Channel | Repi(km) | Rhyp(km) | Rjb(km) | Rrup(km) | Rx(km) | PGA (g) | f1.0SA |
|---|---|---|---|---|---|---|---|---|---|---|---|---|---|---|---|
| 28/09/2021 | 15:07:12 | 4.5 | 31 | 35 | -91 | 13.6 | RODP | HHN | 144.09 | 144.12 | 143.15 | 145.4 | 96.19 | 0.0002 | 0.0002 |
| 28/09/2021 | 15:07:12 | 4.5 | 31 | 35 | -91 | 13.6 | STIA | HHE | 75.07 | 75.12 | 72.16 | 75.9 | -72.33 | 0.0005 | 0.0002 |
| 28/09/2021 | 15:07:12 | 4.5 | 31 | 35 | -91 | 13.6 | STIA | HHN | 75.07 | 75.12 | 72.16 | 75.9 | -72.33 | 0.0005 | 0.0004 |
| 28/09/2021 | 15:07:12 | 4.5 | 31 | 35 | -91 | 13.6 | VAM | HHE | 100.88 | 100.92 | 98.7 | 99.74 | -76.2 | 0.0006 | 0.0003 |
| 28/09/2021 | 15:07:12 | 4.5 | 31 | 35 | -91 | 13.6 | VAM | HHN | 100.88 | 100.92 | 98.7 | 99.74 | -76.2 | 0.0004 | 0.0002 |
| 27/09/2021 | 11:02:24 | 4.6 | 15 | 80 | -93 | 3 | SIVA | HNE | 43.89 | 43.99 | 40.09 | 40.27 | 12.43 | 0.0036 | 0.0010 |
| 27/09/2021 | 11:02:24 | 4.6 | 15 | 80 | -93 | 3 | SIVA | HNN | 43.89 | 43.99 | 40.09 | 40.27 | 12.43 | 0.0049 | 0.0011 |
| 27/09/2021 | 8:24:00 | 4.5 | 232 | 63 | -97 | 12.1 | SIVA | HNE | 46.65 | 46.73 | 42.93 | 43.26 | 24.04 | 0.0023 | 0.0008 |
| 27/09/2021 | 8:24:00 | 4.5 | 232 | 63 | -97 | 12.1 | SIVA | HNN | 46.65 | 46.73 | 42.93 | 43.26 | 24.04 | 0.0023 | 0.0009 |
| 28/09/2021 | 15:07:12 | 4.5 | 31 | 35 | -91 | 13.6 | SIT2 | HNE | 76.56 | 76.61 | 73.69 | 77.25 | -68.83 | 0.0009 | 0.0005 |
| 28/09/2021 | 15:07:12 | 4.5 | 31 | 35 | -91 | 13.6 | SIT2 | HNN | 76.56 | 76.61 | 73.69 | 77.25 | -68.83 | 0.001 | 0.0007 |
| 28/09/2021 | 15:07:12 | 4.5 | 31 | 35 | -91 | 13.6 | SIVA | HNE | 43.67 | 43.76 | 39.87 | 43.95 | 33.23 | 0.0033 | 0.0023 |
| 28/09/2021 | 15:07:12 | 4.5 | 31 | 35 | -91 | 13.6 | SIVA | HNN | 43.67 | 43.76 | 39.87 | 43.95 | 33.23 | 0.0034 | 0.0013 |
| 27/09/2021 | 7:26:24 | 4.4 | 4 | 41 | -172 | 14.2 | CHAN | HHE | 117.05 | 117.08 | 115.34 | 116.24 | -4.99 | 0.0006 | 0.0009 |
| 27/09/2021 | 7:26:24 | 4.4 | 4 | 41 | -172 | 14.2 | CHAN | HHN | 117.05 | 117.08 | 115.34 | 116.24 | -4.99 | 0.0006 | 0.0009 |
| 27/09/2021 | 7:26:24 | 4.4 | 4 | 41 | -172 | 14.2 | IDI | HHE | 36.54 | 36.63 | 32.53 | 36.66 | 16.59 | 0.0022 | 0.0004 |
| 27/09/2021 | 7:26:24 | 4.4 | 4 | 41 | -172 | 14.2 | IDI | HHN | 36.54 | 36.63 | 32.53 | 36.66 | 16.59 | 0.002 | 0.0004 |
| 27/09/2021 | 7:26:24 | 4.4 | 4 | 41 | -172 | 14.2 | SIVA | HNE | 41.43 | 41.51 | 37.56 | 42.72 | 35.67 | 0.0037 | 0.0019 |
| 27/09/2021 | 7:26:24 | 4.4 | 4 | 41 | -172 | 14.2 | SIVA | HNN | 41.43 | 41.51 | 37.56 | 42.51 | 35.67 | 0.0026 | 0.0015 |
| 27/09/2021 | 7:26:24 | 4.4 | 4 | 41 | -172 | 14.2 | IMOD | HHE | 44.28 | 44.35 | 40.49 | 42.99 | -7.83 | 0.0122 | 0.0018 |
| 27/09/2021 | 7:26:24 | 4.4 | 4 | 41 | -172 | 14.2 | IMOD | HHN | 44.28 | 44.35 | 40.49 | 42.99 | -7.83 | 0.01 | 0.0008 |
| 27/09/2021 | 7:26:24 | 4.4 | 4 | 41 | -172 | 14.2 | KNDR | HHE | 147.48 | 147.5 | 146.63 | 149.77 | 146.58 | 0.0002 | 0.0002 |
| 27/09/2021 | 7:26:24 | 4.4 | 4 | 41 | -172 | 14.2 | KNDR | HHN | 147.48 | 147.5 | 146.63 | 149.77 | 146.58 | 0.0002 | 0.0003 |
| 27/09/2021 | 11:02:24 | 4.6 | 15 | 80 | -93 | 3 | ZKR | HHE | 87.84 | 87.89 | 85.3 | 85.54 | -28.88 | 0.0003 | 0.0002 |
| 27/09/2021 | 11:02:24 | 4.6 | 15 | 80 | -93 | 3 | ZKR | HHN | 87.84 | 87.89 | 85.3 | 85.54 | -28.88 | 0.0005 | 0.0005 |
| 27/09/2021 | 7:26:24 | 4.4 | 4 | 41 | -172 | 14.2 | NPS | HHE | 35.99 | 36.08 | 31.96 | 37.2 | 31.96 | 0.0014 | 0.0009 |
| 27/09/2021 | 7:26:24 | 4.4 | 4 | 41 | -172 | 14.2 | NPS | HHN | 35.99 | 36.08 | 31.96 | 37.2 | 31.96 | 0.0006 | 0.0005 |
| 27/09/2021 | 7:26:24 | 4.4 | 4 | 41 | -172 | 14.2 | PFKS | HHE | 22.98 | 23.12 | 18.58 | 25.52 | -20.84 | 0.0085 | 0.0032 |
| 27/09/2021 | 7:26:24 | 4.4 | 4 | 41 | -172 | 14.2 | PFKS | HHN | 22.98 | 23.12 | 18.58 | 25.52 | -20.84 | 0.0071 | 0.0019 |
| 27/09/2021 | 7:26:24 | 4.4 | 4 | 41 | -172 | 14.2 | RODP | HHE | 142.81 | 142.84 | 141.83 | 144.96 | 140 | 0.0002 | 0.0002 |
| 27/09/2021 | 7:26:24 | 4.4 | 4 | 41 | -172 | 14.2 | RODP | HHN | 142.81 | 142.84 | 141.83 | 144.96 | 140 | 0.0003 | 0.0002 |
| 27/09/2021 | 7:26:24 | 4.4 | 4 | 41 | -172 | 14.2 | STIA | HHE | 77.07 | 77.11 | 74.22 | 76.81 | -38.14 | 0.0003 | 0.0002 |
| 27/09/2021 | 7:26:24 | 4.4 | 4 | 41 | -172 | 14.2 | STIA | HHN | 77.07 | 77.11 | 74.22 | 76.81 | -38.14 | 0.0003 | 0.0002 |
| 27/09/2021 | 7:26:24 | 4.4 | 4 | 41 | -172 | 14.2 | VAM | HHE | 99.54 | 99.57 | 97.32 | 98.5 | 5.5 | 0.0008 | 0.0006 |
| 27/09/2021 | 7:26:24 | 4.4 | 4 | 41 | -172 | 14.2 | VAM | HHN | 99.54 | 99.57 | 97.32 | 98.5 | 5.5 | 0.0007 | 0.0005 |
| 27/09/2021 | 8:24:00 | 4.5 | 232 | 63 | -97 | 12.1 | ZKR | HHE | 83.09 | 83.13 | 80.4 | 79.67 | -46.72 | 0.0002 | 0.0001 |
| 27/09/2021 | 8:24:00 | 4.5 | 232 | 63 | -97 | 12.1 | ZKR | HHN | 83.09 | 83.13 | 80.4 | 79.67 | -46.72 | 0.0004 | 0.0003 |
| 28/09/2021 | 15:07:12 | 4.5 | 31 | 35 | -91 | 13.6 | ZKR | HHE | 86.38 | 86.42 | 83.79 | 86.75 | -62.3 | 0.0001 | 0.0001 |
| 28/09/2021 | 15:07:12 | 4.5 | 31 | 35 | -91 | 13.6 | ZKR | HHN | 86.38 | 86.42 | 83.79 | 86.75 | -62.3 | 0.0003 | 0.0002 |
| 27/09/2021 | 7:26:24 | 4.4 | 4 | 41 | -172 | 14.2 | SIT2 | HNE | 78.57 | 78.61 | 75.75 | 77.94 | -26.9 | 0.0012 | 0.0004 |
| 27/09/2021 | 7:26:24 | 4.4 | 4 | 41 | -172 | 14.2 | SIT2 | HNN | 78.57 | 78.61 | 75.75 | 77.94 | -26.9 | 0.0006 | 0.0004 |
| 27/09/2021 | 7:26:24 | 4.4 | 4 | 41 | -172 | 14.2 | ZKR | HHE | 88.21 | 88.24 | 85.67 | 86.83 | 0.28 | 0.0001 | 0.0001 |
| 27/09/2021 | 7:26:24 | 4.4 | 4 | 41 | -172 | 14.2 | ZKR | HHN | 88.21 | 88.24 | 85.67 | 86.83 | 0.28 | 0.0002 | 0.0002 |

# Bibliography


[1] N. A. Abrahamson, W. J. Silva, and R. Kamai. Summary of the ask14 ground motion relation for active crustal regions. *Earthquake Spectra*, 30(3):1025–1055, 2014.

[2] S. Akkar, M. A. Sandıkkaya, and J. J. Bommer. Empirical ground-motion models for point-and extended-source crustal earthquake scenarios in europe and the middle east. *Bulletin of earthquake engineering*, 12(1):359–387, 2014.

[3] M. Båth. The seismology of greece. *Tectonophysics*, 98(3-4):165–208, 1983.

[4] I. A. Beresnev and K.-L. Wen. Nonlinear soil response—a reality? *Bulletin of the Seismological Society of America*, 86(6):1964–1978, 1996.

[5] D. Bindi, M. Massa, L. Luzi, G. Ameri, F. Pacor, R. Puglia, and P. Augliera. Pan-european ground-motion prediction equations for the average horizontal component of pga, pgv, and 5%-damped psa at spectral periods up to 3.0 s using the resorce dataset. *Bulletin of Earthquake Engineering*, 12(1):391–430, 2014.

[6] S. Bonnefoy-Claudet, C. Cornou, P.-Y. Bard, F. Cotton, P. Moczo, J. Kristek, and D. Fäh. H/v ratio: A tool for site effects evaluation. results from 1-d noise simulations. *Geophysical Journal International*, 167(2):827–837, 2006.

[7] S. S. Bora, F. Scherbaum, N. Kuehn, and P. Stafford. On the relationship between fourier and response spectra: Implications for the adjustment of empirical ground-motion prediction equations (gmpes). *Bulletin of the Seismological Society of America*, 106(3):1235–1253, 2016.

[8] G. Bouckovalas and G. Kouretzis. Stiff soil amplification effects in the 7 september 1999 athens (greece) earthquake. *Soil dynamics and earthquake engineering*, 21(8):671–687, 2001.

[9] K. W. Campbell and Y. Bozorgnia. Nga-west2 ground motion model for the average horizontal components of pga, pgv, and 5% damped linear acceleration response spectra. *Earthquake Spectra*, 30(3):1087–1115, 2014.

[10] R. Caputo, S. Catalano, C. Monaco, G. Romagnoli, G. Tortorici, and L. Tortorici. Active faulting on the island of Crete (Greece). *Geophysical Journal International*, 183(1):111–126, 10 2010.

[11] R. Caputo, S. Catalano, C. Monaco, G. Romagnoli, G. Tortorici, and L. Tortorici. Active faulting on the island of crete (greece). *Geophysical Journal International*, 183(1):111–126, 2010.

[12] J. Chandra. *Nonlinear seismic response of the soil-structure system: experimental analyses*. PhD thesis, Université de Grenoble, 2014.

[13] B.-J. Chiou and R. R. Youngs. An nga model for the average horizontal component of peak ground motion and response spectra. *Earthquake spectra*, 24(1):173–215, 2008.

[14] H. Crowley, V. Silva, and L. Martins. Seismic design code calibration based on individual and societal risk. 06 2018.

[15] H. Crowley, V. Silva, and L. Martins. Seismic design code calibration based on individual and societal risk. In *Proceedings of the 16th european conference on earthquake engineering*, pages 18–21, 2018.

[16] L. Danciu, S. Nandan, C. Reyes, R. Basili, G. Weatherill, C. Beauval, A. Rovida, S. Vilanova, K. Sesetyan, P. Bard, et al. The 2020 update of the european seismic hazard model: model overview. *EFEHR Tech Rep*, 1:v1, 2021.

[17] A. S. Elnashai and L. Di Sarno. *Fundamentals of earthquake engineering: from source to fragility*. John Wiley & Sons, 2015.

[18] C. P. Evangelidis, N. Triantafyllis, M. Samios, K. Boukouras, K. Kontakos, O.-J. Ktenidou, I. Fountoulakis, I. Kalogeras, N. S. Melis, O. Galanis, et al. Seismic waveform data from greece and cyprus: Integration, archival, and open access. *Seismological Society of America*, 92(3):1672–1684, 2021.

[19] i. G. ITSAK Research Unit: Thessaloniki, Greece. Arkalochori earthquakes, 6.0 on 27/09/2021 5.3 on 28/09/2021: Preliminary report—recordings of the itsak accelerometric network and damage on the natural and built environment. 2021.

[20] P. Jennings and C. Kisslinger. International handbook of earthquake and engineering seismology, part b, 2002.

[21] J. Kaklamanos, L. G. Baise, and D. M. Boore. Estimating unknown input parameters when implementing the nga ground-motion prediction equations in engineering practice. *Earthquake Spectra*, 27(4):1219–1235, 2011.

[22] S. R. Kotha, D. Bindi, and F. Cotton. Partially non-ergodic region specific gmpe for europe and middle-east. *Bulletin of Earthquake Engineering*, 14(4):1245–1263, 2016.

[23] S. Kramer. *Geotechnical Earthquake Engineering*. Always learning. Pearson, 2014.

[24] O.-J. Ktenidou. *Experimental and theoretical study of seismic ground motion in the city of Aegion, Greece, focusing on local site and topographic effects*. PhD thesis, Αριστοτέλειο Πανεπιστήμιο Θεσσαλονίκης (ΑΠΘ). Σχολή Πολυτεχνική. Τμήμα ..., 2010.

[25] J. Lermo and F. J. Chávez-García. Site effect evaluation at mexico city: dominant period and relative amplification from strong motion and microtremor records. *Soil Dynamics and Earthquake Engineering*, 13(6):413–423, 1994.

[26] G. Papadopoulos. *A seismic history of Crete*, volume 65. 2011.

[27] Y. M. S. S. P. K. P. L. K. K. B. K. C. T. L. P. e. a. Papakhristidis, Repapis. Arkalochori earthquake of 27/9/2021. preliminary report of the hellenic association for earthquake engineering, athens, greece. 2022.

[28] S. Stiros and G. Horsch. A note on the impacts of the 1810 seismic sequence on crete. *Bulletin of the Geological Society of Greece*, 59(1):104–117, 2022.

[29] B.-C. Sylvette, C. Cécile, B. Pierre-Yves, C. Fabrice, M. Peter, K. Jozef, and D. Fäh. H/V ratio: a tool for site effects evaluation. Results from 1-D noise simulations. *Geophysical Journal International*, 167(2):827–837, 11 2006.

[30] I. Triantafyllou, A. Karavias, I. Koukouvelas, G. A. Papadopoulos, and I. Parcharidis. The crete isl. (greece) mw6.0 earthquake of 27 september 2021: Expecting the unexpected. *GeoHazards*, 3(1):106–124, 2022.

[31] E. Vassilakis, G. Kaviris, V. Kapetanidis, E. Papageorgiou, M. Foumelis, A. Konsolaki, S. Petrakis, C. P. Evangelidis, J. Alexopoulos, V. Karastathis, et al. The 27 september 2021 earthquake in central crete (greece)—detailed analysis of the earthquake sequence and indications for contemporary arc-parallel extension to the hellenic arc. *Applied Sciences*, 12(6):2815, 2022.

[32] S. L. Walser and A. K. Stewart. Earthquake-rotated headstones as a means of re-evaluating epicentral location of the 1944 massena-cornwall earthquake: New york, united states and ontario, canada. *The Compass: Earth Science Journal of Sigma Gamma Epsilon*, 90(1):1, 2019.

[33] R. Xu and L. Wang. The horizontal-to-vertical spectral ratio and its applications. *EURASIP Journal on Advances in Signal Processing*, 2021(1):1–10, 2021.